LI
LABORATORY INVESTIGATION
THE BASIC AND TRANSLATIONAL PATHOLOGY RESEARCH JOURNAL
VOLUME 98 | SUPPLEMENT 1 | MARCH 2018

USCAP 2018

ABSTRACTS

PULMONARY PATHOLOGY

(2011-2128)

107TH ANNUAL MEETING

GEARED TO LEARN

MARCH 17-23, 2018

Vancouver Convention Centre
Vancouver, BC, Canada

Published by
SPRINGER NATURE
www.ModernPathology.org

USCAP Creating a Better Pathologist
AN OFFICIAL JOURNAL OF THE UNITED STATES AND CANADIAN ACADEMY OF PATHOLOGY

EDUCATION COMMITTEE

Jason L. Hornick, Chair
Rhonda Yantiss, Chair, Abstract Review Board and Assignment Committee
Laura W. Lamps, Chair, CME Subcommittee
Steven D. Billings, Chair, Interactive Microscopy
Shree G. Sharma, Chair, Informatics Subcommittee
Raja R. Seethala, Short Course Coordinator
Ilan Weinreb, Chair, Subcommittee for Unique Live Course Offerings
David B. Kaminsky, Executive Vice President (Ex-Officio)
Aleodor (Doru) Andea
Zubair Baloch
Olca Basturk
Gregory R. Bean, Pathologist-in-Training
Daniel J. Brat
Amy Chadburn
Ashley M. Cimino-Mathews
James R. Cook
Carol F. Farver
Meera R. Hameed
Michelle S. Hirsch
Anna Marie Mulligan
Rish Pai
Vinita Parkash
Anil Parwani
Deepa Patil
Lakshmi Priya Kunju
John D. Reith
Raja R. Seethala
Kwun Wah Wen, Pathologist-in-Training

ABSTRACT REVIEW BOARD

Narasimhan Agaram
Christina Arnold
Dan Berney
Ritu Bhalla
Parul Bhargava
Justin Bishop
Jennifer Black
Thomas Brenn
Fadi Brimo
Natalia Buza
Yingbei Chen
Benjamin Chen
Rebecca Chernock
Andres Chiesa-Vottero
James Conner
Claudiu Cotta
Tim D'Alfonso
Leona Doyle
Daniel Dye
Andrew Evans
Alton Farris
Dennis Firchau
Ann Folkins
Karen Fritchie
Karuna Garg
James Gill
Anthony Gill
Ryan Gill
Tamara Giorgadze
Raul Gonzalez
Anuradha Gopalan
Jennifer Gordetsky
Ilyssa Gordon
Alejandro Gru
Mamta Gupta
Omar Habeeb
Marc Halushka
Krisztina Hanley
Douglas Hartman
Yael Heher
Walter Henricks
John Higgins
Jason Hornick
Mojgan Hosseini
David Hwang
Michael Idowu
Peter Illei
Kristin Jensen
Vickie Jo
Kirk Jones
Chia-Sui Kao
Ashraf Khan
Michael Kluk
Kristine Konopka
Gregor Krings
Asangi Kumarapeli
Frank Kuo
Alvaro Laga
Robin LeGallo
Melinda Lerwill
Rebecca Levy
Zaibo Li
Yen-Chun Liu
Tamara Lotan
Joe Maleszewski
Adrian Marino-Enriquez
Jonathan Marotti
Jerri McLemore
David Meredith
Dylan Miller
Roberto Miranda
Elizabeth Morgan
Juan-Miguel Mosquera
Atis Muehlenbachs
Raouf Nakhleh
Ericka Olgaard
Horatiu Olteanu
Kay Park
Rajiv Patel
Yan Peng
David Pisapia
Jenny Pogoriler
Alexi Polydorides
Sonam Prakash
Manju Prasad
Bobbi Pritt
Peter Pytel
Charles Quick
Joseph Rabban
Raga Ramachandran
Preetha Ramalingam
Priya Rao
Vijaya Reddy
Robyn Reed
Michelle Reid
Natasha Rekhtman
Michael Rivera
Mike Roh
Marianna Ruzinova
Peter Sadow
Safia Salaria
Steven Salvatore
Souzan Sanati
Sandro Santagata
Anjali Saqi
Frank Schneider
Michael Seidman
Shree Sharma
Jeanne Shen
Steven Shen
Jiaqi Shi
Wun-Ju Shieh
Konstantin Shilo
Steven Smith
Lauren Smith
Aliyah Sohani
Heather Stevenson-Lerner
Khin Thway
Evi Vakiani
Sonal Varma
Marina Vivero
Yihong Wang
Christopher Weber
Olga Weinberg
Astrid Weins
Maria Westerhoff
Sean Williamson
Laura Wood
Wei Xin
Mina Xu
Rhonda Yantiss
Akihiko Yoshida
Xuefeng Zhang
Debra Zynger

To cite abstracts in this publication, please use the following format: **Author A, Author B, Author C, et al. Abstract title (abs#). *Laboratory Investigation* 2018; 98 (suppl 1): page#**

2011 Immune Microenvironment of Chronic Allograft Dysfunction in Lung Transplantation

Aadil Ahmed[1], *Vijayalakshmi Ananthanarayanan*[2], *Kamran Mirza*[3], *Aliya N Husain*[4]. [1]Loyola University Medical Center, Maywood, IL, [2]LUMC, Maywood, IL, [3]Loyola University Medical Center, Maywood, IL, [4]University of Chicago, Chicago, IL

Background: Long term survival following lung transplantation remains around 50% at 5-years because of chronic lung allograft dysfunction (CLAD) [*J Heart Lung Transplant 2011 Oct;30(10):1104-22*]. The definitive treatment for end-stage CLAD is re-transplantation, but limited organ availability and poorer outcomes make this option difficult. Previous research has shown the positive effect of FOX-P3/CD4 positive T-cells in preventing bronchiolitis obliterans in transplant recepients [Transplantation, 90(5), 540–546]. The purpose of this study was to further understand the immune micro-environment and immunoregulatory effects of PD-L1, FOX-P3 and FOX-M1 markers in CLAD pathogenesis that may have a prognostive value in CLAD prevention.

Design: Explanted lungs of 15 CLAD patients with bronchiolitis obliterans and restrictive allograft syndrome undergoing re-transplantation formed the study population. Using immunohistochemistry, the number of CD3, CD4, CD8, CD20 and CD68 positive cells were counted per five high power fields in the bronchial and interstitial compartments of the explanted lungs. PD-L1, FOX-P3 and FOX-M1 expression were measured in bronchiolar and interstitial compartments.

Results: Total counts of each cell population are shown in Table 1. CD3 population predominated in both the compartments (CD3:CD20 ratio 55:2). Majority of the cases (11/15) had higher number of CD8 than CD4 cells which is consistent with literature [*Am J Respir Cell Mol Biol 2011;44(6):749-754*]. In addition, CD8 cells were significantly more in the bronchiolar compared to the interstitial (p=0.009) compartments; similarly CD4 were observed to be greater in the bronchiolar compared to the interstitial (p=0.012) compartments. PD-L1 was present in only 4 cases with an expression rate of 1-10% in some of the affected airways. However in the interstitium, weak (6 cases) to moderate (5 cases) staining was noted in 11 cases. No correlation was found between PDL1 staining and T-cells (CD4/CD8 ratio) in either of the compartments. FOX-P3 and FOX-M1 staining was negative in all cases.

	Bronchiolar Compartments-Average Counts	Interstitial Compartments-Average Counts
CD3	76	47
CD4	24	12
CD8	40	25
CD20	04	01
CD68	13	15
Ratios		
CD4:CD3	6:19 (0.3)	6:23 (0.6)
CD4:CD8	3:5 (0.6)	1:2 (0.5)
CD68:CD3	13.76 (0.17)	15:47 (0.31)

Conclusions: CD3 cells dominated the immune microenvironment of CLAD patients with bronchiolar compartment being the major target. Low PD-L1 expression suggests a contributory role in CLAD pathogenesis. Absence of staining for FOX markers further supports the prior evidence on immunomodulatory role of FOXP3/CD4 positive T-cells in predicting the outcome and suppressing bronchiolitis obliterans in lung transplant patients .

2012 Histologic features predictive of response to PD-1 blockade in patients with non small cell lung carcinoma (NSCLC)

Deepu Alex[1], *William Travis*[1], *Natasha Rekhtman*[1], *Darren Buonocore*[1], *Ai Ni*[1], *Hira Rizvi*[1], *Matthew Hellmann*[1], *Jennifer L Sauter*[1]. [1]Memorial Sloan Kettering Cancer Center, New York, NY

Background: Antibodies that block immune checkpoints targeting the programmed cell death protein 1/programmed death-ligand 1 (PD-1/PD-L1) pathway have revolutionized the treatment of NSCLC. Many studies in the pathology literature correlate histologic features in NSCLC with high PD-L1 expression by immunohistochemistry but histologic studies correlating with response to immunotherapy (IT) are lacking. Herein, we evaluate the histologic features of NSCLCs from patients treated with anti-PD-(L)1 IT.

Design: H&E-stained slides of NSCLCs from 50 patients with advanced stage disease treated with anti-PD-(L)1 based IT were reviewed for WHO classification, necrosis and tumor infiltrating lymphocytes (TILs; scored 0, 1+, 2+, 3+). Adenocarcinomas (AC) and NSCLC NOS (NOS) were reviewed for histologic pattern(s) present (lepidic, acinar, papillary [P], micropapillary [MP] and solid). Treatment response was assessed by RECIST v1.1. Clinical variables and histologic patterns were compared between responders and non-responders using Fisher's exact test for categorical variables and Wilcoxon rank sum test for continuous variables.

Results: Response to PD-L1 blockade by histologic subtype of NSCLC were as follows: 14/32 AC, 4/9 NOS, 4/8 squamous cell carcinomas (SQ) and 0/1 large cell neuroendocrine tumor (LCNEC), for a total of 22 patients with responses. Histologic patterns present in AC/NOS tumors included 37, 16, 7, 14 and 1 with solid, acinar, MP, P and lepidic, respectively. In AC/NOS, MP was significantly associated with non-response (7/23 [30.4%] non responders; 0/18 responders; p=0.012), and P was marginally associated with response (5/23 [21.7%] non responders; 9/18 [50%] responders; p=0.056). In SQ, keratinization was seen more often in responders (75% vs 25%), but was not statistically significant. In all 50 tumors, necrosis was associated with response (12/28 [42.9%] non-responders; 16/22 [72.7%] responders; p=0.047). TILs were not associated with response.

Conclusions: These findings in this small cohort suggest that presence of micropapillary pattern may be adversely associated with response while tumor necrosis and presence of papillary pattern in AC/NOS may be associated with response to PD-(L)1 blockade. These preliminary findings will be further investigated in a larger cohort for validation.

2013 Micropapillary and Solid but not Lepidic Components Correlate with Worse Prognosis in 1522 Invasive Predominant Nonmucinous Lung Adenocarcinoma (LADC)

Rania G. Aly[1], *Takashi Eguchi*[1], *Katsura Emoto*[1], *Joseph Montecalvo*[1], *Natasha Rekhtman*[1], *Kay See Tan*[1], *Prasad S Adusumilli*[1], *William Travis*[1]. [1]Memorial Sloan Kettering Cancer Center, New York, NY

Background: The 8th edition TNM classification recommended to determine the size T descriptor in nonmucinous LADC with a lepidic component according to the invasive rather than total size. This was based on data from lepidic (LEP) predominant LADC indicating better prediction of prognosis with this approach. Since data regarding the impact of the LEP component in invasive predominant tumors did not exist, it was suggested to adjust tumor size to the invasive component with the caveat that more evidence was needed to investigate this issue. We sought to evaluate the prognostic impact of histologic typing including the LEP component in a large cohort of invasive predominant LADC.

Design: Histologic subtyping according to the 2015 WHO Classification was performed on 1839 resected stage I-IIA LADC. Minimally invasive adenocarcinoma and LEP predominant LADC cases were excluded (n=317). The remaining invasive predominant cases were categorized according to the presence or absence of any LEP component. Overall survival (OS) and disease free survival (DFS) were estimated using Kaplan-Meier approach and compared between groups (LEP vs non-LEP) using log-rank tests.

Results: Analysis of the 1522 invasive predominant LADC revealed tumors with at least 5% high grade micropapillary (MIP) or solid (SOL) component had the fewest cases with any LEP component (47% and 17% respectively). Tumors with any high grade component had significantly worse OS and DFS compared to other LADC (p=0.005 and <0.001, respectively) (Figure 1) but no statistical significance was found between LEP and non-LEP groups regarding OS and DFS in papillary, MIP or SOL predominant ADC except for marginal difference in acinar group (OS p=0.045 and DFS p=0.033) (Figure 2).

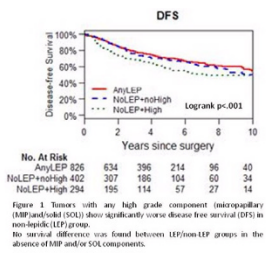

Figure 1 Tumors with any high grade component (micropapillary (MIP)and/solid (SOL)) show significantly worse disease free survival (DFS) in non-lepidic (LEP) group.
No survival difference was found between LEP/non-LEP groups in the absence of MIP and/or SOL components.

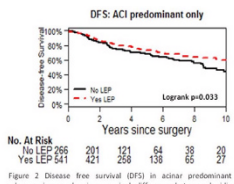

Figure 2 Disease free survival (DFS) in acinar predominant adenocarcinoma showing marginal difference between lepidic (LEP) and non-LEP group (p=0.033)

Conclusions: In invasive predominant LADC, survival appears to mainly be driven by the presence of MIP or SOL rather than LEP components. This suggests that tumor size adjustment for the LEP component may not be necessary in determining the size T-factor in invasive predominant LADC.

2014 Spread Through Air Spaces (STAS) Correlates with Prognosis in Lung Neuroendocrine Tumors (LNET)

Rania G. Aly[1], *Takashi Eguchi*[1], *Kyuichi Kadota*[3], *Natasha Rekhtman*[1], *Prasad S Adusumilli*[1], *William Travis*[1]. [1]Memorial Sloan Kettering Cancer Center, New York, NY, [3]Kagawa University, Kagawa, Japan

Background: Multiple studies have validated spread through air spaces (STAS) as a prognostic marker in lung adenocarcinoma and squamous cell carcinoma. However, the presence and significance of STAS in LNET have been not yet determined. The aim of this study is to investigate the incidence and the prognostic value of STAS in different histologic types of LNET.

Design: 500 p-Stage I-III LNET (1992-2012) were evaluated for mitotic counts, necrosis and Ki67 proliferation index and tumors were classified into typical carcinoid (TC), atypical carcinoid (AC), large cell neuroendocrine carcinoma (LCNEC) and small cell lung carcinoma (SCLC). TC and neuroendocrine tumors combined with other subtypes cases were excluded (n=307). All tumor slides were reviewed and evaluated for STAS lymphovascular invasion, pleural invasion, and necrosis. Recurrence free probability (RFP) and lung cancer-specific survival (LCSS) were analyzed using Kaplan-Meier analysis and Cox hazard model.

Results: The 193 patients (AC, n=35; LCNEC, n=98; and SCLC, n=60) were analyzed. STAS was identified in 41% of tumors. Patients with STAS were associated with worse RFP (Figure 1) and LCSS (Figure 2) compared to patients without STAS in the total cohort as well as in each tumor subtype cohort. In multivariable analysis, STAS was an independent risk factor for recurrence (hazard ratio [HR] 3.55, 95% confidence interval [CI] 2.07-6.08, p<0.001) and lung cancer-specific death (HR 4.07, 95% CI 2.16-7.66, p<0.001), independent of tumor subtypes, tumor size, p-Stage, lymphovascular invasion, and necrosis.

Figure 1. Recurrence free probability – STAS (-) vs. STAS (+)

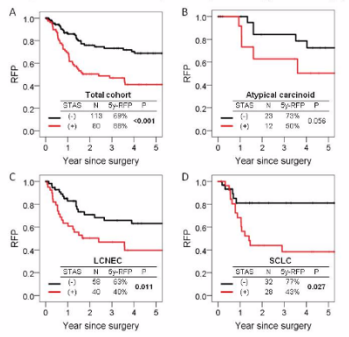

Figure 2. Lung cancer-specific survival – STAS (-) vs. STAS (+)

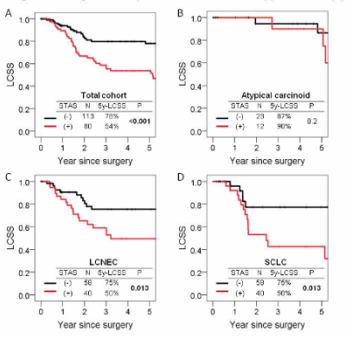

Conclusions: STAS was associated with worse prognosis in all LNET together as well as within each tumor subtype. STAS was also found to be an independent risk factor of RFP and LCSS supporting its prognostic importance.

2015 Validation of PD-L1 Immunohistochemical Stain Using Clone 22C3 in Different Automatic Stainer Platforms

Atreyee Basu[1], *Luis Chiriboga*[2], *Fang Zhou*[3], *Andre Moreira*[3]. [1]NYU Langone Medical Center, New York, NY, [2]NYU, New York, NY, [3]New York, NY

Background: Immunohistochemical stain for PD-L1 as a biomarker for immunotherapy is recommended in non-small cell lung cancer (NSCLC). There are several clones of the antibody, each is paired with a specific drug and has a separate cut off for interpretation. This complexity adds confusion in test selection and interpretation. In the US clone 22C3 is most commonly used, and the interpretation is clearly defined as percentage of positive expression in tumor cells, which has convenient interpretability into therapy applications. However the FDA approval for this test is linked to an automatic stainer not commonly used in US except for select laboratories, and this leads to delays in results. Hence there exists the need for a cross platform validation of the antibody.

Design: The 39 cases of NSCLC used for this validation protocol were sent to a reference laboratory (Keytruda) to obtain the "gold standard" results. The same blocks were evaluated independently in the clinical and research laboratories using 2 different stainer platforms (Ventana). An Optiview detection kit was only used in the clinical setting. 2 extra cases (one negative and another showing high expression) were used for validation of antibody. Results were interpreted as recommended by the FDA: negative (zero or < 1% stain), low expression (1-49%), and high expression (50-100%), independently by 2 pathologists, one with formal training in Keytruda.

Results: The correlation of the gold standard test with both clinical (r=0.88, p <0.001) and research (r=0.75, p <0.001) laboratories were positive and significant. The outcomes were interpreted as negative (for 0% and 1-49% expression) and positive (≥50% expression). There were 2 false negative results in the clinical and 6 in the research laboratory (no false positives). The sensitivity, specificity, positive predictive value and negative predictive value for the clinical laboratory were 92.3%, 100%, 100%, and 86.7% respectively; while those for the research laboratory were 76.9%, 100%, 100%, and 68.4%. The agreement between the trained and untrained pathologists was 71% for clinical and 84% for the research laboratories.

Conclusions: Cross-validation of the clinically used 22C3 anti PD-L1 antibody test is possible in commonly used automated stainer which may reproduce comparable results to the gold standard FDA approved test. The few discrepancies encountered were due to the interpretation of borderline zones. These are intrinsic subjective variations inherent to the test.

2016 Correlation of PD-L1 Expression with Histological Patterns and Treatment Response in Non-Small Cell Lung Cancer

Boulos Beshai[1], *Bo Xu*[1]. [1]Roswell Park Cancer Institute, Buffalo, NY

Background: Programmed death ligand-1 (PD-L1) inhibitors are currently approved for treatment of advanced stage non-small cell lung cancer (NSCLC) patients as either first or second line therapy. In this study, we investigate correlation between PD-L1 expression level in NSCLC tumor cells detected by immunohistochemical method (IHC) to tumor histological growth patterns.

Design: Slides or scanned digital images of NSCLC cases tested for PD-L1 between December, 2015 to August, 2017 were blindly re-reviewed to confirm the level of PD-L1 expression and classification of tumor growth patterns. PD-L1 expression levels were graded as follows: <1%, negative, between 1 to 50%, low expression, >50%, high expression. Metastatic cases with unconfirmed lung primary and specimens with insufficient tumor cells were excluded. In adenocarcinomas, tumors containing lepidic, acinar and papillary patterns are classified as well-to-moderately differentiated (WD to MD). Micropapillary, signet ring cells and solid patterns are classified as moderate-to-poorly differentiated (MD to PD).

Results: Total 47 cases were identified (41 cases of adenocarcinoma, 6 cases of squamous cell carcinoma). Specimens included 8 cytology (1 primary, 7 metastatic), 39 surgical; divided into 2 lung wedges, 5 lobectomies, and 32 biopsies (15 primary, 17 metastatic). Among squamous cell carcinomas, 5 of 6 cases (83%) showed negative or low expression of PD-L1, and one case (17%) displayed high expression. In WD to MD adenocarcinoma, 8 of 10 cases (80%) showed negative or low expression, whereas 2 of 10 cases (20%) had high expression level of PD-L1. On the other hand, MD to PD adenocarcinomas, 17 of 31 cases (55%) displayed low expression and 14 of 31 cases (45%) had high expression. 13 of 17 total "high-expression" cases (76%) demonstrated PD patterns, out of which, 8 cases (62%) had a solid growth pattern.

Conclusions: Among NSCLC, we observed that majority of squamous cell carcinomas display either negative or low expression of PD-L1 protein detected by IHC, regardless of its degree of differentiation. In adenocarcinomas, however, tumors with PD pattern show high PD-L1 expression, with pure solid adenocarcinoma has the highest expression level. The degree of expression becomes lower when combined with other growth patterns of better differentiation. Our next step of investigation will be directed towards reviewing clinical data in patients who received immune check point inhibitors to correlate PD-L1 expression with patient responsive rate.

2017 KI67 Labeling Index in Pulmonary Carcinoid Tumors- Comparison between Small Biopsy and Resection using Tumor Tracing and Hot-Spot Methods

Jennifer Boland[1], *Trynda Kroneman*[1], *Simone Terra*[1], *Hao Xie*[1], *Julian Molina*[1], *Taofic Mounajjed*[1], *Anja Roden*[1]. [1]Mayo Clinic, Rochester, MN

Background: Per WHO criteria, classification of pulmonary carcinoids

as typical (TC) or atypical (AC) requires assessment of necrosis and mitoses. Thus, sampling issues preclude grading on small biopsies unless there are obvious atypical features. Hot-spot (HS) KI67 index is incorporated into grading of gastrointestinal neuroendocrine tumors. While KI67 is not used to grade pulmonary carcinoids, it has particular appeal in the setting of small biopsies, where it may be helpful to determine preliminary grade. However, the rate at which KI67 could under- or over-estimate grade on small biopsies is not known.

Design: Institutional pathology archives were searched for patients with biopsy showing pulmonary carcinoid and subsequent resection. Tumor areas were circled by a pathologist. KI67 stains were performed on both specimens from each patient, and scanned using Aperio ScanScope. Labeling index was determined via digital image analysis by a technologist using tumor tracing (TT, 1% cutoff) and HS (2% cutoff) methods, with 10% re-review by a pathologist. Follow-up was obtained from clinical records.

Results: KI67 results for 31 TCs and 8 ACs are summarized in the table. TT KI67 was in the same category on biopsy and resection in 26 of 39 cases (67%), while the biopsy overestimated KI67 relative to resection in 10 (26%), and underestimated in 3 (7%). HS KI67 was the same in 26 cases (67%), with overestimation relative to resection in 2 (5%), and underestimation in 11 (28%). In resected TCs, HS KI67 was ≤2% in only 22% of cases. Conversely, in resected ACs, TT KI67 was >1% in only 50%. Mean follow-up was 75 months (median 74, range 1-192). Recurrence or metastases occurred in 6 of 8 AC patients (75%), and 6 of 31 TC patients (19%). Metastatic sites included regional lymph nodes (9), liver (3), lung (1), eye (1), bone (1), and soft tissue (1). Two patients died of disease (both AC, 23-74 months). Detailed survival analysis is ongoing to determine the prognostic significance of KI67 by each method compared to WHO classification.

		Typical Carcinoids (n=31)		Atypical Carcinoids (n=8)	
		Hot Spot			
		KI67 ≤2%	KI67 >2%	KI67 ≤2%	KI67 >2%
	Biopsy				
Tumor Tracing	KI67 ≤1%	13 (42%)	4 (13%)	1 (12%)	2 (25%)
	KI67 >1%	2 (6%)	12 (39%)	0	5 (63%)
	Resection				
	KI67 ≤1%	7 (22%)	16 (52%)	0	4 (50%)
	KI67 >1%	0	8 (26%)	0	4 (50%)

Conclusions: KI67 labeling index was in the same category on biopsy and resection in two-thirds of cases, with a tendency to overestimate KI67 on biopsy using TT and underestimate using HS. HS KI67 seems to overestimate grade of resected TCs, possibly because of KI67 hot-spots secondary to prior biopsy procedure. TT KI67 seems to underestimate grade of resected ACs, so assessment for necrosis and mitoses should always be performed for correct grading.

2018 Driver Mutations in Non-Small Cell Lung Cancer Among Hispanics and Native Americans of New Mexico

Cory Broehm[1], *Devon Chabot-Richards*[1]. [1]Albuquerque, NM

Background: The types of driver mutations present in non-small cell lung carcinoma (NSCLC) among Hispanics and Native Americans is not well understood, but is critical for optimizing care for these historically underserved populations. We studied the prevalence of mutations in *EGFR*, *KRAS*, and *BRAF* and *ALK*, *RET*, *ROS*, and *MET* in NSCLC in White (W), Hispanic (H), and Native American (NA) patients treated at University of New Mexico Hospital.

Design: All cases of primary and metastatic NSCLC from January 2010 to January 2017 with molecular or FISH testing performed on formalin-fixed paraffin-embedded tumor tissue and self-identified ancestry available were identified in our archives. Molecular tests included *EGFR* (exons 19 and 21 or exons 18-21), *KRAS* (exons 2-4), and *BRAF* (exons 11 and 15) by next-generation sequencing using the IonTorrent platform (Life Technologies). FISH tests included *ALK*, *RET*, and *ROS* rearrangement and *MET* amplification (Vysis Inc). Histologic subtype for each case and demographic data including age, sex, and self-identified ancestry were also recorded from the medical record.

Results: 193 patients were identified (122 W [53M/69F, Age 38-91y], 64 H [36M/28F, Age 34-94y], 7 NA [2M/5F, Age 44-82y]). Histologic subtypes included adenocarcinoma (93 W, 51 H, 6 NA), adenosquamous (5 W, 3 H), squamous cell (9 W, 3 H), large cell (1 W), and NSCLC NOS (14 W, 7 H, 1 NA). 191 patients had molecular testing (121 W, 63 H, 7 NA), including *EGFR* (all patients), 66 *KRAS* (41 W, 21 H, 4 NA), 65 *BRAF* (40 W, 21 H, 4 NA). *EGFR* mutations were identified in 16 W (13%), 13 H (21%), and 1 NA (14%). *KRAS* mutations were identified in 13 W (32%), 4 H (19%), and 3 NA (75%). *BRAF* mutations were identified in 1 W, 2 H, and none in NA. 187 patients had FISH performed (117 W, 63 H, 7 NA). *ALK* rearrangements were identified in 7 W and 2 H and *ROS* rearrangements in 1 W. *RET* rearrangements were not identified in any patients. *MET* amplification was identified in 3 W patients only. All mutations occurred in adenocarcinoma except 1 *EGFR* (NSCLC NOS, H), 3 *KRAS* (NSCLC NOS and adenosquamous, 2 W/1 H) and 2 *ALK* (NSCLC NOS, 1W/1H). Significant sex and age differences were not noted.

Conclusions: NSCLC in Native Americans shows similar rates of *EGFR* mutations and higher rates of *KRAS* mutations compared to whites. NSCLC in Hispanics shows increased rates of *EGFR* mutations and lower rates of *KRAS* mutations compared to whites. Alterations in *ALK*, *RET*, *ROS*, and *MET* are uncommon but higher in whites.

2019 Methylomic Profiling to Establish Tumour Clonality in Synchronous and Metachronous Non-Small Cell Lung Carcinomas

Michael Cabanero[1], *Yasin Mamatjan*[2], *Kenneth D Aldape*[3], *Ming-Sound Tsao*[2]. [1]University Health Network, Toronto, ON, [2]University Health Network, Toronto, ON, [3]Princess Margaret Cancer Centre MacFeeters-Hamilton Brain Tumour Centre

Background: The distinction between multiple primary lung cancers (MPLCs) and intrapulmonary metastases is important for therapy and prognosis of these patients. Current methods of distinction are based on established clinicopathologic criteria that rely on histomorphologic and temporal associations. However, cases are often difficult to distinguish and have shown marked variation in survival rates observed. More recent studies have incorporated various molecular features, including TP53, X-chromosome inactivation, or loss-of-heterozygosity analysis, as criteria to establish clonality. Since DNA methylation information is conserved during cell division, profiling the tumour methylome could serve as a measure for clonality. We hypothesize that whole genome DNA methylation profiling of synchronous/metachronous lung tumours could serve as a reliable way of establishing clonality.

Design: The methylome of 51 pairs of synchronous NSCLC cases are profiled using the MethylationEPIC Beadchip (850k) chip. Differentially methylated regions will be used as reference points both globally and for paired samples, and differentially methylated points obtained using the highest variant probes. Multidimensional scaling plot will be used to cluster groups based on similarity. Histopathologic characteristics will be reviewed.

Results: Results from the initial 5 profiled cases identified three MPLCs and two intrapulmonary metastases by histopathological evaluation. SNP heat mapping confirmed the identity of 5 matching pairs of NSCLC. Multidimensional scaling plot showed 1/5 cases with a widened gap of mean methylation patterns, suggesting non-clonality. Two cases identified as MPLCs by histopathologic criteria were found to be clonal by methylation analysis. Pathologic review of these cases shows these pairs had different histologically predominant patterns. Results for the remaining 46 cases will be reported.

Conclusions: In cases of multiple primary lung cancers, each lesion is staged and managed as distinct tumours, with surgical resection regarded as treatment of choice for patients with early-stage disease. These cases have better prognosis compared to intrapulmonary metastatic lesions, who are primarily treated with chemo(radiation) therapy. Incorporation of the tumour methylomic profiles with histopathological criteria might improve the reliability of determining tumour clonality.

2020 Acute Lung Injury Complicating Solid Organ Transplantation: A Review of 72 Autopsies

Alain P Cagaanan[1], *Scott W Aesif*[2]. [1]University of Wisconsin Hospital and Clinics, Madison, WI, [2]University of Wisconsin School of Medicine and Public Health, Madison, WI

Background: Organ rejection and secondary infections due to immunosuppression are frequent complications of transplantation for end-stage solid organ failure. Pulmonary complications contribute significantly to post-graft morbidity and mortality. Acute lung injury (ALI) patterns are seen in a variety of clinical settings, infection frequent amongst them. The clinical and pathologic features of ALI following solid organ transplantation have not been well characterized in the literature.

Design: Autopsy reports from 2002 to 2011 were searched for decedents with solid organ transplants. Patients with lung transplants were excluded. Autopsy slides from the native lungs were reviewed by a pulmonary pathologist. Medical records were also reviewed.

Results: Seventy-two patients (47 male) were identified, with a median age of 55 years (range, 2-79 years), median survival following transplantation of 3 years (range, 1 day-22 years). Solid organ transplant type and histologic findings are summarized in the table. Twenty-five patients (18 male) with ALI and infectious organisms identified histologically, died at a median age of 55 years (range, 14-71 years) and median 1 year following transplantation (range, 19 days-17 years). Twenty-one patients (13 male) with ALI and no infectious

organisms identified histologically, died at a median age of 54 years (range, 37-71 years) and median 4 years following transplantation (range, 1 day-17 years). One male patient with *Aspergillus* colonization but no ALI died 10 months after liver transplantation. Another male patient with unclassified fungal colonization but no ALI died 4 months after heart transplantation. One patient who underwent a small bowel, liver, and pancreas transplantation demonstrated no evidence of ALI or organisms.

Transplant(s) (#)	ALI-Pattern(s) Observed (#)	Infectious Organism(s) (#)
Liver (35)	DAD (Acute 11), Mixed (6), OP (7)	B (2), F (7), FV (2), V (1)
Kidney (14)	DAD (Acute 3), Mixed (2), OP (2, Fibrosing 1)	B (1), F (2), FV (1),
Liver & Kidney (5)	DAD (Acute 2), OP (2)	BF (1), BV (1)
Pancreas & Kidney (7)	DAD (Acute 2, Organizing 2), Mixed (1), OP (1)	F (3), V (2)
Heart (10)	DAD (Acute 2), Mixed (2)	BF (1), F (3)

DAD = diffuse alveolar damage, OP = organizing pneumonia, B = bacteria, F = fungus, V = virus

Conclusions: This study demonstrates that ALI frequently complicates the native lungs of solid organ transplant patients (64% of all cases). DAD was common (72% of ALI cases) and infectious organisms were frequently identified histologically (58% of ALI cases). ALI without infectious organisms identified histologically was associated with a longer median survival following solid organ transplantation, when compared to ALI with identifiable infectious organisms. The significance of this finding warrants future investigation.

2021 Expression of GATA3 in Primary Lung Carcinomas: Correlation with Histopathologic Features and TTF-1/p40 Expression

Guoping Cai[1], *Peter Chen*[2]. [1]Wallingford, CT, [2]Yale New-Haven Hospital, Branford, CT

Background: GATA binding protein-3 (GATA3) is a transcription factor that regulates cell differentiation and is considered a sensitive biomarker for tumors of breast and urothelial origin. However, GATA3 expression is not specific and can also been seen in other malignant neoplasms including tumors of the lung. This study assessed GATA3 expression in primary lung carcinomas and correlated its relationship with histopathologic features as well as TTF-1 and p40 expression.

Design: A total of 184 primary lung carcinomas were retrieved from the pathology archives, from which representative cores were taken to construct tissue microarrays (TMA). Immunohistochemistry was performed on TMA sections using GATA3, TTF-1, and p40 antibodies. GATA3 expression was evaluated and semi-quantitatively reported as negative, low, or high according to percentile and density of tumor nuclear staining. Histopathologic features and TTF-1/p40 immunostaining patterns were also reviewed and correlated with GATA3 expression.

Results: Of 184 tumors, positive GATA3 staining was seen in 26 cases (14%), including adenocarcinoma (10 cases), squamous cell carcinoma (10 cases), adenosquamous carcinoma (3 cases), large cell carcinoma (2 cases) and large cell neuroendocrine carcinoma (1 case). Among the GATA3-expressing tumors, low (focal <50% and weak) and high (diffuse >50% and strong) GATA3 expressions were seen in 20 and 6 cases, respectively. High GATA3 expression was more likely observed in poorly differentiated carcinomas, including adenocarcinoma (3 cases), squamous cell carcinoma (2 cases) and large cell carcinoma (1 case). These tumors were also negative for TTF-1 and p40, excluding the cases of squamous cell carcinoma.

FOR TABLE DATA, SEE PAGE 762, FIG. 2021

Conclusions: Our study demonstrates GATA3 expression in a significant number of primary lung carcinomas. Thus, caution should be exercised when interpreting GATA3 expression and assigning tumor origin, especially in the setting of poorly differentiated lung carcinomas.

2022 T Cell Profiling to Predict "Hot" Immunophenotype Correlates with Mutational Drivers, Epithelial Mesenchymal Transition and Outcome in Non-Small-Cell Lung Cancer

Vera Luiza Capelozzi[1], *Juliana Machado*[2], *Tabatha Prieto*[3], *Vanessa Martins*[3], *Cecilia Fahrat*[3], *Alexandre Fabro*[4], *Edwin R Parra*[5]. [1]University of Sao Paulo, Sao Paulo, [2]São Paulo State University, [3]University of São Paulo, [4]Botucatu, [5]UT MD Anderson Cancer Center, Houston, TX

Background: Immune checkpoint blockade increases survival in a subset of patients with non–small-cell lung cancer (NSCLC), but robust biomarkers that predict response to PD-1 pathway inhibitors are lacking. Additionally, our understanding of tumor factors that influence PD-L1 response, such as tumor immune microenvironment, driven mutations and epithelial mesenchymal transition (EMT) remains incomplete.

Design: Tumor tissue specimens from stage I–III NSCLC [84 adenocarcinomas; 51 squamous cell carcinomas (SCCs), 19 large cell carcinomas (LCC) and 10 large cell neuroendocrine carcinomas (LCNEC)] were examined. Multiplex immunofluorescence was performed for macrophages, CD3, CD8, CD57, differentiation status (FOXP3 and CD45RO), and inhibitory receptors (PD-1). This analysis was integrated with clinical, histopathologic characteristics, and Real Time-qPCR.

Results: Significant higher levels of PD-L1 expression were detected in LCNEC compared with other histologies (Table 1; Figure 1). Immunofluorescence profiling identified an immunologically "hot" cluster with abundant CD3+CD8+ and CD3CD45RO T cells and an immunologically "cold" cluster with lower relative abundance of these markers. We found a higher density of suppressor/cytotoxic T lymphocytes (CD3+CD8+) in metastatic LCNEC when compared to SCC (P=0.02). Equally significant was the high expression of inhibitory marker CD3+PD-1+ in metastatic adenocarcinoma compared to SCC (P=0.01). Metastatic LCC presented high levels of naïve/memory T cells CD3CD45RO when compared to SCC (P=0.04; Table 1, Figure 2). A high density of B lymphocytes (CD20+) was found in metastatic LCC compared to adenocarcinoma (P=0.04). There was no correlation between immunophenotype and driver mutations, but we did observe a correlation between the "hot" cluster for PD-L1 and immune regulator genes (CTLA-4 and PDCD1LG2, P<0.01). High CD3+FOXP3+CD45RO+ and CD3+PDL1+ expression, low CD3+CD8+ and absence of CTLA-4 mutation were independent favorable prognostic factors for DFS and OS.

ADC, adenocarcinoma; Scc, squamous cell carcinoma; LCC, large cell carcinoma; LCNE, large cell neuroendocrine carcinoma;

Prim, primary; Met, metastatic

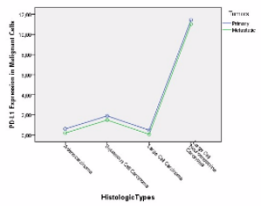

Figure 1. General linear model controlling PD-L1 expression in malignant cells in primary and metastatic tumors according histologic types.

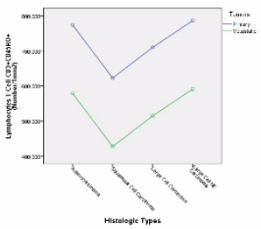

Figure 2. General linear model controlling lymphocytes T Cell CD3+CD45RO+ in microenvironment of primary and metastatic tumors according to histologic types

Conclusions: Our results may support the use of quantitative immune profiling to study prognosis, response and resistance to immunotherapy in lung cancer.

2023 Prognostic value of architectural components in pulmonary adenocarcinoma brain metastases

François Casteillo[1], *Mousa Mobarki*[2], *Jean-Baptiste Guy*[3], *François Vassal*[3], *Pierre Fournel*[4], *Georgia Karpathiou*[3], *Michel Peoc'h*, *Fabien Forest*. [1]University Hospital of Saint-Etienne, Saint-Etienne, Loire, [2]Saint Etienne, [3]University Hospital of Saint-Etienne, [4]Lucien Neuwirth Cancer Institute

Background: Although the WHO 2015 classification recommends the screening of architectural components of primary pulmonary adenocarcinomas as prognostic determinants for overall survival, it remains unknown whether this predictive approach could be extended to the evaluation of metastases. Herein, our aim was to investigate the prognostic value of the different architectural components in brain metastases of pulmonary adenocarcinomas.

Design: *We conducted a retrospective, monocentric study.* Surgical specimens of brain metastases of pulmonary adenocarcinomas were studied. Slides were re-evaluated by two pathologists following the recommendations of the WHO 2015, allowing semi-quantitative estimation of the various architectural components (i.e., acinar, solid, papillary and micropapillary) and determination of

the predominant one. We also studied the occurrence of molecular abnormalities including mutations of *KRAS*, *EGFR*, *BRAF*, *HER2* and *ALK* rearrangements.

Results: One hundred and one excision specimens were included (101 patients). The predominant component was solid in 56.9% of cases, papillary in 22%, acinar in 15.4%, and micropapillary in 1.6%. The presence of a predominant solid or micropapillary component (high grade group) was associated with decreased overall survival compared to the papillary or acinar component (low grade group) (hazard ratio 2.52 [95% confidence interval: 1.48–4.3, $p < 0.01$). This difference was also observed in multivariate analysis. Other factors of poor prognosis were: age ≥ 55 years ($p = 0.0417$); performans status ($p < 0.01$); primary tumor > 25 mm ($p = 0.022$); absence of TTF-1 expression ($p = 0.0412$); presence of an infra-tentorial metastasis ($p < 0.01$); presence of several brain metastases ($p = 0.0182$). The frequency of *EGFR* and *KRAS* mutations were 4.9 % and 28.1 %, respectively. Tumor architecture and prognosis were not associated with the presence of the studied molecular alterations.

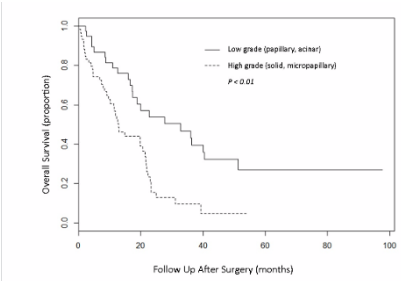

Conclusions: Architectural evaluation of pulmonary adenocarcinomas brain metastases has prognostic value. The presence of a predominant solid or micro-papillary component was associated with decreased overall survival compared to the predominant acinar or papillary architectures. This work allows the identification of different prognostic subgroups in patients with pulmonary adenocarcinoma cerebral metastases.

2024 Identification of a Senescence Associated Secretory Phenotype with p16 Positive Fibroblastic Foci in Interstitial Lung Disease

Matthew J Cecchini[1], *Mariamma Joseph*[2], *Christopher J Howlett*[3], *Marco Mura*[4]. [1]London Health Sciences Centre, Western University, London, ON, [2]London Health Sciences Centre, Western University, [3]Western University, London, ON, [4]London Health Sciences Centre

Background: Usual interstitial pneumonia (UIP) and non-specific interstitial pneumonia (NSIP) are common forms of interstitial lung disease (ILD). Recent studies have identified potential links between UIP and senescence. Senescence is a form of irreversible cell cycle arrest that can be caused by DNA damage, shortened telomeres or oncogene activation. Senescent fibroblasts can develop a senescence-associated secretory phenotype (SASP) to produce profibrotic growth factors and matrix remodeling proteins.

Design: RNA was extracted and hybridized to the Human Gene 1.0 set array (Affymetrix) from explanted lungs in 22 patients with definitive UIP pattern in the native lungs and typical CT features of UIP, 10 subjects with histological pattern of NSIP, 5 with mixed UIP-NSIP pattern, and 11 normal controls. Differentially expressed genes were identified based on a fold change ≥1.5 and a q value (false discovery ratio) <0.05. Immunohistochemistry for p16, p53, Periostin and IDO1 was performed on surgical lung biopsies from 22 UIP, 9 NSIP and 5 mixed cases.

Results: Analysis of the microarray revealed a gene expression signature associated with a senescence associated secretory phenotype in ILD cases. UIP cases showed a unique pattern with an increased expression of MMP2, ACTA2, IGFBP5, MMP7, POSTN and OPN compared to the NSIP cases. Immunohistochemistry identified p16 positive fibroblastic foci in 15 of 22 (68%) of UIP cases, 0 of 9 (0%) NSIP cases and 2 of 5 (40%) mixed cases. P16 fibroblastic foci were also positive for p53 by immunohistochemistry. CDKN2A (p16) gene expression correlated with reduced FVC and increase GAP scores in UIP. No difference in Perositin or IDO1 was identified by immunohistochemistry.

Conclusions: Genome-wide gene expression profiles identified a SASP signature in ILD cases. UIP cases expressed a distinct subset of growth factors and matrix remodeling genes. P16 positive fibroblastic foci were identified in the majority of UIP cases and expression correlated with worsening lung function. Taken together, these results highlight an important etiological basis for senescence in UIP and support the ongoing development of senolytic therapies to disrupt this process. Further, there is a potential use for p16 as an adjunct marker to distinguish UIP from NSIP.

Supported by the Lawson Internal Research Fund, the Western Strategic Support for CIHR Success, Seed Grant and La Roche Multi Organ Transplant Academic Enrichment Fund.

2025 Next-Generation Sequencing and Clinicopathologic Analysis of 101 Pulmonary Invasive Mucinous Adenocarcinomas Focusing on Comparison Among Molecular Subtypes

Jason Chang[1], *Maria Arcila*[2], *Joseph Montecalvo*[1], *Patrice Desmeules*[3], *Ryma Benayed*[4], *Sarah Teed*[4], *Joshua Sabari*[5], *Laetitia Borsu*[4], *William Travis*[6], *Marc Ladanyi*[6], *Alexander Drilon*[4], *Natasha Rekhtman*[6]. [1]Memorial Sloan Kettering Cancer Center, New York, NY, [2]New York, NY, [3]Quebec Heart and Lung Institute, QC, [4]Memorial Sloan Kettering Cancer Center, [5]Memorial Sloan Kettering CC, [6]Memorial Sloan-Kettering CC, New York, NY

Background: Invasive mucinous adenocarcinoma (IMA) is a distinct subtype of lung adenocarcinoma, characterized genomically by frequent *KRAS* mutations or specific gene rearrangements, most commonly in *NRG1*. Whether IMAs with *KRAS* mutations vs *NRG1* fusions have distinct clinicopathologic features is not well established.

Design: A total of 101 IMAs (82 pure, 19 mixed IMA) were included in the study. Targeted 410-gene hybridization capture-based next generation sequencing (NGS) was performed on 77 IMAs. Targeted 62-gene RNA sequencing was performed on 4 driver-negative cases from the NGS cohort and on 24 additional IMAs previously determined to be *KRAS*-wild type by high sensitivity non-NGS assays. Detailed clinicopathologic and genomic analysis was performed, focusing on the comparison of *KRAS*$^+$ vs *NRG1*$^+$ IMAs.

Results: By NGS, the most prevalent alterations in IMAs involved *KRAS* (75%), *NKX2.1* (28%), *CDKN2A* (22%), *STK11* (17%), *TP53* (14%) and *GNAS* (13%). Importantly, we identified 3 (4%) IMAs with *SMAD4* hotspot mutations in patients with no clinicoradiologic evidence of pancreatic adenocarcinoma. Fusions were identified in a total of 18 cases (46% of *KRAS*-wild type IMAs), including 9 *NRG1*, 4 *ALK*, 2 *NTRK1*, 2 *ROS1*, and 1 *FGFR3-TACC3*. *NRG1*$^+$ (n=9) and *KRAS*$^+$ (n=62) IMAs had a similar distribution of pure vs mixed histology. Interestingly, at least focal areas of higher nuclear grade were overrepresented in *NRG1*$^+$ (67%) compared to *KRAS*$^+$ (19%) IMAs (P=0.002). Furthermore, *NRG1*$^+$ tumors tended to be larger in size (median 7.4 vs 3.2 cm, respectively) and had higher rate of lymphovascular invasion (43% vs 7%, respectively; P=0.005) and regional lymph node metastases (50% vs 4%, respectively; P=0.0001) compared to *KRAS*$^+$ IMAs. Patient characteristics for *NRG1*$^+$ and *KRAS*$^+$ IMAs were similar, and included a high rate of never/light smokers (89% and 63%, respectively).

Conclusions: This is the largest study to-date of IMAs with combined targeted DNA and RNA NGS and detailed clinicopathologic analysis. This is the first documentation that *NRG1*$^+$ IMAs have distinctive clinicopathologic features, including higher nuclear grade and greater propensity for nodal spread. Presence of *SMAD4* mutations is another novel finding, which expands the spectrum of pancreatic adenocarcinoma-type alterations in IMAs. This study also highlights the essential role of incorporating fusion detection assays for all *KRAS*-wild type IMAs given the availability of effective emerging and established targeted therapies for *NRG1* and other fusions.

2026 Immunohistochemistry for Loss of Nuclear 5-Hydroxymethylcytosine (5-Hmc) and BAP1 Offers Excellent Sensitivity and Specificity in Diagnosis of Malignant Mesothelioma

David B. Chapel[1], *Aliya N Husain*[2], *Thomas Krausz*[3]. [1]Univ of Chicago Medicine, Chicago, IL, [2]University of Chicago, Chicago, IL, [3]The Univ. of Chicago Hosp, Chicago, IL

Background: Loss of nuclear 5-hydroxymethylcytosine (5-hmc), a marker of epigenetic methylation, is reported in some cancers, including melanoma, gliomas, and hematologic cancers. Retention or loss of 5-hmc has not been reported in benign or malignant mesothelial proliferations, where distinguishing benign reactive and malignant mesothelial cells determines diagnosis and affects patient management and prognosis. Loss of nuclear BAP1, in contrast, is a robust marker of malignant mesothelioma (MM), but shows limited sensitivity, particularly in sarcomatoid MM. Homozygous loss of p16 by FISH is specific for MM and can diagnose 93% of MM when paired with BAP1 IHC. However, FISH is expensive, time-consuming, and not widely available.

Design: Representative sections from 49 cases containing benign or malignant pleural or peritoneal mesothelium (10 reactive mesothelial lesions, 16 epithelioid MM, 12 biphasic MM, and 11 sarcomatoid MM) were examined by IHC for nuclear 5-hmc (scored as percentage of cells exhibiting total nuclear loss) and nuclear BAP1 (scored as retained or lost).

Results: The average degree of 5-hmc loss was significantly greater in MM (mean 72% of cells, 95% CI 64-80%) than in reactive mesothelial proliferations (mean 16% of cells, 95% CI 3-27%)(p<0.001). Furthermore, >50% loss of nuclear 5-hmc was seen in 36/39 cases

(92%) of MM (12/12 biphasic MM, 14/16 epithelioid MM, and 10/11 sarcomatoid MM), but in 0/10 reactive mesothelial lesions. The average degree of 5-hmc loss did not differ significantly between epithelioid, biphasic, and sarcomatoid MM. Within a given biphasic MM, the malignant epithelioid and sarcomatoid components both showed significantly greater 5-hmc loss than adjacent benign reactive spindled mesothelium ($p<0.001$). Nuclear BAP1 was lost in 7/12 biphasic MM, 13/16 epithelioid MM, 0/11 sarcomatoid MM, and 0/10 reactive mesothelial proliferations. Together, BAP1 loss or loss of 5-hmc in >50% of tumor cells identified 38 of 39 MM (sensitivity 97%, specificity 100%).

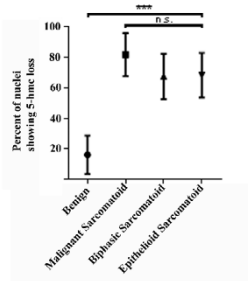

Malignant mesothelioma shows significantly greater loss of nuclear 5-hmc than benign mesothelial proliferations (dots show group mean; whiskers show 95% confidence intervals; *** $p<0.0001$; n.s. = not significant).

Conclusions: Quantitative assessment of nuclear 5-hmc, using >50% loss as a cutoff, helps confirm malignancy in challenging mesothelial lesions, including distinction of true biphasic MM from epithelioid MM with reactive spindled mesothelial cells. Additionally, evaluating 5-hmc and BAP1 together has 97% sensitivity and 100% specificity in diagnosis of MM. Accordingly, IHC for 5-hmc and BAP1 can be performed in the routine workup of suspicious mesothelial lesions, reducing the need to perform FISH for p16 loss.

2027 Strong and Diffuse TTF-1 Expression Does Not Preclude the Diagnosis of NUT Carcinoma

Athena Chen[1], *Martin Taylor*[2], *Tiffany Huynh*[1], *Marina Kem*[1], *Jochen Lennerz*[3], *Richard Kradin*[1], *Mari Mino-Kenudson*[1]. [1]Massachusetts General Hospital, Boston, MA, [2]Boston, MA, [3]Massachusetts General Hospital and Harvard Medical, Boston, MA

Background: Nuclear protein in testis (NUT) carcinoma, an aggressive carcinoma harboring chromosomal rearrangements of *NUT* resulting in NUT fusion oncoproteins, is comprised of monomorphic, primitive epithelioid cells with or without foci of abrupt keratinization. It typically exhibits squamous differentiation by immunohistochemistry (IHC); thus, it is in the differential diagnosis of poorly-differentiated carcinomas without glandular differentiation. Recently, we encountered a case of NUT carcinoma primary to the thorax in which the biopsy diagnosis of lung adenocarcinoma was suggested initially based on clinical IHC demonstrating diffuse TTF-1 expression in the tumor cells. The diagnosis of NUT carcinoma was made after detection of a *BRD4-NUT* fusion by a targeted rearrangement (fusion) assay using anchored multiplex PCR. We retrospectively screened lung adenocarcinomas diagnosed between 2000 and 2016 for cases of missed NUT carcinomas.

Design: Biopsy and subsequent autopsy tissue from the original case were further evaluated histologically and with IHC. Tissue microarrays (TMAs) constructed from 427 resected lung adenocarcinomas were evaluated with NUT IHC. Data from fusion assays performed on lung adenocarcinomas between September 2013 and February 2016 were also reviewed.

Results: The original biopsy showed nests and sheets of primitive, medium-sized epithelioid cells with scant cytoplasm and round nuclei with fine to rarely granular chromatin and prominent central nucleoli. No overt glandular or squamous differentiation was evident histologically. IHC showed strong and diffuse tumor cell positivity for TTF-1 and NUT and focal positivity for p40. The autopsy showed similar tumor morphology with focal, weak TTF-1 and NUT expression and essentially negative p40. None of the resected lung adenocarcinomas (0/427), including 56 (13.1%) cases with predominantly solid growth pattern, were positive for NUT. Furthermore, no additional NUT fusion-positive cases were found in 1389 lung adenocarcinomas tested using the fusion assay (0/1389).

Conclusions: Rare NUT carcinomas may express diffuse TTF-1, which may be aberrant expression like that seen in small cell lung carcinomas, rather than a marker of pneumocyte origin. Thus, pathologists should be judicious but not stingy in their use of NUT IHC when confronted with a primitive-appearing carcinoma, including in the lung.

2028 Is molecular testing overutilized for patients with non-small cell lung cancer?

LI Chen[1], *Arundhati Rao*[2], *Sheila Dobin*[3], *Bing Leng*[4]. [1]Baylor Scott & White, Temple, TX, [2]Scott & White Memorial Hospital, Temple, TX, [3]Baylor Scott & White, [4]Temple, TX

Background: Lung cancer is the leading cause of cancer death in the USA. Identify targetable gene mutations/alterations has become a routine care for patients with non-small cell lung cancer (NSCLC). CAP/IASLC/AMP guideline strongly recommends performing molecular testing for lung adenocarcinoma patients with advanced stage disease. Early stage testing is an institutional policy decision. CAP/IASLC/AMP also established a benchmark turnaround time (TAT) of 10 working days for the results to be available to oncologists. It is not feasible to reach TAT target if molecular tests are studied after a complete cancer staging. Performing molecular testing for all patients with NSCLC regardless of clinical staging brings the possibility of test overutilization.

Design: 764 cases diagnosed with lung NSCLC/adenocarcinoma from July 2014 to June 2017 were included in this study. PCRs were performed to detect EGFR mutations. FISH was performed to detect ALK, ROS1 and RET gene rearrangements. Electronic medical record was reviewed for patient's staging and treatment.

Results: Molecular studies were performed for all 764 cases. Among them,184 were at stage I (24.1%), 52 at stage II (6.8%),122 at stage III (16.0%), 361 at stage IV (47.3%), 45 with unknown or available stage (5.9%). 130 cases showed EGFR mutation (17.0%), 9 with ALK rearrangement (1.2%), 5 with ROS1 rearrangement (0.7%) and 2 with RET rearrangement (0.3%). The TAT was 5.4 ± 1.9 working days. Among patients with EGFR mutation, 33 were at stage I (25.4%) , 5 at stage II (3.8%), 12 at stage III (9.2%), and 65 at stage IV (50.0%). 87.7% of patients at stage IV and 41.7% of patients at stage III were treated with EGFR tyrosine kinase inhibitor, while none of patients at stage I or II received targeted therapy. For the 9 patients with ALK rearrangement, 6 patients had stage IV cancer and 4 of them were treated with ALK kinase inhibitor. 3 other patients were at stage I or stage III and did not receive targeted therapy.

Conclusions: In our hospital, only NSCLC patients at clinical stage III/IV are treated with targeted therapy, which is compliable with guideline recommendation. Molecular testing was performed for 30.9% patients (236/764) with stage I/II disease, which is potentially over-testing. Optimal process to reduce utilization is in conflict with current TAT guideline. Adjustment of guideline may be helpful to address overutilization.

2029 Value of p40/Napsin A (NapA) Dual Immunohistochemistry (IHC) in Subtyping Poorly-Differentiated Non-Small Cell Lung Cancer (NSCLC)

Athena Chen[1], *Marina Kem*[1], *Tiffany Huynh*[1], *Mari Mino-Kenudson*[1], *Amy Ly*[1]. [1]Massachusetts General Hospital, Boston, MA

Background: NSCLC patients often present with advanced stage disease. Small biopsies or cytology samples may be the only tissue available for diagnosis and molecular testing, while accurate subtyping of NSCLC is critical for treatment decision making. WHO guidelines recommend a 2-marker IHC panel for small samples to conserve tissue for molecular testing, suggesting TTF-1 as an adenocarcinoma (ACA) marker and p40 as a squamous cell carcinoma (SCC) marker. TTF-1 sensitivity for ACA is reportedly lower than NapA, while TTF-1 is expressed in >50% of LCNEC and may not discriminate LCNEC from cribriform ACA. Thus, we have developed and clinically implemented a p40/NapA IHC cocktail. In this study, we test it as part of a 3-marker panel (TTF-1 and p40/NapA cocktail) compared to a 2-marker panel (TTF-1 and p40 single stains) for subtyping small NSCLC samples.

Design: TTF-1, p40, and p40/NapA IHC was performed on 47 cases of poorly-differentiated NSCLC using cytology cell block or core biopsy material. Three pathologists each evaluated TTF-1 and p40 single stains and chose one of the following categories: ACA; NSCLC, favor ACA; NSCLC, NOS; SCC; NSCLC, favor SCC; NSCLC, possible adenosquamous; and other. The process was repeated with TTF-1 single and p40/NapA dual stains. H-scores were tabulated for each stain. Interpathologist reliability for IHC interpretation was analyzed with intraclass correlation coefficient, two-way, random effects (ICC). Fleiss' kappa was used to evaluate diagnostic concordance. Subsequent resection diagnosis, molecular data, and/or consensus diagnosis served as the gold standard diagnoses.

Results: Gold standard diagnoses were rendered in 36 cases (24 ACA, 10 SCC, and 2 adenosquamous). For the entire cohort of 47 cases, ICC for the 2-marker panel H-scores was excellent, ranging from 0.95 to 0.98 for all markers in ACA cases, and 0.86 to 0.91 for SCC cases. Fleiss's Kappa for the 2-marker panel was 0.704 ($p=0$) and for the 3-marker panel was 0.687 ($p=0$). Using the 2-marker panel, individual pathologists had diagnostic accuracy rates of 86.1%, 88.9%, and 86.1% on the 36 cases with gold standard diagnoses, while using the 3-marker panel, accuracy rates were 86.1%, 91.7%, and 88.9%.

Conclusions: Our results show good to excellent interobserver concordance and consistency with both panels. Diagnostic accuracy does not appear improved by addition of NapA in this small cohort that does not include LCNEC cases. A larger cohort study with a broader spectrum of NSCLC samples is underway.

2030 Detection of ALK and ROS1 Rearrangements Using Next Generation Sequencing in Lung Cancer Patients: Comparison Between FISH, IHC and NGS

Sergi Clavé[1], *Natalia Rodon*[2], *Lara Pijuan*[1], *Alba Dalmases*[3], *Álvaro Taus*[4], *Marta Lorenzo*[5], *Pedro Rocha*[4], *Ana M Muñoz-Mármol*[6], *Glòria Oliveras*[7], *Joaquim Bosch-Barrera*[8], *Blanca Espinet*[9], *Beatriz Bellosillo*[3], *Xavier Puig Torrus*[10], *Edurne Arriola*[4], *Marta Salido*[11]. [1]Hospital del Mar, Barcelona, [2]Biopat. Biopatologia Molecular SL., Barcelona, Spain, [3]Barcelona, [4]Hospital del Mar, [5]Hospital del Mar-Parc de Salut Mar-IMIM, [6]Hospital Germans Trias i Pujol, Badalona, Barcelona, [7]Institut Català d'Oncologia, Hospital Universitari Dr. Josep Trueta, [8]Institut Català d'Oncologia, Hospital Universitari Dr. Josep Trueta, Girona, [9]IMIM-Hospital del Mar, Barcelona, Catalonia, [10]Biopat, Biopatologia Molecular SL, Barcelona, [11]Hospital del Mar, Barcelona

Background: Detection of *ALK* and *ROS1* rearrangements in non-small cell lung cancer (NSCLC) is required for directing patient care. While fluorescence *in situ* hybridization (FISH) and immunohistochemistry (IHC) have been established as gold standard methods, next generation sequencing (NGS) platforms are called to be at least equally successful, but also more compatible with multiplexing and diagnostic workflows. Our aim was to investigate the performance of NGS in the detection of rearranged cases.

Design: Thirty NSCLC samples were selected retrospectively from our database (n=2.399) based on previous ALK (n=25) and ROS1 (n=5) FISH results (positive or inconclusive) and material availability. Cases were tested by both FISH (Abbott Molecular) and IHC (D5F3,Ventana) in paraffin blocks, and were reviewed centrally to determine the tumor area. Both DNA and RNA were manually extracted from paraffin sections. Ion Torrent sequencing technology with Oncomine™ Focus Assay (ThermoFisher Scientific) were applied using 10 ng of DNA and RNA from each sample.

Results: Patient's characteristics were: median age 62 years, 57% were males and adenocarcinoma (ADC) was the most common histology (72%). Regarding FISH results, 14 cases had split signals, 14 had isolated 3' signals, and two had negative FISH patterns with isolated 5' signals. Testing with IHC, four out of the 30 cases were negative: two cases with isolated 5' signals and two with isolated *3'ALK* signals (discordance FISH vs. IHC). Remarkably, tumor material came from small biopsies in 18 cases and from cytology specimens in six cases. Ten cases (33%) were non-evaluable by NGS due to insufficient sequencing coverage (seven were small biopsies with low DNA and RNA input). NGS technology detected positive *ALK* and *ROS1* fusions in 75% of the assessable samples, being *EML4-ALK* (E13;A20) and *EZR-ROS1* (E10;R34) the most prevalent. Regarding the five cases with negative NGS result: two showed isolated 5'*ALK* signals; two presented isolated *3'ALK* signals although IHC test was negative; and one case had borderline FISH positive result and was re-classified as non-rearranged.

Conclusions: NGS technology for detecting *ALK* and *ROS1* rearrangements in NSCLC could be considered as a screening test although the success rate is closely related to the correct evaluation of the initial amount of tumor tissue, particularly in small biopsies. NGS technology could be used as an additional molecular technique for cases with inconclusive or discordant FISH/IHC results.

2031 Concordance Levels of PD-L1 Expression by Immunohistochemistry, mRNA In Situ Hybridization, and Outcome in Lung Carcinomas

Joseph D Coppock[1], *Ashley Volaric*[2], *Anne Mills*[2], *Alejandro A. Gru*[1]. [1]University of Virginia, Charlottesville, VA, [2]Charlottesville, VA

Background: Targeted inhibition of programmed death-ligand 1 (PD-1) and its ligand (PD-L1) has emerged as first-line therapy for patients with advanced non-small cell lung cancer. While tumors with high PD-L1 expression have demonstrated improved clinical outcomes with anti-PD-1/PD-L1 directed therapy, its use as an exclusionary predictive biomarker has been complicated by robust responses in some patients with low levels of expression. Furthermore, reported levels of PD-L1 expression in any given lung cancer histology vary widely, and discrepancies between expression exist with the use of different antibodies.

Design: We compared PD-L1 expression by immunohistochemistry (IHC) (Ventana, SP263) and RNA in situ hybridization (ISH) (RNAScope, Advanced Cell Diagnostics) in 112 lung cancer cases by tissue microarray (TMA): 51 adenocarcinoma, 42 squamous cell carcinoma, 9 adenosquamous carcinoma, 5 carcinoid tumor, 3 undifferentiated large cell carcinoma, 1 large cell neuroendocrine carcinoma, and 1 small cell carcinoma. At least 1% tumor cell staining was considered positive for both modalities.

Results: An overall positive concordance of only 60% (67/112) was found between PD-L1 IHC and RNA ISH, with 50% (56/112) positive by IHC and 50% (56/112) positive by RNA ISH. 20% (22/112) of cases were positive by RNA ISH but negative by IHC. Conversely, 21% (23/112) were positive by IHC but negative by RNA ISH. There was no significant stratification of PD-L1 positivity by histologic subtype. A trend of increased PD-L1 positivity by RNA ISH versus IHC in stage I cancers was identified, however was not statistically significant (50% (27/54) by IHC and 64% (35/55) by RNA ISH, p=0.18). No significant difference in survival was identified, with an average of 5.3 months in IHC positive cases and 5.2 months in RNA ISH positive cases.

Conclusions: Discordance exists between detectable PD-L1 RNA levels and protein expression in non-small cell lung cancers. While the biologic implications are unclear, this may represent undetectable protein expression in early stage disease or alternatively deregulation of RNA in later stage disease. Future work comparing prediction of response to anti-PD-1/PD-L1 directed therapies in IHC versus RNA ISH positive tumors is warranted.

2032 A Single Institution Study to Compare the 7th and 8th Editions of the AJCC TNM Classification of Lung Tumors in Typical and Atypical Carcinoid Tumors of the Lung

Josephine Dermawan[1], *Carol Farver*[1]. [1]Cleveland Clinic, Cleveland, OH

Background: Pulmonary carcinoid tumors are relatively uncommon and have an indolent clinical course compared to non-small cell lung carcinomas. The applicability of the AJCC TNM classification system in predicting long-term recurrence and survival in carcinoid tumors is unclear and controversial. We report a large, single institution study of carcinoid tumors and correlate pathologic stage (7th and 8th editions) with clinical outcome (recurrence).

Design: We reviewed all surgical lung resection cases from 1995-2013 with a diagnosis of primary lung carcinoid tumor. We collected pathologic parameters including tumor size, nodal status, histology (typical versus atypical carcinoid), and staged these tumors based on the 7th and 8th edition of the *AJCC* TNM Classification of Lung Tumors. Clinical data collected included demographics, smoking history, recurrence, and survival. We excluded patients with concurrent or preexisting malignancies and cases with positive resection margins.

Results: We identified 199 carcinoid tumor cases (73 male, 126 female; aged 10-81). Among all typical carcinoid cases (187), 25 (13%) had positive nodal status (17 [9%] N1, 8 [4%] N2). Among atypical carcinoid cases (12), 3 (25%) had positive nodal status (2 [17%] N1, 1 [8%] N2). Clinical follow-up information was available for 169 cases. Only 13 cases (7.7%) experienced recurrence. Five (3.0%) patients died with metastatic carcinoid tumor. Patients with atypical carcinoid tumors were significantly more likely to experience tumor recurrence compared to those with typical carcinoid tumors (log-rank $P < 0.0001$, Figure 1). Staging the tumors based on the TNM 8th edition correlated with likelihood of tumor recurrence more significantly than that based on the TNM 7th edition ($P < 0.0001$ vs $P = 0.0599$, Figure 2). The type of resection procedure and smoking history had no correlation with clinical outcome.

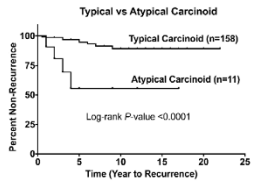

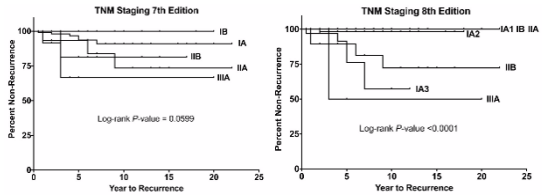

Conclusions: Pulmonary carcinoid tumors have an excellent non-recurrence rate. Classifying carcinoid tumors based on typical versus atypical histology types is the best predictor of tumor recurrence. The TNM 8th edition de-emphasized main bronchus involvement and placed more emphasis on tumor size in staging and was superior in predicting recurrence compared to the TNM 7th edition.

2033 Ex Vivo Lung Perfusion Induces a Time and Perfusate Dependent Molecular Repair Response in Explanted Lungs

Peter Dromparis[1], *Nader Aboelnazar*[2], *Siegfried Wagner*[2], *Sayed Himmat*[2], *Christopher White*[2], *Sanaz Hatami*[2], *Jessica G Luc*[2], *Darren Freed*[2], *Jayan Nagendran*[2], *Michael Mengel*[2], *Benjamin Adam*[2]. [1]Edmonton, AB, [2]University of Alberta, Edmonton, AB

Background: Acute lung injury (ALI) secondary to lung explant and cold static preservation (CSP), the current standard of preservation, result in only 20% of donated lungs being transplanted. Ex vivo lung perfusion (EVLP) shows promise in expanding the suitable lung pool, however the mechanisms underlying this empirical success are poorly understood. The aim of this large animal study is to assess the utility of using molecular markers for quantifying ALI and monitoring ex vivo repair.

Design: 167 swine lung samples were collected in vivo (IV; n=25) and at 0 and 12 hours of CSP (n=22) or 0, 6, and 12 hours EVLP (n=114) with either acellular (AC), packed red blood cells (pRBCs) or whole blood (WB) perfusates, as well as either positive or negative pressure ventilation strategies. Functional and histological parameters of ALI were assessed. 48 previously described ALI genes were assessed from FFPE samples using NanoString nCounter. Data were analyzed with nSolver and R.

Results: Volcano plot analysis identified 28 "repair" genes significantly upregulated and 6 "injury" genes significantly downregulated by 12hrs of EVLP (Figure 1). Both repair and injury gene sets significantly correlated with histological and functional parameters using Spearman's coefficient (Table 1), which was independently confirmed with principal component analysis. Repair gene sets were significantly upregulated and injury gene sets downregulated after 12 hours of EVLP (p<0.001 and p<0.001, respectively), but not CSP (p=0.438 and p=0.652, respectively). Time course analysis showed repair gene expression significantly increased at 6hrs (p<0.001), without further benefit at 12hrs (p=0.505). In contrast, injury gene expression was significantly reduced at 12hrs (p<0.001), but not 6hrs (p=0.161). pRBCs and WB significantly reduced injury gene set expression compared to AC (p=0.008 and p=0.038, respectively), but the change in repair gene set expression did not differ between pRBC and AC (p=0.315), or WB and AC (p=0.193). The change in repair and injury gene set expression did not differ between ventilation strategies (p=0.206 and p=0.675, respectively).

Figure 1

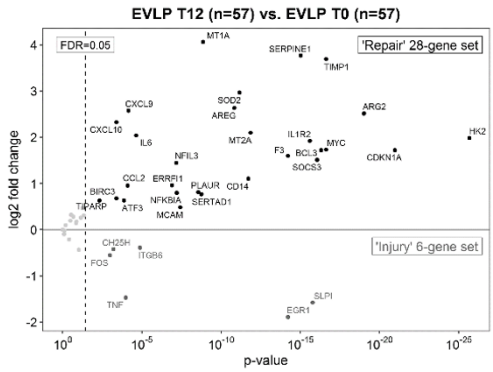

Table 1

	'Repair' 28-gene set		'Injury' 6-gene set	
	Spearman's rank correlation coefficient	p-value	Spearman's rank correlation coefficient	p-value
Functional parameters				
PaO_2/FiO_2 ratio	**0.302**	**<0.001**	**-0.501**	**<0.001**
Lung compliance	**0.200**	**0.027**	**-0.477**	**<0.001**
Pulmonary artery pressure	-0.078	0.395	**0.321**	**<0.001**
Pulmonary vascular resistance	-0.148	0.105	**0.410**	**<0.001**
Pulmonary airway pressure	**-0.189**	**0.037**	**0.269**	**0.003**
Histological parameters				
Hemorrhage	**0.196**	**0.011**	-0.140	0.069
Perivascular neutrophils	0.130	0.091	0.047	0.541
Alveolar inflammation	-0.133	0.085	0.150	0.052
Interstitial neutrophils	**-0.199**	**0.009**	0.128	0.096
Interstitial edema	**-0.329**	**<0.001**	0.124	0.108
Interstitial inflammation	**-0.365**	**<0.001**	**0.215**	**0.005**

Conclusions: EVLP induces a molecular repair response that correlates with clinically utilized histological and functional parameters. This response is time dependent and is influenced by the perfusate, suggesting prolonged EVLP with cellular perfusates may offer beneficial tissue repair over current preservation strategies.

2034 STAT6 Expression in Adenofibroma of the Lung Supports Classification as Intrapulmonary Solitary Fibrous Tumor

Liz Edmund[1], *Nimesh R Patel*[2], *Ece Uzun*[3], *Kara A Lombardo*[2], *Evgeny Yakirevich*[2], *Shamlal Mangray*[2], *Bassam Aswad*[4]. [1]Brown University/ Rhode Island Hospital/ Lifespan, Providence, RI, [2]Rhode Island Hospital, Providence, RI, [3]Rhode Island Hospital, [4]Rhode Island

Background: Adenofibroma (AF) is a rare intrapulmonary biphasic tumor (Figure 1A and 1B). Morphologically, AFs resemble phyllodes tumors of the breast (Figure 1C) with a spindle cell stroma that resembles solitary fibrous tumor (SFT) (Figure 1D). Immunohistochemical (IHC) expression of CD34 in AF has led some to suggest that AFs represent a pseudopapillary variant of SFT. Recently, STAT6 IHC expression and *NAB2-STAT6* fusion has been reported in a series of AFs supporting the notion that they are a variant of SFT with an intratumoral epithelial component. We report our experience in a series of AFs.

Design: Archival cases with spindle cell stromal features of SFT and an epithelial component fulfilling the description of AF without attachment to the pleura were retrieved from our surgical pathology files. Clinical data including demographic information, presentation, imaging and follow-up data were collected. Gross and microscopic features were reviewed. Representative sections from each case were selected for IHC with antibodies to CD34, STAT6 and TTF-1 with appropriate positive and negative controls. AF cases were compared to a group of hybrid SFTs (HTs) with attachment to pleura and typical SFTs. The presence of fusion genes was assessed on FFPE tissue from AFs and a subset of the other cases by next-generation sequencing (NGS) using anchored multiplex PCR technology.

Results: Five cases fulfilled AF criteria and were comapred to 2 HTs and 4 typical SFTs. The clinical, imaging and pathologic features of the tumors are summarized in the table. Diffuse (Diff) strong CD34 and STAT6 IHC positivity were present in the stromal cells and TTF-1 positivity in the epithelium (Epi) of all 5 AFs (Figure 2). *NAB2-STAT6* fusion was present in all AFs (4 of low quality with lower level of supporting reads from ≥ 10 years ago). The 2 HTs were CD34 and STAT6 diffusely positive with TTF-1 positive intratumoral epithelium. Of the two HTs tested by NGS from 4 years ago, one was positive for *NAB2-STAT6* fusion and the other was negative (Table). All typical SFTs were STAT6 diffusely positive by IHC, 3 diffusely CD34 positive and 1 focally (foc) positive. One of these typical SFTs had entrapped TTF-1 positive epithelium even though it was a completely exophytic lesion.

FOR TABLE DATA, SEE PAGE 763, FIG. 2034

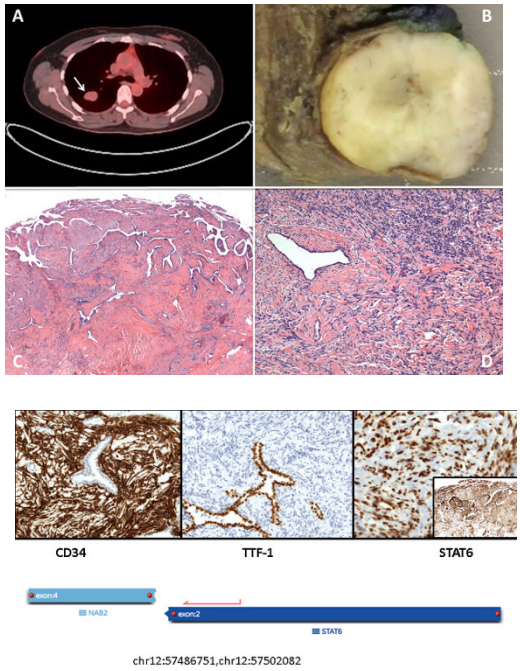

Immunohistochemical profile and *NAB2-STAT6* fusion by NGS in case 3 of the adenofibroma group

Conclusions: This study provides additional cases that support the concept that AFs of the lung represent intrapulmonary SFTs that incorporate pulmonary epithelium during the proliferative process resulting in the characteristic biphasic morphology.

2035 Correlation of Nuclear Grade and Necrosis in Biopsy vs. Resection of Malignant Epithelioid Mesothelioma

Mansooreh Eghtesad[1], *Aliya N Husain*[2]. [1]Chicago, IL, [2]University of Chicago, Chicago, IL

Background: Malignant mesothelioma (MM), a disease with limited therapeutic options, is usually diagnosed by biopsy. Histologic typing and staging have been used as prognostic factors and to make treatment decisions. The recently proposed nuclear grading system and presence of necrosis have been shown to predict survival in patients with pleural epithelioid MM. In this study we compared the pathologic findings and nuclear grading among biopsy specimens which were followed by resection in both pleural and peritoneal MM.

Design: Of a total of 278 patients diagnosed with pleural MM in the last three years, 52 had a biopsy followed by resection. At the time of diagnosis, pathologic tumor characteristics including histologic type, grade and necrosis had been documented. For this study, the electronic pathology reports were reviewed and compared for each patient.

Results: Of 52 cases, 4 were diagnosed with biphasic malignant mesothelioma in either resection or both original biopsy and resection, which were excluded from study. Of the remaining 48 epithelioid malignant mesothelioma cases, 36 had same nuclear grade (36/48, 75%) in biopsy versus resection while 12 cases had different grades (12/48, 25%). Most of these were upgraded in the following resection specimen, either from grade I to II or III, or grade II to III (11/12, 95%) and only one case had been downgraded from grade II on biopsy to grade I on resection. Of the 12 cases, one was followed by two separate resections with the time interval of 4 years between resections, which was graded as grade I on biopsy and first resection and grade II on second resection.

Necrosis was present in 12 cases (12/48, 25%), of which 4 cases had necrosis only on resection (4/12, 33%), 7 cases had necrosis on both biopsy and resection (7/12, 58%) and 1 case was reported to have necrosis only on biopsy (1/12, 8%). Therefore overall, in 43 cases (43/48, 89%), presence or absence of necrosis was concordant in biopsy and following resection.

Conclusions: We found that there is good correlation in nuclear grading and necrosis between biopsy and resection specimens. Since studies have shown that these two factors independently predict overall survival in epithelioid MM, by incorporating these in biopsies, we can stratify patients into prognostic groups and gauge the treatment options accordingly.

2036 YAP Protein Expression in Non-Small Cell Lung Carcinoma (NSCLC): Prognosis Varies with Localization of YAP Overexpression

Tony El Jabbour[1], *Siddhartha Dalvi*[2], *Silva Kristo*[3], *Christine Sheehan*[4], *Timothy Jennings*[5], *Bhaskar Kallakury*[6]. [1]Albany Medical Center, Albany, NY, [2]Delmar, NY, [3]Georgetown University, [4]Albany Medical College, Albany, NY, [5]Loudonville, NY, [6]Georgetown Univ Hosp, Washington, DC

Background: YAP (Yes-associated protein) is a transcriptional activator that is negatively regulated in the Hippo pathway that regulates organ size during growth and development. Overexpression of YAP has been observed in several human tumors, including non-small cell lung carcinoma. Our study is the first to correlate YAP expression with NSCLC subtype and to explore the use of YAP IHC as a prognostic marker in NSCLC

Design: Formalin-fixed, paraffin embedded sections from 118 NSCLC, including 34 squamous cell carcinomas (SCC), 59 adenocarcinomas (AC), and 25 either pure bronchioloalveolar carcinomas (BAC) or AC with BAC features were immunostained by an automated method using YAP (D8H1X) XP® Rabbit mAb (Cell Signaling). Cytoplasmic (cYAP) and nuclear (nYAP) immunoreactivity was scored based on staining intensity (weak, moderate, intense) and percentage of positive cells (focal <= 10%, regional 11-50%, diffuse >50%) in the tumor (T), adjacent benign (B) epithelium and within the tumor microenvironment (cYAPtm and nYAPtm, respectively) in each case. Results were correlated with clinicopathologic variables

Results: Intense diffuse cYAP protein was expressed in 23% tumors and correlated overall with tumor type [32% BAC vs 31% AC vs 3% SCC, p=0.005], tumor stage [31% I vs 0% II vs16% III vs 0% IV, p=0.026], and within the AC subgroup with disease recurrence [60% recurrent vs 26% non-recurrent, p=0.037]. cYAPtm was noted in 30% cases and correlated with tumor type [62% SCC vs 23% AC vs 4% BAC, p<0.0001], male gender (p=0.003) and high tumor grade (p=0.015). nYAP protein was overexpressed in 34% tumors and correlated with tumor size >3.0cm overall (p=0.012) and within the SCC subgroup with LN+ status (p=0.001), high tumor grade (p=0.003) and tumor size >3.0cm (p=0.031). nYAPtm was noted as essentially the same expression as cYAPtm in each of the 30% cases. On multivariate analysis, positive lymph node status (p=0.002) independently predicted overall survival.

Conclusions: YAP overexpression and its impact vary with tumor cell subcellular localization; cYAP is associated with BAC subtype and early stage overall, and correlates with disease recurrence within the AC subgroup, while nuclear localization is associated with a more aggressive behavior. YAP overexpression within the tumor microenvironment is associated with squamous differentiation, male gender and high tumor grade regardless of subcellular localization. Further study of YAP protein expression and its potential role in NSCLC appears warranted.

2037 Clinical Significance of Morphological Patterns of Micropapillary Lung Adenocarcinoma: Classical and Filigree Patterns

Katsura Emoto[1], *Rania G. Aly*[1], *Joseph Montecalvo*[1], *Natasha Rekhtman*[1], *Takashi Eguchi*[1], *Kay See Tan*[1], *Prasad S Adusumilli*[1], *William Travis*[1]. [1]Memorial Sloan Kettering Cancer Center, New York, NY

Background: The classical micropapillary (MP) pattern is defined in the 2015 WHO classification as tumor cells growing in papillary tufts forming florets that lack fibrovascular cores and is associated with poor prognosis. We have observed the filigree pattern as a newly recognized morphologic manifestation of MP lung adenocarcinoma (LADC). Recognition of this histologic subtype is critically important so we sought to investigate the clinicopathological significance of morphological patterns of MP LADC.

Design: Microscopic review of 68 Stage I MP predominant LADC evaluated the extent of classical and filigree MP patterns. Classical MP consisted of tumor clusters within glandular and/or air spaces (Fig.1) or small clusters infiltrating slit-like spaces within fibrous stroma. Filigree MP is composed of tumor cells growing in delicate lace-like narrow stacks of tumor cells where attachments to alveolar walls are frequently visible (Fig.2). Cases were divided into filigree or classical predominant cases. Filigree cases were further categorized as filigree-low or filigree-high at the median. Overall survival (OS) was estimated by the Kaplan-Meier approach and compared between groups using log-rank test. Cumulative incidence of recurrence (CIR) and lung cancer-specific cumulative incidence of death (LC-CID) were estimated by competing risk framework and compared between groups using Gray's test.

Results: We found 33 filigree and 35 classical predominant MP cases. The patients with predominant filigree pattern were associated with smoking history (*p=0.031*) and necrosis (*p=0.001*). No prognostic differences were found between filigree and classical MP patterns (filigree vs. classical: 5-year CIR, 40% vs. 29%, *p=0.521*; 5-year LC-CID, 24% vs. 13%, *p=0.698*; 5-year OS, 64% vs. 62%, *p=0.488*). However, high-filigree cases showed worse prognoses than low-filigree ones (high-filigree vs. low-filigree: 5-year CIR, 57% vs. 31%, *p=0.208*; 5-year LC-CID, 50% vs. 13%, *p=0.067*; 5-year OS, 21% vs. 87%, *p=0.001*).

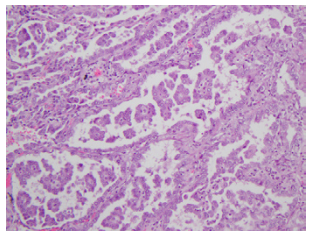

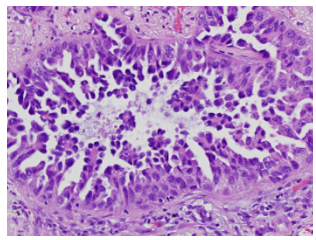

Conclusions: We propose to add the filigree pattern to the classical pattern as an important addition to the morphologic spectrum of the MP subtype. This is supported by our data demonstrating that the filigree pattern is associated with the same poor prognosis as the classical MP pattern.

2038 The Impact of C4d Testing on Tissue Adequacy in Lung Transplant Surveillance

Cynthia Forker[1], *Sarah Hackman*[1], *Daniel D Mais*[1]. [1]University of Texas Health Science Center at San Antonio, San Antonio, TX

Background: Surveillance transbronchial biopsies are routinely used to assess lung allograft rejection, since both asymptomatic and non-specific presentations are common. Although the criteria for diagnosing and grading acute cellular rejection have been well-established, the morphological findings associated with antibody mediated rejection are variable and non-specific. To increase the sensitivity for antibody mediated rejection, a portion of a biopsy can be used for C4d immunofluorescence testing, in combination with routine histology and donor specific antibodies. When the number of alveolar pieces in a routine biopsy is small, the relative utility of sending one piece for C4d testing is unclear.

Design: Pathology reports of 1400 surveillance transbronchial lung forceps biopsies from 2008 to 2017 were reviewed to obtain the number of pieces of alveolar parenchyma in each case. Based on

a standard definition of adequacy as five pieces of well-expanded alveolar parenchyma, reports were grouped according to whether an adequate number of pieces were submitted for morphological evaluation. We considered 4 pieces as a "marginal" sample and 3 or less as an "inadequate" sample. Of the cases considered marginal, we determined whether pieces withheld for C4d immunofluorescence testing could have instead been used to obtain an adequate specimen for morphological evaluation.

Results: Of the 1400 biopsies, 653 specimens had 5 or more pieces of alveolar parenchyma. 747 specimens were submitted with less than 5 pieces, with 290 of those considered marginal. In all 290 marginal cases, a piece was withheld for C4d immunofluorescence testing. In about 21% of all cases, the piece withheld for C4d testing was the difference between a "marginal" versus "adequate" evaluation.

Conclusions: About 21% of specimens would have the recommended 5 pieces of alveolar parenchyma if not for the withholding of pieces for C4d testing. Over the span of 10 years, 290 such cases were recorded at our institution. Given this nontrivial impact, it is unclear if C4d testing should be performed on surveillance transbronchial biopsies when the number of pieces in the specimen is marginal.

2039 Genomic Alterations, Microsatellite Instability and Tumor Mutational Burden in 21 Cases of Primary Pulmonary Sarcomas

Yelena Fudym[1], *Jeffrey S Ross*[2], *Laurie Gay*, *Julia A Elvin*[3], *Jo-Anne Vergilio*[4], *James Suh*[5], *Shakti Ramkissoon*[6], *Eric Severson*[7], *Sugganth Daniel*[8], *Siraj Ali*[3], *Alexa B Schrock*[10], *Jon Chung*[8], *Vincent A Miller*[8], *Philip M Stephens*[8], *Robert Corona*[11]. [1]SUNY Upstate Medical University, Syracuse, NY, [2]Foundation Medicine, Cambridge, MA, [3]Foundation Medicine, Inc, Cambridge, MA, [4]Foundation Medicine, Inc, Cambridge, MA, [5]Foundation Medicine, Inc, Morrisville, NC, [6]Foundation Medicine, Morrisville, NC, [7]Foundation Medicine, Inc, Morrisville, NC, [8]Foundation Medicine, [9]Cambridge, MA, [10]Foundation Medicine, Cambridge, MA, [11]SUNY Upstate Medical Univ, Syracuse, NY

Disclosures:
Jeffrey Ross: *Employee*, Foundation Medicine, Inc.
Laurie Gay: *Employee*, Foundation Medicine, Inc.
Jo-Anne Vergilio: *Employee*, Foundation Medicine, Inc.
James Suh: *Employee*, Foundation Medicine, Inc.
Shakti Ramkissoon: *Employee*, Foundation Medicine, Inc.
Eric Severson: *Employee*, Foundation Medicine, Inc.
Siraj Ali: *Employee*, Foundation Medicine, Inc.
Alexa Schrock: *Employee*, Foundation Medicine, Inc.
Jon Chung: *Employee*, Foundation Medicine, Inc.
Philip Stephens: *Employee*, Foundation Medicine, Inc.

Background: Pulmonary sarcomas (PSRC) are uncommon malignancies which typically pursue an aggressive clinical course. We utilized comprehensive genomic profiling (CGP) to search for novel treatment options in patients with clinically advanced disease.

Design: CGP was performed on hybridization-captured, adaptor-ligation based libraries for up to 315 cancer-related genes on a series of 21 cases of PSRC with 17 of the PSRC also undergoing RNA sequencing to enable expanded gene fusion detection. All classes of genomic alterations (GA) including base substitutions, indels, fusions and copy number changes were assessed simultaneously from a single sample. Clinically relevant GA (CRGA) were defined as GA associated with drugs on the market or under evaluation in mechanism driven clinical trials. Total mutational burden (TMB) was determined on 1.1 Mb of sequenced DNA as previously described.

Results: There were 10 sarcoma NOS, 5 pulmonary artery intimal sarcomas, 4 pleomorphic/MFH sarcomas, 1 primary inflammatory myofibroblastic tumor (IMT) and 1 primary solitary fibrous tumor (SFT) cases. There was 1 stage I, 1 stage II, 9 stage III and 10 Stage IV tumors. The patients had a median age of 58 years (range 33 to 81 years). There were 7 female and 14 male patients. The mean number of GA per sarcoma was 5.8. Notable alterations not considered actionable presently included *TP53* 47%, *CDKN2A* 36%, *CDKN2B* 25% and *RB1* 13%. CRGA included *PDGFRA*, *RICTOR*, *CDK4* and *KIT* all at 11%. When additional CRGA in *EGFR*, *TSC2*, *ALK* and *BRAF* each at 5%, a total 0f 10 (48%) of PSRC featured at least 1 CRGA. The one case with an *ALK* fusion, a patient with IMT initially localized to the lung only and diagnosed as a primary lesion. The mean TMB in the PSRC was 8.3 mutations per Mb with 14% having TMB of >10 mut/Mb and 10% having TMB > 20 mut/Mb. MSI status was available for 9 (43%) of the PSRC cases and all (100%) were MSS (stable) and negative for MSI high. Assessment of therapeutic intervention and responses to targeted and immunotherapies is on-going.

Conclusions: PSRC is characterized by a relative high frequency of GA including driver mutations or fusions in tyrosine kinase and cell cycle regulatory genes. In addition, this study also identified a significant proportion of PSRC that feature an intermediate or high TMB indicating the potential for use of immunotherapies for these patients. Further study of CGP to assist in management of patients suffering from this rare form of pulmonary malignancy appears warranted.

2040 Inter-Pathologist Diagnostic Agreement for Non-Small Cell Lung Carcinomas (NSCLC) Using Current and Recent Classifications

William Funkhouser[1], *Neil Hayes*[2], *Dominic T Moore*[2], *Jason P Fine*[2], *Keith Funkhouser*[3], *Philip T Cagle*[4]. [1]Chapel Hill, NC, [2]University of North Carolina, Chapel Hill, [3]University of Wisconsin, Madison, [4]Houston Methodist Hospital, Houston, TX

Background: Estimating inter-pathologist diagnostic agreement (IPDA) should allow pathologists to improve diagnostic criteria and classifications. IPDA can be estimated using Cohen's kappa, *k*. Published *k* for non-small cell lung carcinoma (NSCLC) diagnosis using the 1981 WHO classification found mean *k*=0.25 using H&E only, and mean *k*=0.39 using H&E/mucin stains. Published *k* for NSCLC diagnosis using the 2004 WHO classification found mean *k*=0.25-0.31 using H&E only, and mean *k*=0.45 using H&E, mucin, and TTF-1/P63/P40 immunostains. We sought to compare IPDA for diagnoses made with H&E stains only, vs. diagnoses made with H&E/mucin/IHC stains, using 4 published NSCLC classifications, and to compare IPDA across pathologist practice settings, practice durations, pulmonary pathology expertise, and lung carcinoma case volumes.

Design: A web-based survey tool presented core biopsy images of 54 NSCLC cases to 22 participant pathologists, initially as H&E-only images, followed by a panel of H&E, mucin, and IHC (CK5/6, P63, TTF-1, Napsin A) images. Each case was diagnosed according to published 2004 WHO, 2011 IASLC, and 2015 WHO NSCLC classifications. Cohen's kappa was calculated for the 231 observer pairs as an estimate of IPDA. Kappa distributions (mean, 95% CI) were compared for the 4 NSCLC classifications, for H&E-only and H&E/mucin/IHC diagnoses, and for the participant pathologists' different practice settings, practice durations, pulmonary path expertise, and lung carcinoma case volumes.

Results: IPDA is higher for each classification when H&E is supplemented with mucin and IHC stains, and is higher for these H&E/mucin/IHC diagnoses using the 2015 classification than with the 2011 or 2004 classifications (Figure 1). For the current 2015 WHO classification using H&E/mucin/IHC stains, IPDA improved with pulmonary pathology expertise, with >6 years practice experience, and with >100 new lung carcinoma diagnoses/year, but was not different by practice setting (community, academic) (Figure 2).

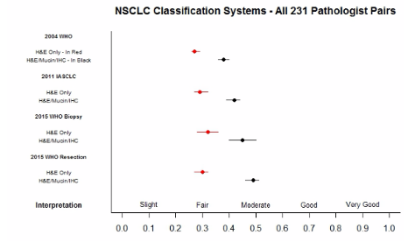

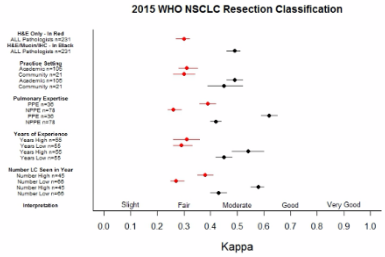

Conclusions: IPDA for each of the 4 NSCLC classifications is higher when H&E is supplemented with mucin and IHC stains. IPDA using H&E/mucin/IHC stains is higher for the WHO 2015 NSCLC classification than for the 2004 or 2011 classifications. Using the 2015 classification and H&E/mucin/IHC stains, IPDA is higher for pathologists who identify as pulmonary pathology experts, have more years of experience, and/or who see a higher number of lung cancer cases, but is the same for community and academic practices.

2041 Influence of Specimen Characteristics on PD-L1 Testing Results in Non-Small Cell Lung Cancer: A Retrospective Study

Andréanne Gagné[1], *Emily Wang*[2], *Nathalie Bastien*[3], *Michèle Orain*[4], *Patrice Desmeules*[5], *Sylvain Pagé*[6], *Sylvain Trahan*[7], *Christian Couture*[8], *Philippe Joubert*[9]. [1]Laval University, Quebec City, PQ, [2]Laval University, Quebec City, QC, [3]Institut Universitaire de Cardiologie et de Pneumologie de Québec Research Center, Quebec City, QC, [4]Institut Universitaire de Cardiologie et de Pneumologie de Québec Research Center, Quebec City, QC, [5]Quebec Heart and Lung Institute, QC, [6]Institut Universitaire de Cardiologie et de Pneumologie de Québec Research

Center, Quebec City, QC, [7]IUCPQ, Quebec City, QC, [8]IUCPQ-UL (Hopital Laval), Quebec City, PQ, [9]Institut de Cardiologie et de Pneumologie de Québec, Quebec, QC

Background: Checkpoint inhibitors targeting PD-1/PD-L1 axis have become the new standard of care for patients diagnosed with advanced non-small cell carcinoma (NSCLC) negative for a targetable mutation or rearrangement. For some molecules, the level of PD-L1 staining by tumor cells determines the eligibility of patients to treatment. However, several questions remain regarding the impact of preanalytical factors on PD-L1 expression assessment, such as the specimen type, the number of viable tumor cells and the primary vs metastatic nature of the sampled tumor.

Design: A retrospective cohort composed of 1359 consecutive patients diagnosed with NSCLC and tested for PD-L1 between September 2016 and April 2017 was reviewed. PD-L1 immunostaining was performed using 22C3 antibody clone. PD-L1 status was measured as the percentage of tumor cells with at least focal positive membranous staining. Pathology reports were reviewed to collect patient and tumor characteristics, specimen type and quality, and PD-L1 results. Descriptive statistics and chi square tests were used.

Results: 1174 patients had an evaluation of PD-L1 on a specimen with sufficient tumor cell content (> 100 tumor cells) and 853 of them had PD-L1 staining: 381 (32.4%) in 1 to 49% of tumor cells and 472 (40.2%) in more than 50% of tumor cells. PD-L1 staining was higher in distant and lymph node metastases, both in cytology and tissue specimens. Overall, cytology showed higher PD-L1 expression than tissue specimens (46.4% vs 36.8% of patients with >50% PD-L1 positive tumor cells). However, when stratifying for primary and metastatic lesions, the staining was similar. Also, 185 patients had an evaluation of PD-L1 in specimens despite limited tumor cell content (< 100 cells) and PD-L1 staining was lower for each sample site and specimen type.

		% PD-L1 stained tumor cells				Mean % PD-L1 stained tumor cells	
Specimen type	Sampled site	< 1% n (%)	1-49% n (%)	>50% n (%)	p value	>100 cells	<100 cells
Cytology	Lung	8 (28.6)	9 (32.1)	11 (39.3)	0.075	37.0	27.1
	Lymph node	65 (30.4)	54 (25.2)	95 (44.4)		41.6	34.5
	Distance metastasis	11 (14.7)	20 (26.7)	44 (58.7)		50.0	33.8
Tissue (biopsy + surgery)	Lung	181 (29.7)	222 (36.4)	207 (33.9)	0.003	33.5	28.1
	Lymph node	19 (20.2)	24 (25.5)	51 (54.3)		48.7	32.0
	Distance metastasis	36 (23.7)	52 (34.2)	64 (42.1)		37.8	23.1

Conclusions: Our results show that while PD-L1 expression is higher in cytology specimens, staining is similar between cytology and tissue specimens when compared by sampled sites. Our results also suggest that cytology specimens are likely suitable for PD-L1 testing, although this will require further validation. We also confirmed the importance of tumor cell content for proper evaluation of patients in a wide range of NSCLC specimens.

2042 Programmed Death Ligand1 (PD-L1) expression in a cohort of 39 pleomorphic pleural malignant mesotheliomas (MMs), compared to conventional mesotheliomas

Francoise Galateau Salle[1], *Nolwenn Le Stang*[2], *Francesca Damiola*[2], *Experts MESOPATH National Center*[3], *Jean-Claude Pairon*[4], *Arnaud Scherpereel*[5], *sylvie lantuejoul*[6]. [1]Mesopath, Caen, [2]Centre Léon Bérard, Lyon, France, [3]Mesopath, [4]Inserm U955, Equipe 4, DHU A-TVB, Faculté de Médecine Créteil, France, Creteil, France, [5]University Hospital, Lille, France, [6]Centre Leon Berard, Lyon, Rhone Alpes Auvergne

Background: Pleomorphic mesothelioma (PM) is a rare and very aggressive tumor with no effective treatment to date. The 2015 WHO classification has considered this subtype to be classified as an epithelioid mesothelioma with a dismal prognosis close to the survival of sarcomatoid type. Immunotherapy against checkpoints inhibitors such as PD-L1 has recently showed encouraging results in pleural malignant mesothelioma trials. We aimed to investigate PD-L1 expression in PM and to perform a comparative study with conventional MMs. Additionally, we are taking the advantages of the HTG EdgeSeq Oncology Biomarker Panel 2465 genes to retrospectively characterize the immunologic profiles between PM samples and the conventional epithelioid (EM) and sarcomatoid (SM) types.

Design: 39 formalin-fixed paraffin-embedded pleural PMs were retrieved from the MESOPATH files, and compared to 20 EMs and 20 SMs and were strictly ascertained according to the French standardized procedure of certification. PD-L1 (clone SP-263) expressions were performed on the automate Benchmark of Ventana and evaluated immunohistochemically by percent of tumor cells staining. According to previous studies PD-L1 positivity was considered when ≥1% membrane tumor cell staining was observed and the expression in TILs and macrophages was evaluated by percent of cytoplasmic positive staining in lymphocytes within the tumor and graded IC0, IC1, IC2, IC3 according to the SP142 Ventana scoring used in the Atezolizumab trials. PD-L1 staining was assessed in tumor and immune cells by two trained thoracic pathologists, experts in mesothelioma field. Categorical variables were compared by Fisher's exact test. Overall survival was assessed using the Kaplan-Meier method.

Results: A total of 90% (35/39) PMs was positive for PD-L1. PMs tended to be more PD-L1 positive (35/39; 90%) than conventional MMs (13/40; 33%) (p<0.0001). The interobserver concordance evaluating PDL-1 staining was good (k=0.77) in the tumor cells and excellent (k=0.80) in immune cells. PD-L1 tumor cells positive PMs had a worst overall survival at 3 years (p=0.006). No significant prognostic difference was observed between the groups of immune cells (IC0 to IC3). Unpublished results of HTG analyses in different cohorts will be given on site.

Conclusions: Pleomorphic mesotheliomas have the highest rate of PD-L1 expression (90%) compared to conventional types (33%). Thus PD-L1 expression in PMs is an important prognostic factor and a major predictive biomarker for PD-L1 therapies.

2043 Detection of BRAF Mutations in EGFR and ALK negative Lung Adenocarcinoma Using BRAF V600E Mutation-Specific Antibody: A Retrospective Study and Correlation with DNA-based analysis of BRAF Gene Status

Michael W Harrell[1], *Karen Buehler*[2], *Mohammad Vasef*[1]. [1]University of New Mexico, Albuquerque, NM, [2]TriCore Reference Laboratory

Background: Identification of actionable oncogenic driver mutations has drastically modified the treatment regimen in non-small cell lung cancer (NSCLC). In addition to actionable *EGFR* mutations and *ALK, ROS1* or *RET* fusions, recent comprehensive genomic profiling of non-squamous NSCLC has identified additional targetable mutations in other genes including *BRAF* V600E in 2-4% of cases. However, mutations involving other codons of *BRAF* have also been reported. The *BRAF* mutations appear to be non-overlapping with other oncogenic driver mutations. Dramatic response to BRAF inhibitors have been reported in *BRAF* V600E mutated lung adenocarcinoma and a phase 2 clinical trial is currently underway. We retrospectively analyzed 110 NSCLC using *BRAF* V600E mutation-specific antibody and correlated the results with PCR-based analysis of *BRAF* gene.

Design: Three tissue microarrays (TMAs) composed of 2 mm in diameter tissue cores of 98 previously characterized NSCLC were constructed. Immunohistochemistry (IHC) was performed on the TMAs and 12 additional molecularly documented *BRAF*-mutated NSCLC using *BRAF* V600E mutation-specific antibody. For *BRAF* molecular testing, DNA was extracted from recuts of paraffin tissue blocks and was subjected to multiplex PCR followed by library preparation using Ion AmpliSeq library kit. The sequencing performed on Ion Torrent PGM platform and the sequence data were analyzed using the Ion Torrent Suite and NextGENe software.

Results: *BRAF* V600E mutation-specific IHC identified in 6 of 110 primary lung adenocarcinoma including 1 of 98 TMA cases and 5 of 5 molecularly documented *BRAF* V600E-mutated cases indicating 100% sensitivity and concordance of IHC results with molecular testing. All 5 non-V600E *BRAF* variant mutated cases were negative by *BRAF* V600E IHC indicating 100% specificity of the antibody. Results are summarized in Table.

Cases	Diagnosis	BRAF Variants By Sequencing	BRAF V600E by IHC
1	Lung adenocarcinoma	V600E	Positive
2	Lung adenocarcinoma	V600E	Positive
3	Lung adenocarcinoma	V600E	Positive
4	Lung adenocarcinoma	V600E	Positive
5	Lung adenocarcinoma	V600E	Positive
6	Lung adenocarcinoma	V600E	Positive
7	Lung adenocarcinoma	G466A	Negative
8	Lung adenocarcinoma	G466V	Negative
9	Lung adenocarcinoma	G469A	Negative
10	Lung adenocarcinoma	G469V	Negative
11	Lung adenocarcinoma	L588H	Negative
12	Lung adenocarcinoma	K601E	Negative

Conclusions: *BRAF* V600E mutation-specific IHC is a rapid and cost effective screening tool in identifying *BRAF* V600E mutated NSCLC that would benefit from BRAF inhibitors. However, a negative result will not exclude the possibility of a *BRAF* variant mutation although efficacy of BRAF inhibitors in *BRAF* variant mutated NSCLC is uncertain at this time.

2044 HEG1 is a Novel Mucin-like Membrane Protein That is Useful for the Diagnosis of Malignant Mesothelioma

Kenzo Hiroshima[1], *Di Wu*[2], *Yasuo Sekine*[3], *Daisuke Ozaki*[4], *Toshikazu Yusa*[5], *Shoutaro Tsuji*[6], *Yohei Miyagi*[7], *Aliya N Husain*[8], *Kohzoh Imai*[9]. [1]Tokyo Women's Med Univ-Yachiyo Medical Ctr., Yachiyo, Chiba, [2]Tokyo Women's Med Univ-Yachiyo Medical Ctr., Yachiyo, Japan, [3]Tokyo Women's Med Univ-Yachiyo Medical Ctr., [4]Chiba Rosai Hospital, Ichihara City, Chiba, [5]Chiba Rosai Hospital, [6]Kanagawa Cancer Center Research Institute, [7]Kanagawa Cancer Center Research Institute, Yokohama, Kanagawa, [8]University of Chicago, Chicago, IL, [9]The University of Tokyo

Background: Calretinin, WT1, and D2-40 are the best positive mesothelioma markers for histological diagnosis of malignant mesothelioma (MM). However, none of these markers are 100% sensitive for MM. We recently discovered that HEG1 is a protein that has high specificity and sensitivity to MM. The aim of this study was to evaluate immunoreactivity of HEG1 as a diagnostic marker for MM.

Design: Tissue microarrays (TMA) composed of MM were constructed by one of the authors. They contained 87 pleural mesotheliomas and 22 peritoneal mesotheliomas. We also collected from the pathology archives of our institutes, biopsies of 65 MMs, 26 pulmonary carcinomas, pleural biopsies from the 11 patients with fibrous pleuritis, and cell blocks of effusion from 11 MM patients.

Results: Most epithelioid mesotheliomas displayed strong membranous reactivity for HEG1. However, of the staining was cytoplasmic in epithelioid mesotheliomas with solid pattern and in sarcomatoid mesotheliomas. TMA from pleural mesothelioma contained 51 epithelioid, 34 biphasic, and two sarcomatoid mesotheliomas. Calretinin, WT1, D2-40, and HEG1 were expressed in 73.3%, 62.8%, 60.5%, and 91.4%, respectively, of epithelioid mesotheliomas, and in 48.5%, 42.4%, 33.3%, and 93.9%, respectively, of biphasic mesotheliomas. Two sarcomatoid mesotheliomas were positive for HEG1, but negative for other markers. Calretinin, WT1, D2-40, and HEG1 were expressed in 81.8%, 68.2%, 68.2%, and 90.9%, respectively, of TMA from peritoneal mesotheliomas containing 19 epithelioid mesotheliomas and three biphasic mesotheliomas. In biopsies, 37 of 39 epithelioid mesotheliomas (94.9%), 15 of 16 biphasic mesotheliomas (93.8%), and 7 of 10 sarcomatoid mesotheliomas (70.0%) were positive for HEG1. All pulmonary adenocarcinomas (0/11) and squamous cell carcinomas (0/7) were negative for HEG1, but 87.5% (7/8) of pleomorphic carcinomas were positive. As a whole, sensitivity of HEG1 for the differentiation between non-sarcomatoid mesothelioma and lung carcinoma is 95.2% and specificity is 73.1%. 10 of 11 biopsies of fibrous pleuritis (90.9%) were positive for HEG1. All of eleven cell blocks from pleural effusion of the patients with pleural mesothelioma were positive for HEG1.

Conclusions: Sensitivity of HEG1 for MM is higher than that of calretinin, WT1, and D2-40. Most importantly, it is higher in biphasic mesotheliomas. HEG1 is a useful marker for the differential diagnosis between MM and pulmonary carcinoma (except for pelomorphic carcinoma).

2045 Targeted Next Generation Sequencing Identifies Recurrent BAP1 Alterations in Malignant Peritoneal Mesothelioma

Yin P. (Rex) Hung[1], *Fei Dong*[1], *Christopher Crum*[1], *Lucian Chirieac*[1]. [1]Brigham and Women's Hospital, Boston, MA

Background: Malignant peritoneal mesothelioma is a rare aggressive neoplasm that arises from the peritoneal lining. Germline and somatic alterations in *BRCA1-associated Protein 1* (*BAP1*) have been implicated in the pathogenesis of pleural and peritoneal mesothelioma. Nevertheless, the mutational landscapes of peritoneal mesotheliomas, including tumors lacking *BAP1* alterations, remain largely unexplored.

Design: Targeted next generation sequencing was performed on 20 malignant peritoneal mesotheliomas using DNA extracted from formalin-fixed paraffin-embedded tissue sections to examine 447 cancer-associated genes and 191 regions across 60 genes for rearrangement detection. Analysis was restricted to pathogenic alterations in tumor suppressor genes and oncogenes (including *BAP1, TP53, NF2, CDKN2A*) and loss of function variants (nonsense, frameshift, splice site variants, and focal deletions). Immunohistochemistry for BAP1 was performed to correlate with molecular alterations.

Results: Malignant peritoneal mesotheliomas (19 epithelioid; 1 biphasic) from 20 patients (11 men, 9 women; age 32-81) were analyzed. Inactivating *BAP1* mutations were identified in 14 tumors (70%; 8 cases with >1 alterations), including 4 frameshift, 2 missense, 2 splice site, 1 nonsense, 3 structural rearrangements/deletion; 10 cases showed *BAP1* copy number loss (monoallelic in 8, biallelic in 1; including 6 with concurrent *BAP1* mutations). Other recurrent copy number changes included loss of *PBRM1*, *SETD2*, *CDKN2A*, and *NF2*. Of the 6 tumors (30%) that lacked *BAP1* mutations, loss-of-function variants in *CHEK2* and *TP53* were found in 1 case each, and focal copy gain in *WT1* and *ARAF* were also noted. By immunohistochemistry, BAP1 expression was intact in 8, partially diminished in 2, and completely lost in 10 cases, overall patterns corresponding to *BAP1* genomic alterations.

Conclusions: Targeted sequencing identifies recurrent inactivating mutations and/or copy number losses of *BAP1* in 70% of malignant peritoneal mesothelioma. Loss of tumor suppressor genes and epigenetic regulators such as *PBRM1, SETD2, CDKN2A, NF2* is often present. Peritoneal mesothelioma with *BAP1* genomic alteration can be readily identified by immunohistochemistry for BAP1 with either complete loss or diminished protein expression. Peritoneal mesotheliomas that lack BAP1 mutations harbor mutations involving *CHEK2* and *TP53*, implicating DNA repair pathway genes as potential therapeutic targets.

2046 Loss of ARID1A is Associated with Distinct Clinicopathologic Features in Lung Carcinomas

Yin P. (Rex) Hung[1], *Amanda Redig*[2], *Jason L Hornick*[1], *Lynette Sholl*[1]. [1]Brigham and Women's Hospital, Boston, MA, [2]Boston, MA

Background: *ARID1A*, a component of the SWI/SNF complex important in epigenetic regulation, is mutated in ~10% of lung carcinomas. Although other members of the SWI/SNF complex such as SMARCA4 have been implicated in aggressive thoracic malignancies, the significance of *ARID1A* mutations in lung cancer remains unclear. We aimed to describe the clinical, histologic, immunohistochemical, and molecular correlates of *ARID1A*-mutated lung carcinomas.

Design: We examined *ARID1A* variants in an institutional cohort of 1743 non-small cell lung carcinomas (NSCLC) via targeted next generation sequencing (NGS) of >300 cancer related genes. Nonsense, frameshift, splice site, and structural variants were defined as loss of function (LOF). Loss of ARID1A expression by immunohistochemistry (IHC) was scored as complete absence or dim expression in tumor cells. Cases with retained nuclear expression or only scattered individual tumor cells with loss were considered intact.

Results: *ARID1A* mutations were detected in 188 (11%) NSCLC, including 153 (of 1488) adenocarcinomas (LUAD) and 35 (of 255) squamous cell carcinomas (LUSC). ARID1A IHC was available for 95 mutated samples, of which 24 had protein loss (6 complete and 18 dim). Of these, 23 (96%) had a LOF mutation. Geographic (subclonal) loss of ARID1A was notable in 4 LUAD. Patients whose tumors showed ARID1A loss had a mean age of 68 years, 46% were female, and all were smokers. 17/24 cases were LUAD, of which 10 (59%) also harbored *KRAS* mutations. No other driver oncogene mutations were detected. All cases showed high-grade histology with a predominantly solid growth pattern; pleomorphic features were also noted including 1 LUAD and 1 LUSC with extensive sarcomatoid differentiation. In one LUAD, areas with loss of ARID1A showed high-grade fetal-like differentiation.

Conclusions: Although *ARID1A* mutations are relatively common in lung carcinoma, only a minor subset appears to lead to functional protein loss. 48% of the cases with *ARID1A* mutations but no protein loss, as well as those with only scattered tumor cell showing loss of expression, require further study. ARID1A protein loss is associated with distinct clinicopathologic features and appears to contribute to the phenotypic spectrum of both LUAD and LUSC. Identification of functional alterations in pathways that contribute to tumorigenesis but that have not yet been widely studied may begin to explain the morphologic and clinical heterogeneity observed in lung cancers.

2047 Expression analysis of CD70, CD27 and FOXP3 with evaluation of their prognostic value in malignant pleural mesothelioma

Shingo Inaguma[1], *Jerzy Lasota*[2], *Zengfeng Wang*, *Markku Miettinen*[3]. [1]Nagakute, Aichi, [2]National Cancer Institute, Bethesda, MD, [3]National Cancer Institute

Background: Diffuse malignant mesothelioma of the pleura is a highly aggressive tumor typically with a short survival. CD70 is a type II transmembrane surface antigen belonging to the tumor necrosis factor (TNF) super family. CD27 is a member of the TNF receptor superfamily. Under physiological conditions, the interaction of tightly-regulated CD70 and CD27 plays a co-stimulatory role in promoting T-cell expansion and differentiation through the NFκB pathway. Aberrant high CD70 expression has been documented in hematological and solid malignancies in association with immune evasion of malignant cells. FOXP3, a master transcription factor of regulatory T-cells (Tregs), plays crucial roles for the differentiation, maintenance, and function of Tregs.

Design: In this study, 172 well characterized primary diffuse pleural mesotheliomas including epithelioid (n=145), biphasic (n=15), and sarcomatoid (n=12) histotypes were evaluated immunohistochemically for CD70, CD27 and FOXP3 expression. Tumor samples were assembled to multitumor blocks containing up to 40 rectangular tissues. Immunohistochemistry was performed using the Leica Bond-Max automation and Leica Refine detection kit (Leica Biosystems, Bannockburn, IL). In mesothelioma cells, immunoreactivity of CD70 (cell membranous) was evaluated at a detection cut-off of 5%. A threshold of ≥50 positive tumor-associated inflammatory cells (TAIs)/high-power field (HPF) was used to define CD70-, CD27-, and FOXP3-positive cases.

Results: Twenty percent (34/172) of mesotheliomas expressed CD70 and 22% (38/172) contained CD70-expressing TAIs. Cases with CD27- and FOX3-positive TAIs were detected in 32% (55/171) and 25% (43/171), respectively. Overall survival was significantly decreased in the cohort of patients with CD70-expressing tumor (P<0.01). On the other hand, the patients with CD27-positive TAIs showed favorable clinical outcome (P=0.03). However, FOXP3 expression was not significantly associated with clinical outcome (P=0.80). The multivariable Cox hazards regression analysis identified CD70-positivity on tumor cells as a potential risk factor (HR, 2.39; 95%CI, 1.35-4.20; P=0.0026). CD27-positivity was revealed as a potential favorable factor (HR, 0.52; 95%CI, 0.31-0.90; P=0.018).

Conclusions: CD70 and CD27 immunostaining could be useful in the prognostication of malignant pleural mesothelioma patients and planning the treatment including CD70/CD27 pathway targeting therapy. However, FOXP3 immunostaining should be further estimated for its clinical use.

2048 PD-L1 expression induced by cancer associated fibroblast-derived factors in human lung adenocarcinoma cells

Chihiro Inoue[1], *Yasuhiro Miki*[2], *Ryoko Saito*[3], *Shuko Hata*[4], *Yoshinori Okada*[5], *Hironobu Sasano*[6]. [1]Tohoku University Graduate School of Medicine, Sendai, Miyagi, [2]Disaster Ob/Gyn, Int. Res. Inst. of Disaster Sci., Tohoku Univ., [3]Tohoku University Graduate School of Medicine, Sendai-shi Aoba-ku, Miyagi-ken, [4]Tohoku Medical and Pharmaceutical University, Sendai, Miyagi, [5]Institute of Development, Aging and Cancer, Tohoku University, [6]Tohoku University, Sendai-shi

Background: Lung adenocarcinoma (LADC) cells are well known to interact with stromal component including inflammatory cells, microvascular, and fibroblasts in cancer microenvironment. Activated fibroblasts are also known as cancer associated fibroblasts (CAFs). CAFs play important roles in cancer development, such as cancer cell growth, invasion, metastasis, and therapeutic resistance, through secreting growth factors and inflammatory cytokines. Results of clinical trials revealed that PD-L1 status in non-small lung cancer cells was significantly related to the response rate for some anti-PD-1/PD-L1 antibodies. However, the influence of CAFs on PD-L1 expression in LADC has remained unknown. Therefore we studied the relationship between CAFs and PD-L1 status in human LADC.

Design: We immunolocalized α-SMA, a well-known CAFs marker, in stromal area in surgical resected specimens of 113 LADC cases, and analyzed its correlation with the status of PD-L1 on LADC cells and the clinicopathological significance. We then established the primary fibroblastic stromal cells derived from lung adenocarcinoma tissues. α-SMA immunoreactivity was detected in fibroblastic stromal cells. We also performed RT-PCR and Western blotting to examine the effects of the conditioned medium collected from fibroblastic stromal cells on the expression levels of PD-L1 mRNA and protein in LADC cells, A549 and PC-9.

Results: The patients were tentatively classified into two groups, high- and low-SMA according to the median score of α-SMA immunoreactivity. High-SMA group was positively and significantly associated with Brinkman index, Stage, and worse overall 5-year survival in 113 LADC cases. In addition, positive status of PD-L1 was significantly associated with population score (%) of α-SMA. In A549 and PC-9 cells, conditioned medium (CM) derived from fibroblastic stromal cells increased the ratio of PD-L1 mRNA/RPL13A mRNA. In addition, protein level of PD-L1 was also increase by CM treatment in A549 and PC-9 cells.

Conclusions: CAFs increased the expression of PD-L1 in LADC cells. CAFs are known to secrete inflammatory cytokines and growth factors, and PD-L1 in carcinoma cells were upregulated by exposure to inflammatory cytokines or activating growth signaling pathways. CAFs could indirectly suppress anti-tumor immunity and promote tumor progression in LADC tissue by promoting the expression of PD-L1 in carcinoma cells, and influence the therapeutic response in these patients.

2049 Expression of intratumoral programmed cell death-ligand 1 (PD-L1) and intratumoral CD8+ T cell and FOXP3+ T cell in lung cancer

Yasuto Jin[1], *Reina Imase*[2], *Hiroyuki Shimada*[2], *Shuta Yamauchi*[2], *Osamu Matsubara*[3]. [1]Hiratsuka Kyosai Hospital, Hiratsuka-shi, Kanagawa, [2]Hiratsuka Kyosai Hospital, [3]Hiratsuka Kyosai Hospital / The Cancer Institute, Hiratsuka, Kanagawa

Background: Overexpression of PD-1 and PD-L1 induces immune evasion by cancer cells. Blockade of this immune checkpoint could reverse the tumor immune system and activate the anti-cancer response. Nivolumab and pembrolizumab, anti-PD-1 antibodies, were recently approved for the treatment of advanced NSCLC. A PD-L1 positive (≥1%) expression status by immunohistochemistry (IHC) has been associated with a favorable response. However responses to these drugs are limited, with the objective response rate ranging between 20%-30%. These results suggest that individual tumor microenvironments vary according to the immune evasion process of each cancer tissue. Consequently, the introduction of biomarkers, which predict the responders to the immune checkpoint blockades are necessary in clinical practice. FOXP3+CD4+ regulatory T (Treg) cells maintain the immunological self-tolerance and suppress the activation of T cells recognizing tumor-specific shared antigens in cancer tissue.

Design: Expression of PD-L1, CD8 and FOXP3 in tumor cells and tumor infiltrating lymphocytes (TILs) were examined by IHC in 35 cases with advanced lung cancer (including 26 cases of adenocarcinoma and 9 cases of squamous cell carcinoma) treated with nivolumab or pembrolizumab. Histologic subtypes, tumor stage and other clinicopathologic conditions were compared with the level of their expression.

Results: Expression of PD-L1 expression in tumor cells was detected in 68.6% of the cases. The objective response rate was 40%, and this was significantly correlated PD-L1 positivity with CD8+TILs (p=0.0079). Nine cases having driver gene mutations did not show a tendency towards favorable response. The patients with high PD-L1 expression showed consistently dense CD8+TILs, even in subgroup analyses according to histological subtype, stage, age and smoking status. In cancer-associated stroma, CD4+ cells and FOXP3+ cells were detected. Cases with no PD-L1, low CD8+, and FOXP3+ status were also detected.

Conclusions: High expression of PD-L1 with CD8+TILs was associated with a favorable response to treatment with immunotherapy. In contrast, no PD-L1 with low CD8+TILs and FOXP3+TILs was not associated with favorable response. Therefore, assessment of PD-L1, CD8+ TILs and FOXP3+ TILs may be valuable for predicting response toimmunotherapy. PD-L1- and CD8+ TILs and FOXP3+ TILs may be indicative of the addition of other therapeutic agent. Investigation of novel combinations of immunotherapy according to individual tumor microenvironments is warranted.

2050 Reduced expression of SMARCB1/INI1 protein in malignant mesothelioma

Toshiaki Kawai[1], *Koji Kameda*[2], *Hiroshi Nakashima*[2], *Kenzo Hiroshima*[3]. [1]Toda Central Medical Laboratory, Toda, Saitama, [2]National Defense Medical College, [3]Tokyo Women's Med Univ-Yachiyo Medical Ctr., Yachiyo, Chiba

Background: Background: Deciduoid mesothelioma is a rare variant of epithelioid mesothelioma. Malignant rhabdoid tumors, renal medullary carcinoma, and some synovial sarcomas show a loss

of SMARCB1/INI1 protein expression in tumor cells, and all of these tumors are known to have rhabdoid cells. Some mesothelioma cases, such as the deciduoid type, have also been reported to possess such rhabdoid features. There has been no study on this topic in malignant mesothelioma. We analyzed the immunohistochemical expression of SMARCB1/INI1 in malignant mesotheliomas [45 epithelioid type (including 9 deciduoid type), 12 biphasic type, and 16 sarcomatoid type].

Design: Design: We employed (a) immunohistochemistry for SMARCB1/INI1 using a mouse monoclonal antibody, BAF47, to the *INI1* gene product and (b) Fisher's exact test, the Kaplan-Meier method, and the Log-Rank test for survival analysis to evaluate the prognostic factor (SAS 9.4).

Results: Results: The results showed that 17 of 73 (23%) malignant mesotheliomas cases (epithelioid: 24%; biphasic; 8%; sarcomatoid; 31%) had reduced SMARCB1/INI1 expression. Statistically, the reduced rate of SMARCB1/INI1 expression was significantly greater in the deciduoid type (67%) than in either the epithelioid type ($p < 0.026$), or the biphasic type ($p < 0.0158$), regardless of the existence of rhabdoid cells, but not significantly different between the deciduoid and sarcomatoid types ($p < 0.1153$). Two cases of the deciduoid type with a complete loss of SMARCB1/INI1 protein expression were recognized. However, there was no statistically significant difference in prognosis between malignant mesotheliomas with reduced versus preserved SMARCB1/INI1 protein expression.

Conclusions: Conclusion: The results suggest that cases with reduced SMARCB1/INI1 protein expression should not be excluded when making a diagnosis of malignant mesothelioma.

2051 Non-necrotizing Granulomatous Pneumonitis in Soldiers Deployed to Southwest Asia

Christine Kim[1], *Mitra Mehrad*[1]. [1]Vanderbilt University Medical Center, Nashville, TN

Background: Reports of respiratory illnesses among soldiers returning from the Southwest Asia (SWA) have been described recently. During deployment to the SWA, soldiers are exposed to various respiratory hazards including dust storms, smoke from burn pits and industrial air pollutants. Few studies have reported increased rates of constrictive bronchiolitis and asthma in these patients. Given the limited data, we sought to expand the pathologic perspective in this cohort of patients.

Design: In a retrospective study, lung biopsies from veterans of SWA with unexplained exertional dyspnea were identified, re-reviewed and assessed for the presence of granulomas and pleural reaction. Special stains for microorganisms when appropriate were performed to exclude an infectious etiology.

Results: Overall, 59 patients with history of exposure to at least one of the following were identified: smoke from burn pit, dust storms, and sulfur plant fire. The majority of the biopsies were video-assisted thoracoscopic lung biopsies (57/59, 96.6%) with 2 (3.4%) cases being cryobiopsies. Patients were predominantly male (54/59, 91.5%) with an age range of 24 to 55 years (mean and median: 35). Non-necrotizing, poorly formed granulomas were identified in 22 cases (22/59, 37.2%). The granulomas had a bronchiolocentric distribution and were associated with chronic lymphoplasmacytic bronchiolitis, similar to hypersensitivity pneumonitis (HP). Pleural reaction in the form of focal chronic lymphocytic pleuritis and/or focal pleural adhesions were seen in 43 (43/57, 75.4%) biopsies, predominantly limited to the areas overlying collections of subpleural pigmented macrophages. No pleura was available to assess in the two cryobiopsies.

Conclusions: In our series, a significant number of patients had pleural reaction and approximately 1/3 showed features of hypersensitivity pneumonitis, suggesting that pleural reaction and HP may be part of the spectrum of SWA deployment-related lung diseases.

2052 Genomic Profiling and Pathologic Characterization of Neuroendocrine Tumors of the Lung in East Asian Patients

Moonsik Kim[1], *Hyo Sup Shim*[2]. [1]Yonsei University College of Medicine, Seoul, [2]Boston, MA

Background: Neuroendocrine tumors (NETs) of the lung are categorized based on their histologic features. Recently, the genomic data based on next-generation sequencing have been investigated. Integrating genetic profiling with clinical-pathologic findings is critical for the understanding and treatment of NETs. However, most of the NET studies have come from the Western population. Therefore, it is necessary to characterize the NET of the lung in East Asian patients.

Design: Retrospectively selected clinical and pathological data were collected from a total of 77 NET cases including 26 large cell neuroendocrine carcinoma (LCNEC), 22 small cell lung carcinoma (SCLC), 8 atypical carcinoid and 21 carcinoid tumors. 48 cases underwent targeted next generation sequencing including 46 genes among the collected data. Comprehensive review of the NGS results and analyses with histopathology and clinical outcome were performed.

Results: Among LCNEC, *TP53* and *RB1* co-mutation was observed in 7 out of 19 samples. Overall survival rate was lower in those with co-mutation than not, though it is not statistically significant. Driver or targetable gene alterations, such as *KRAS* mutation (1/19), *FGFR1* amplification (1/19), and *ERBB2* amplification (1/19) were also found. In SCLC group, alteration of *TP53* (13/15), *RB1* (14/15), *TP53* and *RB1* co-mutation (12/15), *PTEN* mutation (6/15), *MYCN* amplification (1/15) and *PIK3A* mutation (2/15) were found. High grade neuroendocrine carcinoma groups, LCNEC and SCLC, had at least one alteration of either *TP53* or *RB1*. Among typical carcinoid samples, only one sample had co-mutation of *TP53* and *RB1* (1/7). The patient had lymph node metastasis at the time of diagnosis. In atypical carcinoid groups, *TP53* mutation was found in a single sample (1/6). None had *RB1* mutation from the collected data.

Conclusions: Mutational status of *TP53* or *RB1* was associated with NET categorization, and can be a reference. *TP53* and *RB1* co-mutant NETs tend to show aggressive behavior. A NGS panel test is recommended since a targetable mutation has been found in NETs, although the frequency is low.

2053 A Combination of MTAP and BAP1 Immunohistochemistry is Effective for Distinguishing Sarcomatoid or Biphasic Mesothelioma from Fibrous Pleuritis

Yoshiaki Kinoshita[1], *Makoto Hamasaki*[2], *Masayo Yoshimura*[1], *Shinji Matsumoto*[3], *Ayuko Sato*[4], *Tohru Tsujimura*[4], *Kazuki Nabeshima*[5]. [1]Fukuoka University School of Medicine and Hospital, Fukuoka, [2]Fukuoka University Hospital, Fukuoka, [3]Fukuoka University Hospital and School of Medicine, [4]Hyogo College of Medicine, [5]Fukuoka University, Fukuoka, Japan

Background: Histologic diagnosis of malignant pleural mesothelioma (MPM) is not always straightforward. Loss of BRCA1-associated protein 1 (BAP1) expression detected by immunohistochemistry (IHC) and homozygous deletion (HD) of 9p21 detected by fluorescence *in situ* hybridization (FISH) are useful to distinguish malignant mesothelial proliferations from benign proliferations. We have previously reported that IHC expression of the protein product of the methylthioadenosine phosphorylase (*MTAP*) gene, which is localized in the 9p21 chromosomal region, is correlated with the deletion status of 9p21 FISH in MPM tissues. In this study, we investigated whether a combination of MTAP and BAP1 IHC could distinguish sarcomatoid MPM from fibrous pleuritis.

Design: We examined IHC expressions of MTAP and BAP1 and 9p21 FISH in sarcomatoid/desmoplastic (n=17) and biphasic MPM (n=12) and in fibrous pleuritis (n=24). In biphasic MPM, only sarcomatoid components were evaluated for IHC and FISH. Sensitivity and specificity of each detection assay for discriminating MPM cases from fibrous pleuritis was determined. In addition, we compared the IHC expression of MTAP with the deletion status of 9p21 FISH.

Results: MTAP IHC and BAP1 IHC showed 82.8% and 37.9% sensitivity, respectively and 100% specificity each in differentiating MPM from fibrous pleuritis. A combination of MTAP and BAP1 IHC yielded greater sensitivity (96.6%) than that detected for BAP1 IHC alone (37.9%) or 9p21 FISH alone (93.1%). Moreover, a high degree of concordance was observed between the results of MTAP IHC and 9p21 FISH ($\kappa = 0.62$).

Conclusions: A combination of MTAP and BAP1 IHC is a reliable and effective method for distinguishing sarcomatoid or biphasic MPM from fibrous pleuritis, when the results were interpreted accurately.

2054 PD-L1 Protein and Messenger RNA Expression in Non-Small Cell Lung Cancer: Correlations with Clinicopatholgic and Genetic Alterations

Hyun Jung Kwon[1], *Hyojin Kim*[2], *Soo Young Park*[3], *Yeon Bi Han*[3], *Eunhyang Park*[4], *Jin-Haeng Chung*[5]. [1]Seoul National University Bundang Hospital, Seongnam-si, Gyeonggi-do, [2]Seongnam Gyeonggi-do, Korea, [3]Seoul National University Bundang Hospital, [4]Seoul, [5]Seoul Nat'l Univ/Medicine, Seongnam, Gyeongido

Background: Monoclonal antibodies targeting the programmed cell death-1 (PD-1) receptor and its ligand (PD-L1) have shown promising results in advanced non-small cell lung cancer (NSCLC). In this study, we present the clinicopathological features associated with PD-L1 protein as well as mRNA expression in a large Asian cohort of NSCLC and performed subgroup analysis according to histologic subtype and pathologic stage.

Design: We retrospectively analyzed 687 NSCLC tissues (476 adenocarcinoma and 211 squamous cell carcinoma) using tissue microarray. PD-L1 IHC was performed using Dako 22C3 pharmDx assay and *PDL1* mRNA was measured using RNAscope® assay. Correlation of PD-L1 IHC and RISH results were evaluated, to each

other and to clinicopathologic parameters including genetic status of *EGFR*, *KRAS* and *ALK*. Survival analysis was performed.

Results: The overall prevalence of PD-L1 protein expression was 25.2% in tumor cells and *PDL1* mRNA expression was 11.9%. There was a strong positive correlation between PD-L1 IHC and RISH results (Spearman's rho = 0.6, p<0.001). In adenocarcinoma (ADC), PD-L1 protein and mRNA expressions significantly correlated with histologic subtype (p<0.001 and p=0.002, respectively). PD-L1 showed higher expression in poorly differentiated (solid and micropapillary predominant) histologic subgroup than well differentiated (lepidic predominant) subgroup. PD-L1 expression was also associated with genetic alteration. While PD-L1 protein and mRNA expression were lower in EGFR mutated group compared to EGFR-negative group (p=0.001 and p=0.016, respectively), PD-L1 protein expression were higher in KRAS-mutated group than KRAS-negative group (p=0.017). In SqCC, only tumor size was associated with PD-L1 protein expression with marginal significance (p=0.049). With a 1% cut-off value, PD-L1 IHC positivity showed a short overall survival duration in early stage ADC with marginal significance (p=0.05, HR= 1.947 with 1.000-3.791 (95% C.I)). PD-L1 mRNA expression, however, showed no prognostic significance.

Table 1. Association between PD-L1 status and clinicopathologic variables including histologic subtype and genotype in lung adenocarcinoma

		PD-L1 IHC (number (%))				PD-L1 RNA scope (number (%))		
	Total	Negative	Weak positive	Strong positive	**p** value	Negative	Positive	**p** value
Smoking history								
Yes	192	156 (81.3%)	22 (11.5%)	14 (7.3%)	> 0.05	180 (93.8%)	12 (6.2%)	> 0.05
No	284	243 (85.6%)	26 (9.2%)	15 (5.3%)		267 (94.0%)	17 (6.0%)	
Histologic subtype*								
WD	42	41 (97.6%)	1 (2.4%)	0	<0.001	41 (97.6%)	1 (2.4%)	0.002
MD	360	309 (85.8%)	33 (9.2%)	18 (5.0%)		343 (95.3%)	17 (4.7%)	
PD	68	43 (62.7%)	14 (20.9%)	11(16.4%)		57 (83.6%)	11 (16.4%)	
Mucinous	6	6 (100%)	0	0		6 (100%)	0	
Pathologic stage								
IA-IIA	340	286 (84.1%)	33 (9.7%)	21 (6.2%)	> 0.05	320 (94.1%)	20 (5.9%)	> 0.05
IIB-IV	136	113 (83.1%)	15 (11.0%)	8 (5.9%)		127 (93.4%)	9 (6.6%)	
EGFR mutation								
Present	223	201 (90.1%)	17 (7.6%)	5 (2.2%)	0.001	216 (96.9%)	7 (3.1%)	0.016
Absent	229	179 (78.2%)	27 (11.8%)	23 (10.0%)		209 (91.3%)	20 (8.7%)	
KRAS mutation								
Present	23	15 (65.2%)	4 (17.4%)	4 (17.4%)	0.017	20 (87.0%)	3 (13.0%)	> 0.05
Absent	237	203 (85.7%)	23 (9.7%)	11 (4.6%)		223 (94.1%)	14 (5.9%)	
ALK rearrangement								
Present	24	21 (87.5%)	1 (4.2%)	2 (8.3%)	> 0.05	24 (100%)	0	> 0.05
Absent	181	161 (89.0%)	12 (6.6%)	8 (4.4%)		177 (97.8%)	4 (2.2%)	

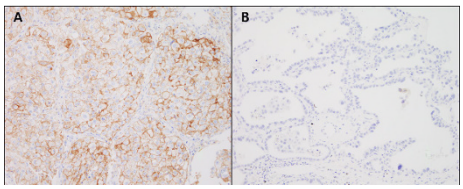

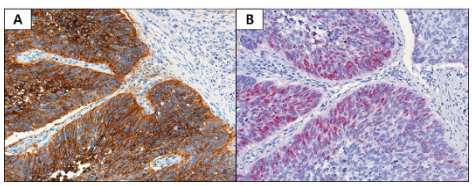

Conclusions: Our study revealed that PD-L1 expression was closely associated with histologic subtype and genomic alteration status in lung ADC, and activation of the PD-L1 pathway might be a poor prognostic factor especially in early stage lung ADC. In addition, *PDL1* RISH showed promising results in predicting PD-L1 protein expression in NSCLC.

2055 Limiting ROS-1 immunohistochemistry to a population of patients either aged 55 years or younger, or never smokers of any age, as a method for cost-efficient screening ROS-1 gene rearrangements

Ute Laggner[1], *Toyin Adefila-Ideozu*[2], *Eric Lim*[3], *Sanjay Popat*[4], *Lisa Thompson*[5], *Suzanne Macmahon*[5], *Alexander D Bowman*[6], *Andrew Nicholson*[7]. [1]Royal Brompton Hospital, London, United Kingdom, [2]Royal Brompton Hospital, [3]Royal, [4]Royal Marsden Hospital, [5]Institute of Cancer Research, [6]Royal Brompton & Harefield NHS Trust, London, [7]Royal Brompton Hospital, London, Great Britain

Disclosures:
Eric Lim: *Employee*, Informative Genomics

Background: ROS-1 translocations are rare genetic abnormalities in lung cancers that, when identified, are a target for personalised therapy. The current test of choice is FISH, although with a rate of no more than 1-2%, screening using FISH is an expensive proposition. Furthermore, immunohistochemistry is not inexpensive and time consuming. The literature reports that most cases occur in younger patients and/or never smokers with lung cancer, so we sought to review a cohort of such patients to determine the incidence of ROS-1 positive patients, correlating with FISH testing.

Design: Patients aged 55 years or under, diagnosed with lung cancer between 2005 and 2016, were amalgamated with patients who were never smokers. Slides were stained on the Benchmark Ultra (Ventana) automated platform with an antibody for ROS-1 (D4D6, Cell Signalling), using heat retrieval CC1 method for 72mins, followed by a 1/100 dilution, with an incubation of 60 minutes at 37oC. After this an Optiview amplification kit was used for a further 8 minutes. Cases were scored using an h-score. All positive tumours were then sent for FISH analysis for the ROS-1 translocation, with a cut-off of > or = to15%, and the sensitivities of positive IHC staining for ROS-1 were generated at different h-score levels.

Results:

A total of 247 cases were screened with immunohistochemistry. Of these, 134 were aged 55 years or under, and 113 patients were aged over 55 years but were never smokers. 211 were negative (adenocarcinoma n=183; squamous cell carcinoma n=20, large cell carcinoma n=1, large cell neuroendocrine carcinoma n=3, non-small cell carcinoma, NOS n=2, and adenosquamous carcinoma n=2).

36 cases showed positivity (adenocarcinoma n=35, non-small cell carcinoma, NOS n=1) with h scores ranging from 5-300. Of these, 20 were aged 55 years or under, and 16 patients were never smokers aged over 55 years. Of these 36 cases, there were 9 positive, 5 failed and 22 negative FISH tests. Using an h-score of ≥100, 9 out of 12 (75%) cases (excluding fails) were positive using FISH and, for h<100, 19 of 19 were negative. Of cases positive for FISH, 7 of the 9 were in the 55 years or younger, with only 2 never smokers of 60 and 64 years of age respectively.

Conclusions: Limiting immunohistochemical screening for ROS1 to a population of patients either aged 55 years or younger, or never smokers of any age, identified IHC-positive and FISH-positive patients in 3.6% of patients. This may be a more cost effective way of screening for this rare genetic abnormality.

2056 Expression analysis of autophagy related markers LC3B, p62 and HMGB1 indicate an autophagy independent negative prognostic impact of high p62 expression in pulmonary squamous cell carcinomas

Rupert Langer[1], *Christina Neppl*[1], *Ralph A Schmid*[2], *Mario P Tschan*[1], *Sabina Berezowska*[1]. [1]University of Bern, Bern, [3]Inselspital University Hospital Bern

Background: Autophagy is a cellular mechanism involved in maintaining cellular homeostasis under stress conditions. LC3B and p62 are key players in autophagosome formation and degradation, whereas the stress-linked protein HMGB1 can act as a regulator of autophagy. Pulmonary squamous cell carcinomas (pSQCC) lack targetable molecular genetic alterations, and demand alternative tumor directed therapeutic options. Autophagy has been investigated in the context of cancer and is considered a potential target for antitumoral therapy. We therefore investigated the relevance of the expression of LC3B, p62 and HMGB1 in pSQCC as a rationale for potential autophagy directed therapy in pSQCC.

Design: Expression levels of LC3B, p62 and HMGB1 were assessed in 334 primary resected pSQCC by immunohistochemistry. Expression patterns were correlated with pathological and clinical parameters.

Results: Dot-like staining of LC3B, dot-like, cytoplasmic and nuclear staining of p62 and nuclear staining of HMGB1 were observed in various levels. $LC3B^{high}p62^{low}$ staining, suggested to be indicative for intact activated autophagy, was observed in 11 cases (3.3%) and $LC3B^{high}p62^{high}$ expression, indicative for activated but late stage impaired autophagy, was observed in 37cases (11.1%) but none of them was significantly linked to patients' outcome. High p62 levels regardless of LC3B expression (n=209), however, were associated with significantly worse disease specific survival (p=0.009), which was confirmed using an internal validation model (split sample validation; p=0.049 and p=0.085). High p62 expression was also an independent negative prognostic factor in multivariate analysis (HR=2.7; 95%CI 1.3-5.5; p=0.005; besides UICC/AJCC TNM stage; HR=1.7; 95%CI=1.4-2.1; p<0.001). Of note, HMGB1 expression was correlated neither with expression of LC3B and p62, nor patients' outcome.

Conclusions: Basal intact or late stage impaired activated autophagy characterized by $LC3B^{high}p62^{low}$ or $LC3B^{high}p62^{high}$ expression levels, respectively, is only observed in few cases of primary resected pSQCC. Our results rather point to a predominant autophagy independent role of p62 in pSQCC with an association between high expression levels and unfavorable prognosis.

2057 Reproducibility of PD-L1 scoring for immune cells in NSCLC. A study from the French group of thoracic pathologists PATTERN

Sylvie Lantuejoul[1], *Lucie Tixier*[2], *Nolwenn Le Stang*[3], *Isabelle Rouquette*[4], *Aurélie Cazes*[5], *Francoise Galateau Salle*[6], *Hugues Begueret*[7], *Veronique Hofman*[8], *Jean Vignaud*[9], *Stéphane Garcia*[10], *Julien Adam*[11], *Francesca Damiola*[3], *Frederique Penault-Ilorca*[12], *Diane Damotte*[13]. [1]Centre Leon Berard, Lyon, Rhone Alpes Auvergne, [2]Centre Jean Perrin, Clermont Ferrand, [3]Centre Léon Bérard, Lyon, France, [4]University Hospital, Toulouse Oncopole, France, [5]Hopital Bichat, AP-HP Paris, France, [6]Mesopath, Caen, [7]University Hospital Bordeaux, France, [8]University Hospital Nice, France, [9]Nancy, [10]University Hospital Nord AP-AM, Marseille, France, [11]Gustave Roussy, Villejuif, IDF, [12]Clermont-Ferrand, France, [13]University Hospital Cochin, AP-HP, Paris, France

Background: Whereas PD-L1 expression by tumor cells is a predictive biomarker for nivolumab and pembrolizumab in lung cancer, a high PD-L1 expression by Immune cells (IC) is correlated with the highest survival rate for patients treated by atezolizumab. However, several comparison studies have reported a poor reproducibility of PD-L1 scoring for IC.

Design: In order to evaluate the reproducibility of IC0, IC1, IC2 and IC3 scores and the value of 2 or 3 step scoring systems, 40 surgical samples of NSCLC stained with the 22C3, 28.8, SP263 and SP142 assays on DAKO and VENTANA platforms were analyzed by 10 trained pathologists. Seven of them have attended multi-head microscope sessions before starting the study.

Results: IC2 and IC3 scores were more frequent with SP142 and 28.8 assays (53% and 52% of IC2.IC3 scores for SP142 and 28.8, respectively), than with the 22C3 and the SP263 assays (42% and 40%, respectively) (p<0.0001). Using a 2 step scoring system (IC0IC1 versus IC2IC3), kappa values were 0.48 for SP263, 0.35 for 22C3, 0.20 for 28.8 and 0.19 for SP142. With a 3 step scoring system (IC0 versus IC1.IC2 versus IC3), kappa values were 0.39 for SP142, 0.36 for SP263, 0.36 for 22C3, and 0.28 for 28.8. Kappa values increased when the slides were analysed only by the 7 pathologists who attended the multi-head microscope session using the 3 step scoring system (k=0.51 for 22C3, 0.44 with SP263, 0.42 for SP142, 0.40 for 28.8); overall, the highest concordance was with SP263 assay when IC0IC1versus IC2IC3 scores were taken into account (k=0.60). The kappa value was below 0.26 when interface or intra-lobular patterns were considered, and as expected, cases were highly discordant when the evaluation of the IC staining was hampered by a large amount of positive tumor cells admixed with IC (p=0.005).

Conclusions: Although SP142 and 28.8 stained the most the IC, the reproducibility among pathologists was higher with the SP263 and 22C3 assays. The reproducibility increased when pathologists who attended multihead microscope sessions were involved and with the use of a 2 or a 3 step scoring sytem. This study emphasizes the importance of training pathologists to PD-L1 testing, and the potential usefulness of such scoring systems, which need now to be clinically validated.

2058 Molecular and Ultrastructural Features of Diffuse Intrapulmonary Malignant Mesothelioma, a Rare Variant Simulating Interstitial Lung Disease

Brandon Larsen[1], *Maxwell Smith*[1], *Anja Roden*[2], *William R Sukov*[3], *Helena Hornychova*[4], *Seshadri Thirumala*[5], *Thomas Colby*[6], *Henry Tazelaar*[6]. [1]Mayo Clinic Arizona, Scottsdale, AZ, [2]Mayo Clinic Rochester, Rochester, MN, [3]Mayo Clinic, Rochester, MN, [4]Charles University in Prague, Hradec Králové, Czech Republic, [5]Lubbock, TX, [6]Mayo Clinic, Scottsdale, AZ

Background: Diffuse intrapulmonary malignant mesothelioma (DIMM) is an exceedingly rare variant of mesothelioma characterized by diffuse intrapulmonary growth with minimal pleural involvement, clinically simulating interstitial lung disease. We recently published 5 cases of DIMM, the largest series to date of this peculiar phenomenon, but DIMM remains poorly understood and its putative mesothelial nature has been based on morphologic and immunophenotypic grounds alone. The molecular and ultrastructural characteristics of this variant have never been evaluated.

Design: Four patients with DIMM from our pathology consultation practice were studied further, including 3 cases reported previously as part of our initial series and one additional newer case (mean age 63 yrs, all men). Ultrastructural evaluation was performed by transmission electron microscopy. Cases were then tested for molecular alterations that are common in conventional forms of mesothelioma, using immunohistochemistry for *BRCA1*-associated protein-1 (BAP1) and fluorescence in situ hybridization (FISH) of the *CDKN2A* (p16) gene.

Results: Clinically, the additional patient's presentation was strikingly similar to the other 3 cases as previously reported, with nonspecific pulmonary symptoms and radiologic features suggestive of interstitial lung disease, but lacking pleural thickening or masses. As before, DIMM was only recognized after wedge biopsies were obtained. Ultrastructural evaluation of all 4 cases demonstrated numerous long, sinuous, smooth microvilli on the tumor cells, further confirming their mesothelial nature as suspected. BAP1 expression was lost in the tumor cells in all 4 cases. *CDKN2A* (p16) FISH showed heterozygous loss of this gene region in one case, suggesting that the molecular pathogenesis of DIMM and conventional mesothelioma may be similar, at least in some cases, but the mechanism responsible for its peculiar intrapulmonary growth pattern remains unknown.

Conclusions: DIMM shows ultrastructural and molecular features that are similar to conventional forms of mesothelioma, suggesting that transmission electron microscopy, BAP1 immunohistochemistry, and *CDKN2A* (p16) FISH may be useful adjunctive assays in an appropriate histologic context to further support a diagnosis of DIMM, especially in difficult cases or small biopsies.

2059 The Papanicolaou Society of Cytopathology Guidelines for Respiratory Cytology: Reproducibility of Categories among Observers

Lester Layfield[1], *Magda Esebua*[2], *Leslie Dodd*[3], *Tamar Giorgadze*[4], *Robert Schmidt*[5]. [1]University of Missouri, Columbia, MO, [2]Columbia, MO, [3]Women's and Children's Hospital, Chapel Hill, NC, [4]Medical College of Wisconsin, Milwaukee, WI, [5]Salt Lake City, UT

Background: The Papanicolaou Society of Cytopathology has developed a set of guidelines for reporting respiratory cytology. While the malignancy risk for each category is known, the interobserver reproducibility of these diagnostic categories has not been well-described.

Design: Fifty-five cytologic specimens obtained by FNA from pulmonary nodules were independently reviewed by four board-certified cytopathologists and assigned to the diagnostic categories described by the Papanicolaou Society of Cytopathology guidelines for respiratory specimens. Statistical analysis for diagnostic accuracy was performed for absolute agreement and chance-corrected agreement (kappa). Differences in frequency of distribution of diagnoses between raters was assessed using the Kruskal-Wallis test.

Results: No significant differences in distribution of scores by raters was observed. On average the absolute agreement was 49.5% and the chance-corrected agreement (kappa) was 20%. 34.5% of interrater comparisons were in full agreement and total lack of agreement between the four categories was found in 3% of cases. Combining the "suspicious for malignancy" category with the "malignant" category did not significantly alter interrater agreement statistics.

Conclusions: Agreement between raters was at best fair and did not improve significantly when the categories "suspicious for malignancy" and "malignant" were combined. The most common source of disagreement appeared to be between the categories "suspicious" and "malignant".

2060 Utilization of Next Generation Sequencing vs. Sequential Individual Testing for Therapeutically Important Mutations in Lung Cancer: A Cost Effectiveness Study

Lester Layfield[1], *Richard Hammer*[1], *Sandra K White*[2], *Robert Schmidt*[3]. [1]University of Missouri, Columbia, MO, [2]University of Utah, [3]Salt Lake City, UT

Background: Testing of pulmonary adenocarcinomas for therapeutically important mutations is standard of care. Initially,

mutations were tested individually starting with EGFR. Next generation sequencing (NGS) is an alternative with either a single or two panel approach. We investigated the cost effectiveness of five approaches.

Design: Five testing protocols were compared.

1. Testing of four genes (*EGFR, ALK, ROS1, CMET*) (4_GENE).
2. Stepwise testing of four genes where each gene is tested sequentially (4_STEP) until a positive result.
3. Stepwise testing for five genes (*ALK, CMET, EGFR, KRAS, ROS1*) (5_STEP).
4. Full panel NGS, 11 genes (*ALK, BRAF, CMET, EBRR2, EGFR, HRAS, KRAS, NRAS, NTRKI, RET, ROS1*) tested simultaneously (FP_NGS)
5. Two panel NGS (2P_NGS), with six genes (EGFR, BRAF, KRAS, ALK, ERBB2, MET) tested. If EGFR is negative, a second panel of four genes (ALK, RET, ROS1, UTKR1) is tested.

Positivity rates for mutations were from available references. Costs were based on Mayo Medical Laboratories' price list.

We found the average cost of each testing pathway and used the expected value of information, E_i as a measure of effectiveness.

$E_i = N_A + \square N_P$

N_A is the number of positive results for actionable mutations and N_P is the number of positive results for prognostic markers.

Results: The optimal four-test sequence is EGFR, ALK, CMET, ROS1. This strategy had a cost-effectiveness of $8974 per actionable result. The average cost of testing varied from $1970 (4 STEP) to $2500 (full panel NGS). If no value was placed on prognostic information the 4 STEP and GENE approaches were most cost-effective. If prognostic information was valued, the 4 STEP, 5 STEP and full panel NGS methods were most cost effective.

Conclusions: Our analysis indicates that the traditional step-wise analysis of EGFR, ALK, CMET and ROS1 was most cost effective. This strategy had a cost-effectiveness ratio (CER) of $8974 per actionable result. The CER of the 4 GENE and the 4 STEP strategies were independent of the value placed on prognostic information while the CERs of the two panel NGS and full panel NGS improved as more value was placed on prognostic information. A two-panel NGS approach is least cost effective even when prognostic and actionable results are equally valued.

2061 Automated Quantification of Ki-67 Index Associates With Pathologic Grade and Prognosis of Pulmonary Neuroendocrine Tumors

Dongmei Lin[1], *Zhong Wu Li*[2], *Haiyue Wang*[3]. [1]Peking University Cancer Hospital & Institute, Beijing, [2]Peking University, Beijing, China, [3]Peking University Cancer Hospital

Background: Pulmonary neuroendocrine tumors (PNETs) can be classified as four variants: typical carcinoid (TC), atypical carcinoid (AC), small cell lung cancer (SCLC) and large cell neuroendocrine carcinoma (LCNEC). Classification of the four tumor categories is a step-wise process identified by the presence of necrosis and number of mitoses per 2mm². In NE tumor pathology, Ki-67 was first described as a prognostic factor in the pancreas and was incorporated into the grading system of digestive tract NE neoplasms in the 2010 World Health Organization (WHO) classification. However, the significance of Ki-67 has not been fully studied in PNETs. The purpose of our research is to investigate the potentially diagnostic value of Ki-67.

Design: We retrieved 157 surgical specimens of pulmonary neuroendocrine tumors (37 TC, 2 AC, 29 LCNEC, 89 SCLC) based on mitotic rate and histologic features. Manual Conventional Method (MCM) and a nuclear quantitation algorithm performed by Computer Assisted Image Analysis Method (CIAM) were used to calculate the Ki-67 proliferative index (PI). In CIAM, six equivalent fields (500 × 500μ) at 10× magnification were manually annotated for digital image analysis.

Results: The median mitotic count and Ki-67 index for TC, AC, LCNEC, and SCLC were 1 and 3.61%, 3.5 and 22.91%, 58 and 57.62%, 118.5 and 79.66%, respectively. However, the Ki-67 index overlapped among the four groups, with ranges of 0.38-12.66% for TC, 4.34-41.48% for AC, 30.67-93.74% for LCNEC, and 35.71-96.87% for SCLC. The tumor histologic grade can be divided into two groups by Ki-67 index of 10%. For the univariate survival analyses, both the Overall Survival (OS) and Progression Free Survival (PFS) correlated with Ki-67 index, mitotic number and nodal metastasis. But multivariate analysis revealed that none of Ki-67 index and mitotic figure were proved to be an independent prognostic factor for OS or PFS. In contrast, nodal metastasis was demonstrated to be an independent prognostic factor for OS in PNETs (P=0.002) and high grade NECs (P=0.009). Moreover, the Ki-67 index performed by CIAM was proved to be of great positive correlation with MCM.

Conclusions: Our results indicate that software-automated quantitation of Ki-67 index is a reliable method to predict the prognosis of PNETs. Ki-67 index can be a useful adjunct to pathologic grade in PNETs. Moreover, nodal metastasis was proved to be a more important prognostic factor among clinicopathological parameters.

2062 Adult Bronchopulmonary Dysplasia for Lung Transplantation: A Two Case Summary

Natalia Liu[1], *Oscar Cummings*[2], *Chadi A Hage*[3], *Chen Zhang*[4]. [1]Indiana University School of Medicine, Indianapolis, IN, [2]Indiana University School of Medicine, Indianapolis, IN, [3]Indiana University School of Medicine, [4]Indiana University, Indianapolis, IN

Background: Bronchopulmonary dysplasia (BPD) is a chronic lung disease in infancy and is usually seen in premature infants who require mechanical ventilation and oxygen therapy for acute respiratory distress. Although most patients wean from oxygen therapy by age 2-3 years, re-hospitalization for respiratory problems is common in these patients in their adulthood. There have been few studies that document the long-term outcomes of BPD survivors. Data on pulmonary function and radiographic findings of adult BPD are scarce; data on pathologic features of adult BPD are essentially non-existent.

Design: Two adult patients who underwent recent double lung transplantation for BPD at our institution were identified. Clinical data including clinical presentation, results of chest radiographic images, pulmonary function tests (PFT), cardiac catheterization, and echocardiography were retrieved from the electronic medical records. Hematoxylin & eosin (H&E) stained sections of the explant lungs were examined. Elastin stain was performed and examined on selective sections of each case.

Results: Both patients had similar clinical features including history of prematurity and long term mechanical ventilation after birth, severe obstructive ventilation defect with hyperexpanded lungs on PFT, airtrapping and mosaic attenuation on chest CT scan, and severe pulmonary arterial hypertension. Pathologic examination of the two cases showed some common features including fibrosis surrounding the bronchovascular bundles and within the interlobular septa and subpleural areas, thickening in the walls of the veins by fibromuscular hyperplasia, narrowing/obliteration of the small airways by muscular hypertrophy, and enlargement of airspace with thin alveolar septa (emphysematous changes). Small airway narrowing/obliteration were more prominent in one case. The other case showed more prominent acute bronchitis and bronchiolitis.

Conclusions: The two adult patients with BPD demonstrated similar pathological changes in their lungs, which may explain the common clinical findings in the two patients.

2063 Assessment of MUC4 and HER2 Protein Expression in Lung Tissue Sections of Severe Asthma Patients Using Digital Image Analysis

Oscar F Lopez Nunez[1], *Sally E Wenzel*[2], *Humberto Trejo Bittar*[3]. [1]University of Pittsburgh Medical Center, Pittsburgh, PA, [2]University of Pittsburgh Medical Center (UPMC), [3]University of Pittsburgh Medical Center (UPMC), Pittsburgh, PA

Background: In severe asthma, we have reported a significantly lower expression of the HER2 (ErbB2) receptor mRNA in bronchial epithelial cells in-vitro compared to milder asthma and healthy controls, which is associated with increased expression of its ligand MUC4. Here, we aimed to characterize and quantify in lung tissue sections the expression of MUC4 and HER2 in the small airways of severe asthmatics using immunohistochemistry and digital image analysis.

Design: Distal lung tissue obtained from video-assisted thoracoscopic surgery biopsy specimens from 5 control subjects (non-asthmatic and never smokers), 5 severe asthmatics and 6 severe asthmatics/asthmatic granulomatosis, were available for examination. Formalin-fixed paraffin-embedded tissue sections were stained for MUC4 (ThermoFisher Scientific, 1G8 clone) and HER2 (Ventana, 4B5 clone) followed by whole slide imaging. Protein expression was further assessed in the small airways by using the Aperio ImageScope software with the positive pixel count algorithm. The results were expressed as percentage of positive pixel counts (positivity) over the total number of pixels.

Results: HER2 protein expression was significantly diminished in the small airways of severe asthmatics and patients with asthmatic granulomatosis when compared to controls (positivity 0.9% and 1.5% vs. 17.3%, respectively, $p < 0.05$) (Figure 1). In contrast, MUC4 protein expression was elevated in the severe asthmatics and asthmatic granulomatosis patients when compared to the controls (positivity 9.3% and 11% vs 4.6%, respectively, $p<0.05$) (Figure 2).

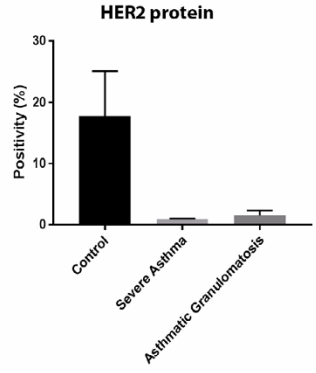

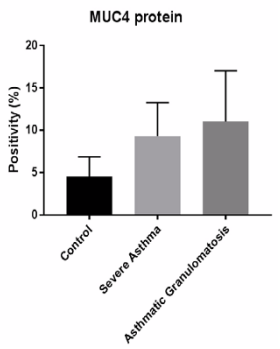

Conclusions: This is the first report using lung tissue sections from asthmatic patients demonstrating less HER2 protein with an associated upregulation of its ligand MUC4 in small airways. We hypothesize that the reduced HER2 expression might be associated with impaired proliferation and healing/repair, which might contribute to the bronchiolar scarring identified in the small airways of asthmatics.

2064 Interobserver Agreement on Frozen Section-based Substaging of T1 Lung Adenocarcinoma – Preliminary Results on an Institutional Experience

Xunda Luo[1], *Abir Mukherjee*[1], *Amandeep Aneja*[2]. [1]Temple University Hospital, Philadelphia, PA, [2]Temple University Hospital, Philadelphia, PA

Background: Sublobar lung resection is gaining popularity among thoracic surgeons as a less radical alternative treatment option for adenocarcinoma in situ (AIS) and microinvasive adenocarcinoma (MIA) because of excellent prognosis of these two lesions after a margin-negative resection. However, intraoperative frozen section (FS)-based diagnoses of these lesions is still lagging, especially in non-cancer centers with a general surgical pathology practice setting. The present study aimed to examine whether satisfactory interobserver agreement on FS-based diagnoses of AIS and MIA could be achieved under these circumstances.

Design: FS and corresponding permanent section (PS) slides of T1 lung adenocarcinoma cases surgically treated in the present institution between 2015 and 2017 were independently reviewed by two general surgical pathologists. The review process was not timed. Inter-observer and FS-PS concordance was examined by a third investigator.

Results: Seventeen T1 lung adenocarcinoma cases were reviewed and divided into AIS/MIA and non-AIS/MIA groups for agreement testing. The 2 pathologists agreed upon the diagnoses of 2 AIS/MIA and 12 non-AIS/MIA cases, disagreed upon the remaining 3 cases on the extent of the invasive component, with a moderate strength of agreement (*kappa*=0.46, *SE*=0.26). FS- and PS-based diagnoses by one pathologist agreed for 1 AIS/MIA and 14 non-AIS/MIA cases, disagreed upon the remaining 2 cases, with a moderate strength of agreement (*kappa*=0.45, *SE*=0.31). As of the second pathologist, FS- and PS-based diagnoses agreed for 3 AIS/MIA and 12 non-AIS/MIA cases, disagreed upon the remaining 2 cases, with a good strength of agreement (*kappa*=0.67, *SE*=0.21).

Conclusions: The concordance rates observed under these circumstances were comparable to those reported previously by several cancer centers. Despite the small sample size and non-timed review process of the present study, these results are encouraging in terms of promoting the practice of frozen section-based substaging of T1 lung adenocarcinoma. Interobserver variability on degree of invasion, frozen section quality, and timed diagnosis are major challenges faced by the pathologist in this scenario.

2065 Cancer Stem Cells of the Lung Adenocarcinoma, Emphasizing the Level during the Progression from Atypical Adenomatous Hyperplasia to Invasive Adenocarcinoma

Osamu Matsubara[1], *YASUTO JIN*[2], *Eugene Mark*[3]. [1]Hiratsuka Kyosai Hospital / The Cancer Institute, Hiratsuka, Kanagawa, [2]Hiratsuka Kyosai Hospital, Hiratsuka-shi, Kanagawa, [3]Massachusetts General Hospital, Boston, MA

Background: Cancer stem cells (CSCs) are considered to be responsible for tumorigenesis, progression and maintenance, so targeting CSCs metabolism has become a therapeutic approach to improve survival. Appreciation of cancer stem cells in lung adenocarcinoma is in a formative stage. Invasive adenocarcinoma, especially lepidic predominant adenocarcinoma, is thought to progress in a stepwise fashion from atypical adenomatous hyperplasia (AAH) to adenocarcinoma in situ (AIS), and to minimally invasive adenocarcinoma (MIA). This study was aimed to examine the change of the character and nature of cancer stem cells (CSCs) during the progression from AAH to invasive adenocarcinoma.

Design: We studied a series of 80 Japanese patients with lung adenocarcinoma who underwent resection by video-assisted thoracoscopic surgery or thoracotomy and who had no chemotherapy or radiotherapy before surgery. There were 56 males and 24 females with a median age of 72 years ranging from 45 to 86 years at the time of surgery. Fourty-six patients had a smoking history. The pathological stages were TNM stage I in 30 cases and stage II in 50 cases. All tissue specimens were formalin-fixed and paraffin-embedded. We found 22 cases of AIS, 8 cases of MIA, 50 cases of invasive adenocarcinoma, and 10 cases with multiple AAH lesions. An immunohistochemical analysis of CD133 (Miltenri Biotec), aldehyde dehydorogenase-1A1 (ALDH1A1) (Abcam) and CD44 (Abcam) was performed using Vectastain ABC Kit methods after antigen retrieval.

Results: The CD199 expression of the tumor cells showed membranous staining, and there were three distinct patterns appeared from the distribution and density of expression. In pattern 1, CD199-positive cells appeared in a group, usually lining small acinar or glandular structures of the adenocarcinoma. In pattern 2, there were one or two CD199-positive cells in the basal layer of small acinar or gland structures of the adenocarcinoma. In pattern 3, CD199-positive cells were not present. Patterns 1-2 were seen in 12 (24%) and 8 (16%) cases of invasive adenocarcinoma, individually. CD199-positive cells were not observed in any cases of AAH, AIS or MIA. In non-tumorous tissue

Conclusions: Our results provide that invasive adenocarcinomas of the lung commonly have higher expression levels of CD199-positive cells within the tumor and that CD199-positive cells were not observed in any cases of AAH, AIS or MIA. These findings suggest that CSCs might have an important role in progression and invasion of lung adenocarcinoma.

2066 EGFR and p53 Mutation Status in Lepidic and Non-Lepidic Lung Adenocarcinomas

Lauren Mecca[1], *Hanna Rennert*[2], *Qiulu Pan*[3], *Nasser Altorki*[4], *Sebron W Harrison*[2], *Mohamed K Hussein*[2], *Alain Borczuk*[5] [1]New York Presbyterian Hospital - Weill Cornell, New York, NY, [2]Weill Cornell Medicine, [3]Weill Cornell Medicine, New York, NY, [4]Weill Cornell Medicine, New York, NY, [5]Cornell University Medical Center, New York, NY

Background: Lung adenocarcinomas (AdCa) with exclusive or near-exclusive non-mucinous lepidic pattern are thought to be precursors of invasive subtypes. The origin of tumors without lepidic precursor is not as well understood, although one hypothesis is that morphologic evidence of the lepidic origin has been obliterated. The purpose of this study is to examine mutation rates among AdCa with (LEP-POS) and without (LEP-NEG) an identifiable non-mucinous lepidic component to unearth differences in trunk driver mutations that may reveal different origins, as well as differences in other mutations types among LEP-POS vs LEP-NEG subgroups.

Design: Consecutive resected primary lung AdCa (n=305) from a North American cohort were studied using an Ion Torrent Ion AmpliSeq™ Cancer Hotspot Panel. The cases were grouped according to predominant pattern (adenocarcinoma in situ (AIS), minimally invasive (MIA), acinar, lepidic, micropapillary, solid, papillary) and further subdivided into LEP-POS vs LEP-NEG cases. Mutations were tallied by group, including subtypes of EGFR mutation and KRAS mutations (transversion vs transition). The percentages of cases with mutations in each category were recorded and their proportions assessed for significance by Fisher exact test.

Results: EGFR mutations were found in 33% (70/211) of all LEP-POS primary lung AdCa versus 8% (8/95) of LEP-NEG cases(p = 0.0001). This finding was also identified in LEP-POS vs LEP-NEG acinar-predominant AdCa (35% (24/68) vs 5% (1/19), p = 0.009). While the

EGFR rate was higher in LEP-POS micropapillary tumors than LEP-NEG (36 vs 18%), this difference was not significant.

No cases of AIS (0/10) or MIA (0/39) were found to have p53 mutations. However, p53 was mutated in 14% of lepidic-predominant AdCA (8/58), p =.007. The rate of TP53 mutation in LEP-POS acinar predominant AdCa is 26.5%, also increased as compared to AIS and MIA. Rates of KRAS mutation, including transversion and transition types, were not different in the LEP-POS vs LEP-NEG subgroups.

Predominant Pattern	EGFR	KRAS	TP53
AIS	2/10 (20%)	2/10 (20%)	0/10 (0%)
MIA	12/39 (31%)	12/39 (31%)	0/39 (0%)
Lepidic	20/58 (34%)	20/58 (34%)	8/58 (14%)
Acinar – LEP-POS	24/68 (35%)	26/68 (38%)	18/68 (26%)
Acinar – LEP-NEG	1/19 (5%)	7/19 (37%)	1/19 (5%)
Micropapillary – LEP-POS	9/25 (36%)	9/25 (36%)	4/25 (16%)
Micropapillary – LEP-NEG	6/32 (19%)	12/32 (38%)	6/32 (19%)
Solid – LEP-POS	2/5 (40%)	0/5 (0%)	0/5 (0%)
Solid – LEP-NEG	1/26 (4%)	13/26 (50%)	13/26 (50%)

Table 1. Summary of AdCa Mutation Status

Conclusions: LEP-POS AdCa exhibit driver type EGFR mutations significantly more often than LEP-NEG AdCa and raises the possibility of a non-lepidic precursor for these latter tumors. The increasing presence of p53 mutations from AIS and MIA to lepidic-predominant AdCa indicates a role for p53 in a progression of lepidic pattern carcinogenesis and provides molecular support for the hypothesis that AIS and MIA may be precursor lesions to lepidic-predominant and LEP-POS acinar-predominant AdCa.

2067 Histologic ancillary findings in the distinction between idiopathic and secondary UIP patterns: a multidisciplinary approach in 100 consecutive open lung biopsies

Maria Cecilia Mengoli[1], *Gloria Montanari*[2], *Alberto Cavazza*[2], *Paolo Spagnolo*[3], *Giovanni Della Casa*[4], *Giovanni Sotgiu*[5], *Luisella Righi*[6], *Francesca Barbisan*[7], *Giuseppe Pelosi*[8], *Giulio Rossi*[9]. [1]Arcispedale Santa Maria Nuova-IRCCS Reggio Emilia, Reggio Emilia, Emilia Romagna, [2]Arcispedale S. Maria Nuova-IRCCS, Reggio Emilia, [3]University of Padova, [4]Policlinico of Modena, Modena, MO, [5]University of Sassari, [6]Orbassano, Italy, [7]Ospedali Riuniti di Ancona, Ancona, Ancona, [8]IRCCS MultiMedica Group Science & Technology Pole, Milan, MI, [9]Regional Hospital

Background: Usual interstitial pneumonia (UIP) pattern defines, when idiopathic, IPF, but may be encountered in several chronic ILD. We evaluated the utility of histologic "ancillary findings" in differentiating idiopathic *vs* secondary UIP in a multidisciplinary setting.

Design: We collected 100 open lung biopsies displaying UIP pattern. A pathological diagnosis of idiopathic *vs* secondary UIP was performed evaluating: honeycombing, fibroblastic foci, smoking-related findings, interstitial giant cells/granulomas, bronchiolocentric damage, bridging fibrosis, lympho-plasmacellular or eosinophilic infiltrates, lymphoid follicles, chronic pleuritis, metaplastic (bone/smooth muscle/adipose) tissue, intraalveolar proteinosis-like material. Demographic, clinical, functional, serological and imaging data were retrospectively collected. A multidisciplinary diagnosis was finally reached and compared with the original diagnosis.

Results: The study population included 74 male and 26 female patients (mean age 64 years). Thirty-eight patients reported environmental/occupational exposures. Serological autoimmune abnormalities were detected in 14 patients. Giant cells and/or granulomas, peribronchiolar metaplasia, bridging fibrosis lympho-plasmacellular infiltrate, follicles with germinal centers and eosinophils were present in 35%, 44%, 34%, 52%,7% and 6% of cases, respectively. Chronic pleuritis, metaplastic tissue and proteinosis-like alveolar material were detected in 6%, 50% and 16% of cases. Histologic examination favoured "idiopathic" UIP in 54% and "secondary" UIP in 46% of cases. Overall, following MDD and taking into account the presence of ancillary findings, the initial diagnosis changed in 21% of cases. Specifically, the proportion of IPF diagnoses dropped from 86% to 65%, while that of chronic HP and CTD-ILD increased from 13% to 24% and from 2% to 7%, respectively.

Conclusions: Interstitial giant cells and/or granulomas, peribronchiolar metaplasia, chronic pleuritis and lymphoid follicles significantly (p<0.001) correlated with a non-idiopathic UIP pattern. The presence of histologic ancillary features increases the diagnostic accuracy of fibrotic ILD in a MDD setting.

2068 Micropapillary Adenocarcinoma (MPC) of the Lung: Diagnostic Reproducibility and Morphologic Criteria Amongst Pulmonary Pathologists

Ross Miller[1], *Paloma Monroig-Bosque*[2], *Joel A Morales*[3], *Anja Roden*[4], *Andrew Churg*[5], *Roberto Barrios*[6], *Philip T Cagle*[7], *Yimin Ge*[7], *Timothy Allen*[8], *Henry Tazelaar*[9], *Maxwell Smith*[10], *Brandon Larsen*[10], *Lynette Sholl*[11], *Mary B Beasley*[12], *Alain Borczuk*[13], *Kirtee Raparia*[14], *Alberto Ayala*[1], *Jae Y. Ro*[15]. [1]Houston Methodist Hospital, [2]Houston Methodist, Houston, TX, [3]University of Puerto Rico School of Medicine, [4]Mayo Clinic Rochester, Rochester, MN, [5]Vancouver General Hospital, Vancouver, BC, [6]The Methodist Hospital, Houston, TX, [7]Houston Methodist Hospital, Houston, TX, [8]Univ. of Texas Medical Branch, Galveston, TX, [9]Mayo Clinic, Scottsdale, AZ, [10]Mayo Clinic Arizona, Scottsdale, AZ, [11]Brigham & Women's Hospital, Boston, MA, [12]Mount Sinai Health System, [13]Cornell University Medical Center, New York, NY, [14]Northwestern University, Chicago, IL, [15]Houston Methodist Hospital, Cornell University, Houston, TX

Background: MPC of the lung is considered an aggressive variant of lung adenocarcinoma frequently manifesting with advanced stage and having a poor prognosis. Recent studies have proposed that the presence of any micropapillary component, regardless of the overall percentage, is critical to identify as it has negative prognostic implications, particularly shortened survival. To date, no studies have investigated the morphological criteria used by pathologists to classify MPC of the lung.

Design: Sixty digital images, each from hematoxylin and eosin-stained slides representing possible MPC (2 images per case), were distributed to 16 pulmonary pathologists; each pathologist was asked to classify cases as MPC or not. The following morphological features were recorded as present or absent for each case independent of the reviewers' diagnosis: columnar cells, elongate slender cell nests/processes, extensive stromal retraction, lumen formation with internal epithelial tufting, epithelial signet ring-like forms, intracytoplasmic vacuolization, multiple nests in stromal lacunar spaces, or alveolar spaces, back-to-back lacunar spaces, epithelial nest anastomosis/confluence, marked pleomorphism, peripherally oriented nuclei, randomly distributed nuclei, tumor cell nest size (≤4, ≤12 or >12), fibrovascular core, and spread through air-spaces (STAS). Heatmap representations with hierarchical clustering of the diagnostic interpretations were created, and dendograms denoting the frequency of pathologists reporting the pre

Results: Cluster analysis of the diagnostic interpretations showed three subgroups: micropapillary (MPC3), combined papillary and micropapillary (MPC2), and others (MPC1). These subgroups correlated with the median percentage of MPC component reported. In addition, three subgroups were identified by cluster analysis when looking at the morphologic features. These significantly correlated with the three diagnostic subgroups. The most common morphological features being utilized to diagnose MPC were: "multiple tumor cell nests in the same lacunar/alveolar space, small-medium tumor cell nest size (≤4 cells thick), and absence of central fibrovascular cores". In cases with mixed histologic components; "peripherally oriented nuclei (inverted polarity) and lumen formation with internal epithelial tufting" were also features being used to identi

Conclusions: Overall, there was good agreement for diagnosing MPC. The most common utilized diagnostic features include "multiple nests within the same lacunar/air

2069 Thoracic Hyalinizing Clear Cell Carcinoma: A Series of 3 Cases

Joseph Montecalvo[1], *Lei-Chi Wang*[2], *Chih-Jung Chen*[3], *Natasha Rekhtman*[1], *Nora Katabi*[1], *Ronald Ghossein*[1], *Cristina R Antonescu*[1], *William Travis*[1]. [1]Memorial Sloan Kettering Cancer Center, New York, NY, [2]Taipei Veterans General Hospital, Taipei, Taiwan, [3]Changhua Christian Hospital, Changhua, Taiwan

Background: Hyalinizing clear cell carcinoma (HCCC) is a well-known, typically low grade salivary gland tumor in the head and neck region but only five cases have previously been reported arising in the lung. We examined the clinicopathologic, radiologic, and cytogenetic features of 3 new cases of primary thoracic HCCC (THCCC).

Design: Three cases of THCCC from the pathology files and the personal consults of one of the authors were included in our study. The tumor location, gross anatomic features, clinical history, and clinical outcomes were reviewed. H&E slides and immunohistochemical stains were re-reviewed, and fluorescence in situ hybridization (FISH) with *EWSR1* and *ATF1* probes was performed in all cases.

Results: Patients were 40, 61, and 76 years old with 1 male and 2 females. All patients were asymptomatic and nonsmokers. Two tumors were located adjacent to the bronchioles, and one tumor was located endobronchially. In 2 cases chest computed tomography scans showed solitary, solid, and well-circumscribed tumors measuring 2.0 and 2.7 cm. No tumors were identified elsewhere, in particular the salivary glands or oropharngolaryngeal area. The histologic features were similar in all cases; namely, monotonous and polygonal tumor cells showing clear to eosinophilic cytoplasm forming nests and cords

as well as a background of diffusely hyalinized and focally fibrocellular myxoid stroma. No necrosis and virtually no mitotic figures were seen. The periphery of the tumor showed a cuff of lymphoid follicles and lymphoplasmacytic infiltrate. All three cases were diffusely positive for cytokeratin, p40 and/or p63, while consistently negative for TTF1. No myoepithelial cells were seen morphologically or by immunohistochemistry with negativity for S100, SMA, and calponin. Focal intracytoplasmic mucin was seen by mucicarmine stain. All cases showed the presence of *EWSR1* and *ATF1* gene rearrangements. Follow up showed no evidence of recurrence in all cases.

Conclusions: THCCCs show characteristic morphologic, immunophenotypic, and cytogenetic findings. However, due to their rarity presenting in the lung, they present a diagnostic challenge due to overlapping features with other entities of both primary and metastatic tumors to the lungs. Recognition of the characteristic morphologic and immunohistochemical features followed by confirmation of *EWSR1* and *ATF1* gene rearrangements by FISH are critical for accurate diagnosis.

2070 Pulmonary BRG1 (SMARCA4)-deficient undifferentiated neoplasms represent an exceptionally aggressive type of sarcomatoid carcinoma: Clinicopathologic and genomic evidence supports a link to non-small cell carcinoma

Joseph Montecalvo[1], *Deepu Alex*[1], *Ryan Ptashkin*[2], *Ai Ni*[3], *Jennifer L Sauter*[1], *Jason Chang*[1], *Achim Jungbluth*[3], *Amanda Beras*[2], *Azadeh Namakydoust*[2], *Charles Rudin*[2], *Marc Ladanyi*[4], *Cristina R Antonescu*[1], *William Travis*[4], *Natasha Rekhtman*[4]. [1]Memorial Sloan Kettering Cancer Center, New York, NY, [2]MSKCC, [3]MSKCC, New York, NY, [4]Memorial Sloan-Kettering CC, New York, NY

Background: Highly aggressive, undifferentiated thoracic neoplasms characterized by BRG1 (*SMARCA4*) deficiency and rhabdoid-like morphology have been recently described and proposed to represent a type of sarcoma. *BRG1* deficiency also occurs in a subset of conventional lung non-small cell carcinomas (NSCC) with poor differentiation and aggressive behavior. We sought to assess whether these tumors represent distinct entities.

Design: We identified 22 BRG1-deficient undifferentiated neoplasms (BDUNs) involving the lung with morphologic features of "*SMARCA4*-deficient thoracic sarcomas" and 45 BRG1-deficient conventional lung carcinomas (BDC), and compared their clinicopathological and immunohistochemical features. Next generation sequencing (NGS) of 341+ genes was performed on 16 BDUNs, 45 BDCs and 39 conventional sarcomas.

Results: Of 22 BDUNs, 17 were entirely undifferentiated (rhabdoid-like, monomorphic, discohesive), whereas 5 had composite histology, containing areas of both BDUN and conventional NSCC. BRM (*SMARCA2*) co-deficiency occurred in 17/22 (77%) BDUNs vs 1/45 (2%) BDCs ($P<0.0001$). Similarly, claudin-4 was negative in all BDUNs vs only 1/45 BDCs ($P<0.0001$). Although keratins were absent or minimal in 82% of BDUNs, EMA was consistently positive. Focal TTF-1 was detected in 3 BDUNs. By NGS, 56% of BDUNs harbored classic NSCC mutations (*STK11*, *KEAP1*, *KRAS*, *NF1*). Importantly, 85% of BDUNs exhibited a strong genomic smoking signature, similar to BDCs, whereas none of 39 conventional sarcomas in a control group had this signature. Clinically, BDUNs occurred primarily in smokers (90%), and were associated with dismal survival (median 5.2 mo), which was significantly worse than that for stage-matched BDCs (20.7 mo; $P=0.004$).

Conclusions: Pulmonary BDUN represents an exceptionally aggressive, de-differentiated variant of NSCC. The relationship with NSCC is supported by 1) existence of composite tumors, 2) consistent EMA and occasional TTF-1 expression, 3) genomic alterations typical of NSCC, and 4) strong genomic smoking signature, in line with predominance in smokers. Nevertheless, BDUNs are phenotypically and prognostically distinct from conventional BDCs. We propose that BDUNs represent a distinct type of sarcomatoid carcinoma, in which emergence of de-differentiated, claudin-4-negative component is mediated by co-deficiency of BRG1+BRM and possibly other components of SWI/SNF complex, analogous to BRG1-deficient undifferentiated carcinomas of endometrium and other sites.

2071 SMARCA4 (BRG1) deficiency in lung carcinomas correlates with poor differentiation and aggressive clinical behavior

Joseph Montecalvo[1], *Deepu Alex*[1], *Ryan Ptashkin*[1], *Ai Ni*[1], *Jennifer L Sauter*[1], *Jason Chang*[1], *Amanda Beras*[1], *Azadeh Namakydoust*[1], *Charles Rudin*[1], *Marc Ladanyi*[1], *Cristina R Antonescu*[1], *William Travis*[1], *Natasha Rekhtman*[1]. [1]Memorial Sloan Kettering Cancer Center, New York, NY

Background: *SMARCA4* (BRG1), a key member of SWI/SNF chromatin remodeling complex, is mutated in a subset of lung carcinomas. There are only limited data on the prevalence of *SMARCA4* mutations in various lung carcinoma subtypes, as well as their clinicopathologic and genomic associations, although proclivity for poor differentiation and aggressive behavior has been suggested. Furthermore, the concordance between *SMARCA4* mutations and BRG1 expression is not well established.

Design: We queried the 341+ gene targeted next-generation sequencing results of 2668 lung cancers to identify cases with *SMARCA4* truncating mutations or deletions. Mutated cases with available tissue were analyzed for BRG1 expression by immunohistochemistry (IHC). Clinicopathologic and genomic features of carcinomas with BRG1 loss were reviewed. Undifferentiated, rhabdoid-like tumors were excluded.

Results: Out of 2668 lung cancers, 116 (4.3%) harbored *SMARCA4* deleterious alterations (DA). These alterations were more prevalent in lung adenocarcinomas (AdCA; 90/2024; 4.4%) than squamous cell carcinomas (4/261; 1.5%; $P=0.03$), and were entirely absent in small cell carcinomas (0/131; $P=0.006$). Increased prevalence was seen in unclassified non-small cell carcinomas (NSCC; 16/130; 12%; $P=0.0003$), adenosquamous carcinomas (2/22; 9%) and sarcomatoid carcinomas (1/15; 7%). By IHC, BRG1 expression was lost in 45 of 60 (75%) carcinomas with *SMARCA4* DAs ($BRG1^-$). By NGS, $BRG1^-$ carcinomas exhibited typical profiles of smoking-related NSCC, including *STK11* (53%), *KEAP1* (49%), and *KRAS* (38%) mutations, in line with predominance in smokers (91%). $BRG1^-$ AdCAs had at least focal (88%) or predominant (63%) solid histology, and were commonly TTF-1-negative (60%). Conversely, cases with *SMARCA4* DAs but retained BRG1 expression ($BRG1^+$) were more common in never smokers (27%), lacked the solid histology/TTF-1-negative association, and had lower *STK11* ($P=0.008$) and higher *EGFR* ($P=0.01$) mutation rate. $BRG1^-$ patients had significantly worse overall survival than $BRG1^+$ patients (median survival 16 vs 26 mo, respectively; $P=0.026$).

Conclusions: This is the largest study to date on *SMARCA4* mutations and BRG1 expression in lung carcinomas. *SMARCA4* deficiency has a predilection for AdCAs and is associated with poor/aberrant differentiation and aggressive clinical behavior. Tumors with *SMARCA4* DAs but intact BRG1 expression lack the aggressive phenotype of $BRG1^-$ carcinomas, highlighting the importance of IHC in the analysis of SWI/SNF pathway aberrations.

2072 Lung adenocarcinoma with MET exon 14 skipping mutation; clinicopathological characteristics and immunohistochemical MET expression

Noriko Motoi[1], *Kuniko Sunami*[2], *Yuichiro Ohe*[2], *Shun-ichi Watanabe*[2], *Takashi Kohno*[3]. [1]National Cancer Center Hospital, Chuoku, Tokyo, [2]National Cancer Center Hospital, [3]National Cancer Center Research Institute

Background: A subset of lung adenocarcinoma (LAD) has a MET exon 14 skipping mutation that is a promising therapeutic target. In this study, we examined clinicopathological characteristics of surgically resected LAD with MET 14 skipping mutation as well as MET protein expression.

Design: Out of 608 consecutive surgically resected LAD between 1997 and 2008, 7 cases with MET exon 14 skipping mutation were recruited. The MET mutation was screened by a formalin-fixed paraffin-embedded (FFPE) tissue-based molecular counting assay (nCounter system (NanoString technologies) with combination of RT-PCR. The detailed pathological evaluation was performed including WHO 8th edition based predominant subtype and cellular features on whole FFPE slides. Clinicopathological features, including the 8th UICC-TNM staging and patient outcome, were reassessed and retrieved from the medical chart. Immunohistochemical examination of 4-um thick FFPE section slides was performed using antibodies against c-MET (SP-44, Ventana) and phosphorylated MET (Tyr1234/1235) (D26; Cell Signaling technology). The H-score (range 0-300) was calculated.

Results: LAD with MET exon 14 skipping mutation was average age group at operation was 64-year-old (range 58-81) and 5 male and 2 female. Total and invasion size of the tumor was 30/22 mm in average, ranging 15-58/ 4-58mm, respectively. There were each two cases of stage IA1, IA2, and IA3 and one case of stage IIB1. All but one stage IIB1 cases were alive without disease (median observation period was 124 months). WHO histological subtype was 3 lepidic, 2 papillary 1 acinar and 1 solid. All stage I cases had hobnail/cuboidal tumor cell type, with one case of mild pleomorphism. One stage IIB case showed pleomorphic tumor cells with nuclear atypia. Clear cell features were noted in four cases including stage IIB. MET-mutated LAD showed a wide range of immunoreactivity for c-MET (H-score median 100, range 10 to 180) and all cases were negative for p-MET.

Conclusions: LAD with MET exon 14 skipping mutation shows a various histological pattern of hobnail/ cuboidal cells with clear cell features in some cases. By immunohistochemical staining, c-MET/p-MET protein was not constantly detectable on FFPE section. Our study results indicated that morphology-based and/or immunohistochemistry-based screening has low predictive power.

2073 Is Insulinoma-Associated Protein 1 (INSM1) A Reliable Neuroendocrine Marker in Lung Pathology? An Immunohistochemical Study of 324 Cases

Sanjay Mukhopadhyay[1], *Josephine Dermawan*[1], *Carol Farver*[2]. [1]Cleveland Clinic, Cleveland, OH, [2]Cleveland Clinic, Cleveland, OH

Background: Recent evidence suggests a role for the nuclear marker INSM1 in the diagnosis of neuroendocrine lung neoplasms. Our aim was to validate these findings in a large series of whole-tissue sections and investigate INSM1 expression in lung lesions whose INSM1 status has not been previously reported.

Design: We stained 274 primary lung neoplasms (246 whole-tissue sections 246, 13 biopsies, 15 tissue microarray) with INSM1 (A-8, Santa Cruz). A subset of these cases was stained with synaptophysin (SYN), chromogranin (CHR) and CD56. There were 37 small cell lung carcinomas (SCLC), 23 large cell neuroendocrine carcinomas (LCNEC), 34 carcinoid tumors (32 typical, 2 atypical), 128 adenocarcinomas, and 32 squamous cell carcinomas. Previously untested primary lung tumors included adenosquamous carcinoma (4), large cell carcinoma (4), sarcomatoid carcinoma (4) and 1 case each of sclerosing pneumocytoma, adenoid cystic carcinoma, mucoepidermoid carcinoma, epithelial-myoepithelial carcinoma and hamartoma. We also stained 20 carcinoid tumorlets and 30 meningothelial-like nodules. Any nuclear staining for INSM1 was considered positive.

Results: The sensitivity of INSM1 for SCLC (97%) was equal to SYN (97%) and greater than CHR (74%) and CD56 (86%) (Table 1). For LCNEC, CD56 (94%) and SYN (87%) were more sensitive than INSM1 (75%). All markers stained 100% of carcinoid tumors. INSM1 staining was focal (<10%) in 8% of SCLC, 67% of LCNEC and 0% of carcinoids. All INSM1-positive non-neuroendocrine tumors stained only focally. The sensitivity of INSM1 for neuroendocrine lung neoplasms as a group (93%) was identical to CD56 (93%) and SYN (93%) and higher than CHR (72%). The specificity of INSM1 for neuroendocrine lung neoplasms (98%) was similar to CHR (98%) but higher than SYN (88%) or CD56 (88%). All previously untested primary lung tumors were INSM1-negative. Carcinoid tumorlets were positive (20/20) for INSM1 and meningothelial-like nodules were negative (0/30).

Table 1: INSM1 in Lung Neoplasms

	INSM1	SYN	CHR	CD56
SCLC	36/37 (97%)	23/24 (97%)	17/23 (74%)	12/14 (86%)
LCNEC	18/24 (75%)	20/23 (87%)	11/24 (46%)	15/16 (94%)
Carcinoid tumor	34/34 (100%)	12/12 (100%)	21/21 (100%)	15/15 (100%
Adenocarcinoma	4/128 (3%)	3/25 (12%)	1/79 (1%)	7/86 (8%)
Squamous cell carcinoma	0/32 (0%)	0/1 (0%)	0/22 (0%)	5/22 (23%)
Adenosquamous carcinoma	0/3 (0%)	N/A	1/2 (50%)	1/3 (33%)
Large cell carcinoma	0/4 (0%)	N/A	0/1 (0%)	0/1 (0%)
Sarcomatoid carcinoma	0/4 (0%)	N/A	0/1 (0%)	1/1 (100%)
Other neoplasms	0/5 (0%)	N/A	0/1 (0%)	0/1 (0%)

Conclusions: INSM1 is highly sensitive for SCLC, less sensitive than CD56 and SYN for LCNEC, and equally sensitive as other neuroendocrine markers for carcinoid tumors. The specificity of INSM1 for neuroendocrine differentiation is comparable to CHR and considerably higher than SYN or CD56. In whole-tissue sections of resected tumors, INSM1 staining is focal in a small subset of SCLC and a significant proportion of LCNEC. INSM1 positivity in carcinoid tumorlets and absence of INSM1 staining in meningothelial-like nodules are novel observations.

2074 Prominent Expression of the Negative Immune Checkpoint Regulator VISTA in Malignant Pleural Mesothelioma (MPM)

Stephanie Muller[1], *Marjorie Zauderer*[1], *Patrice Desmeules*[2], *Achim Jungbluth*[1], *Miriam Fayad*[1], *Denise Frosina*[1], *Ai Ni*[1], *Marc Ladanyi*[1], *Jennifer L Sauter*[1]. [1]Memorial Sloan Kettering Cancer Center, New York, NY, [2]Quebec Heart and Lung Institute, QC

Background: VISTA, a V-domain Ig-containing suppressor of T cell activation is an immune checkpoint gene involved in inhibition of anti-tumor responses and is a potential mechanism of resistance in cancers that fail to respond to anti-PD-L1 immunotherapy (IT). As many MPMs, especially of epithelioid (E) subtype, respond poorly to the latter, we sought to examine VISTA expression in MPM by immunohistochemistry (IHC).

Design: VISTA (D1L2G) and PD-L1 (E1L3N) IHC was performed on 55 MPMs (52 on tissue microarray [TMA]; 3 whole tissue section [WTS]; 40 E, 11 biphasic [B], 4 sarcomatoid [S]), 10 benign pleura (BP) (VISTA only; WTS) and on MPMs from 10 patients (WTS; 8 E, 2 S) subsequently treated with anti-PD-L1 IT. Percentage cytoplasmic (VISTA)/membranous (PD-L1) staining in tumor cells and in inflammatory cells was scored. High expression was defined as > 50% of tumor cells positive. Clinical follow up (response, stable or progressive disease, progressive) was obtained for patients in the IT cohort.

Results: 49 (89%) of MPMs on TMA demonstrated VISTA expression (90% of E, 100% of B and 50% of S). High expression was seen in 31 (63%) MPMs (69%, 45% and 50% of E, B and S, respectively) positive for VISTA. VISTA stained inflammatory cells in 38 (73%; n=52) MPM cases. VISTA was expressed in all BP tested. 14 (29%; n=49) MPMs were positive for PD-L1 (9/35 E, 3/10 B and 2/4 S), 6 with high expression. PD-L1 positivity in inflammatory cells was seen in 5/49 (10%) MPM cases.

Of 10 MPM patients treated with IT, 9 expressed VISTA and 7 expressed PD-L1: 8 cases showed high expression of VISTA; 1 case with low expression was negative for PD-L1; and none displayed high PD-L1 expression. On follow up, stable disease was seen in 3 patients and 7 progressed. Pretreatment MPMs in all patients with stable disease and in 3 patients with progression were positive for both markers. MPMs in 3 patients with progression were positive for VISTA only, and 1 was positive for PD-L1 only.

Conclusions: We report strong expression of the negative checkpoint regulator VISTA in a majority of MPMs versus lower expression of PD-L1. High VISTA expression in MPM may be related to poor responses to anti-PD-L1 IT seen in some patients. VISTA may also represent a novel IT target in MPM as anti-VISTA therapies are on the horizon.

2075 Proteomic Analysis of Tracheobronchial Amyloidosis Demonstrates Polytypic Immunoglobulins

Prasuna Muppa[1], *Jason D Theis*[2], *Surendra Dasari*[1], *Ellen McPhail*[1], *Paul Kurtin*[1], *Karen Rech*[1]. [1]Mayo Clinic, Rochester, MN, [2]Mayo Clinic

Background: Tracheobronchial amyloidosis (TBA) presents as multifocal deposits in the tracheobronchial tree, and is not associated with systemic disease. Studies using immunohistochemistry (IHC) have characterized these deposits as AL (immunoglobulin light chain) type. However, in contrast to other forms of AL amyloid, an underlying clonal process has not been demonstrated. In this study, we used liquid chromatography-mass spectrometry (LC-MS) to characterize these amyloid deposits.

Design: Ninety-five tracheobronchial amyloidosis cases were identified in the Mayo Clinic Mass Spectrometry laboratory. Amyloid deposits were isolated from formalin-fixed, paraffin-embedded specimens using laser microdissection, digested into tryptic peptides and analyzed by LC-MS. MS spectra were identified through validated database search engines augmented with known protein sequences from human light chain variable (LCV) region peptides to assess clonality of the immunoglobulins. In a subset of cases (25), clinical information was obtained and additional studies to assess clonality were performed (IHC for kappa and lambda light chains and immunoglobulin gene rearrangement studies).

Results: All cases showed peptide profiles consistent with AL type amyloid. 52% had a predominance of kappa peptides and 48% lambda peptides. The profiles were distinct from previously analyzed systemic AL amyloid cases, in that LCV region peptides originating from multiple different LCV genes were identified in 91% of patients, suggesting a polytypic immunoglobulin composition. In the other 9%, data were insufficient to determine immunoglobulin composition. In the patients with available clinical information, none developed systemic amyloidosis within 48 months median follow up. Only 1 of 25 samples showed a clonal immunoglobulin gene rearrangement. The plasma cell infiltrate in this vocal cord biopsy also appeared clonal by IHC studies, suggesting that this case does not fit with the category of TBA.

Conclusions: By proteomic analysis, TBA appears to be comprised of polytypic immunoglobulins. The most likely source of the immunoglobulins is the local plasma cells, which also appear polytypic by IHC and molecular genetic studies. The predisposing conditions that lead to amyloid fibril formation in the setting of these polyclonal plasma cell infiltrates requires further investigation.

2076 Unexpected Pathology Findings in Lung Explants: A 5-Year Retrospective Review at a High Volume Transplant Center

Charlotte Myers[1], *Ross Miller*[1]. [1]Houston Methodist, Houston, TX

Background: High volume lung transplant centers receive a number of explanted organs for pathologic evaluation. With regard to lung transplantation, the underlying disease process is typically known on account of clinical and radiographic findings. Microscopic review of these lungs often shows end-stage lung disease. However, pathology evaluation of lung explants may still reveal unexpected findings and add relevant clinical information.

Design: We reviewed lung explanted specimens from 385 patients from our institution (a high volume transplant center) from July 2012 to July 2017. Collected data included age, gender, underlying indication

for the transplant, type of transplant (single, double, or multi-organ), and pathologic findings seen in the explanted lung. Retrospective review of pre-operative imaging was performed in cases where an unexpected finding was detected in the explanted specimen.

Results: Data analysis from July 2012 to July 2017 identified 14 cases (3.6%) of incidentally discovered neoplasms in lung explants and 10 cases (2.7%) with incidental infectious organisms. The vast majority of cases showed correlation between the presumed underlying clinical diagnosis and the final pathologic diagnosis (99%), yet one case showed chronic hypersensitivity pneumonitis in a patient undergoing transplant for clinically diagnosed COPD. In the cases where incidental neoplasms were found, 8 were carcinoid tumors, 3 were invasive primary adenocarcinomas, 2 were primary squamous cell carcinomas, and 1 was metastatic adenocarcinoma.

Conclusions: Unanticipated findings in explanted lungs do occur. In our cohort, neoplasms were the most commonly identified incidental finding. However fungal organisms and hypersensitivity pneumonitis were also seen. None of these were suspected on preoperative imaging studies.

2077 Clinicopathologic Features of Patients with Lung Adenocarcinoma in Central New York Harboring BRAF V600E Mutations

Rochelle Nagales Nagamos[1], *Shengle Zhang*[2]. [1]SUNY Upstate Medical University, Syracuse, NY, [2]SUNY Upstate Medical Univ, Syracuse, NY

Background: BRAF mutation is a driver mutation in lung adenocarcinomas which accounts for about 2-3% of NSCLC cases. Recently, FDA approved dabrafenib (BRAF inhibitor) and trametinib (MEK inhibitor) as combined targeted therapy for patients with BRAF V660Emutation positive lung adenocarcinoma. BRAF V600E mutation is a predictive biomarker of treatment response to BRAF inhibitor. Its clinicopathologic features are not well studied, particularly its histologic presentation.

Design: Demographics, histologic type and BRAF V600E mutation of 314 patients diagnosed with primary or metastatic lung adenocarcinoma between the periods of 01/2015 to 07/2017 (34 months) in multiple hospitals in central New York were reviewed and evaluated. BRAF V600E mutations were tested by lab-developed real time PCR assay. The specimen is comprised of surgical (66%) routine and biopsy tissues as well as cytology (34%) tissues and fluid.

FOR TABLE DATA, SEE PAGE 763, FIG. 2077

Conclusions: The BRAF V600E mutation is found in 1.3 % of patients with lung adenocarcinoma, slightly lower than national average of 2.1%. BRAF V600E mutation tends to occur in male patients with smoking history. Majority of the cases (75%) were at advanced stage at the time of diagnosis, and had poorly differentiated histologic subtype (75%). These findings may aid in decision-making on tumor selection for BRAF V600E mutation testing and identify patients for targeted therapy.

2078 Histopathologic Clues to the Diagnosis of Lung Cysts Associated with Birt-Hogg-Dubé Syndrome (BHDS): An analysis of 57 Cases in Comparison with Idiopathic Bullae/Blebs

Yukio Nakatani[1], *Mitsuko Furuya*[2]. [1]Chiba University Hospital, Chiba, Japan, [2]Yokohama City University Graduate School of Medicine, Yokohama, Kanagawa

Background: Birt-Hogg-Dubé syndrome (BHDS) is a hereditary disorder caused by *FLCN* germline mutation. Approximately 30 % of *FLCN* mutation carriers develop renal cell carcinomas (RCCs), and over 90% of BHDS patients have lung cysts which frequently cause pneumothorax before the onset of RCCs. Therefore, it is critical for pathologists to diagnose the BHDS lung cysts correctly, but these specimens are frequently misdiagnosed as non-specific bullae/blebs (NSB/B). The aim of this study was to clarify the histopathologic clues to the differential diagnosis between the two.

Design: We performed histopathological analysis of lung specimens resected either for pneumothorax or for diagnostic purpose in 57 patients who had final genetic confirmation of *FLCN* mutations. Lung specimens diagnosed as NSB/B in 25 patients with spontaneous pneumothorax were also analyzed for comparison. Cystic lesions were subdivided into intraparenchymal lesions (IPL) and pleural/subpleural lesions with protrusion into pleural cavity (P/SPL) and separately analyzed. Immunostaining for CAM5.2 and TTF-1 was performed in selected cases of BHDS lung cysts and in all cases of NSB/B.

Results: IPL type cysts were observed in 86% (49/57) of the BHDS cases. These cysts were thin-walled and well-demarcated with pneumocyte lining, resembling a giant alveolus. Peculiar involvement of the interlobular septum and bronchovascular bundle by part of the cyst wall was seen in 82% (40/49) and 16% (8/49) of the BHDS cases, respectively. An intracystic alveolar septum-like or complex alveolus-like structure (CAS), was present in 72% (35/49). The IPL type cyst with these features was not seen in 25 NSB/B cases. Perilesional fibrosis/inflammation was less frequently associated with IPL type cysts of BHDS cases (16%, 8/49) than with those of NSB/B cases (80%, 16/20). P/SPL type cyst walls showed fibrous thickening and chronic inflammation in both BHDS and NSB/B cases, closely resembling each other; however, those in BHDS cases showed epithelial lining, and CAS was seen in 88% (23/26); NSB/B cases had cysts with absent or near absent epithelial lining in 92% (23/25), and CAS-like changes, seen in 24% (6/25), were mostly in continuity with emphysematous change.

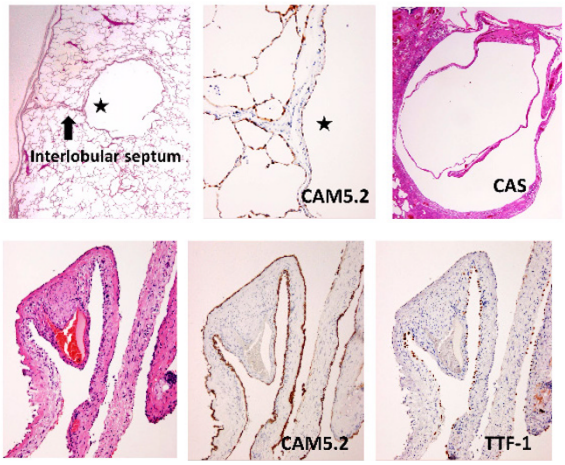

Conclusions: Complete epithelial lining**,** intimate association with the interlobular septum/bronchovascular bundle, and CAS are the useful features that can distinguish BHDS-associated lung cysts from NSB/B, and thereby help us determine whether the cases should be considered for genetic testing.

2079 Immune Microenvironment Markers (PD-L1, WARS, IDO) and Clinical Outcomes in Mucinous Lung Adenocarcinomas

Gahie Nam[1], *Yiang Hui*[1], *Liz Edmund*[2], *Kara A Lombardo*[3], *Ece Uzun*[4], *Nimesh R Patel*[3], *Maria Garcia-Moliner*[3], *Shaolei Lu*[5], *Li Juan Wang*[6]. [1]Alpert Medical School of Brown University, Providence, RI, [2]Brown University/ Rhode Island Hospital/ Lifespan, Providence, RI, [3]Rhode Island Hospital, Providence, RI, [4]Rhode Island Hospital, [5]Brown University, Providence, RI, [6]Barrington, RI

Background: The tumor immune microenvironment is increasingly recognized in understanding the behavior and predicting the clinical outcome in a variety of tumors. Mucinous lung adenocarcinoma (MLA) is a unique variant of lung adenocarcinomas with a distinct immunohistochemical and molecular profiles but little is known regarding its tumor immune microenvironment. We studied PD-L1, WARS, IDO expressions in MLAs.

Design: Tissue microarrays were constructed with MLA resections from 1995 to 2015. Immunohistochemistry for PD-L1, IDO and WARS were performed. Staining was scored based on intensity (strong=3, weak=1) and extent (0-1%=0, 1-4%=1, 5-50%=2, >50%=3). Total score of ≥4 was considered positive. Targeted next generation sequencing for KRAS mutations was performed. Clinical and survival data were documented.

Results: Eighty patients were identified with a mean age of 66.6 years (38-90) and female-to-male ratio of 1.35. 78.8% were known smokers. The mean tumor size was 3.51 cm (0.6-9.5 cm). 34 patients (43%) were diagnosed at pT1, 31 (39%) at pT2, 8 (10%) at pT3, 6 (8%) at pT4, 1 (1%) at Tis. KRAS mutations were detected in 16 of 25 cases. 37 cases (46%) were positive for PD-L1 in the tumor cells. 38 (48%) were PD-L1-positive within the stroma/lymphocytes. IDO was positive in 60 cases (75%) while WARS was positive in 66 cases (83%). The median follow-up time was 35 months (2-159) and median time to disease progression was 15.5 months (7-63). Recurrence was associated with higher tumor grade (46% vs 16%, p=0.0236) and multifocality (62.5% vs 26.9%, p=0.0388). Distant metastasis was associated with lymph node metastasis (39% vs 14%, p=0.041). IDO-positive tumors were associated with lymphovascular invasion (p=0.0298). WARS-positive tumors were associated with higher T stage (p=0.033). PD-L1 positivity in tumor epithelium was associated with longer overall survival (median survival: 114 vs 59 months, p= 0.0068) [Figure 1]. PD-L1 positivity in the stroma/lymphocytes did not correlate with overall survival or disease free survival. No associations between PD-L1 expression and KRAS mutation were identified.

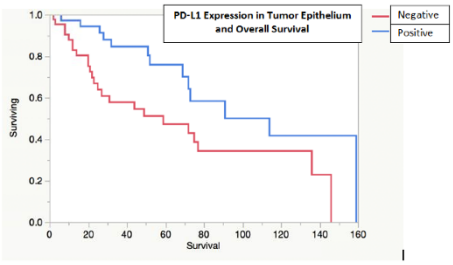

Conclusions: In contrast to other lung carcinomas, PD-L1 expression in the tumor cells of MLAs is associated with longer overall survival. IDO and WARS expression were associated with poor prognostic factors. IDO and PD-L1 expression is widely prevalent in MLAs and may lend credence to the use of IDO or PD-L1 inhibitors as therapeutic options in these tumors.

2080 Compound EGFR Mutations Frequently Occur on the Same Allele (in Cis) and Define a Unique Subset of EGFR Mutant Non-Small Cell Lung Cancer

Catherine Nicka[1], *Jason Peterson*[2], *Francine de Abreu*[2], *Keisuke Shirai*[3], *Gregory Tsongalis*[4], *Konstantin H Dragnev*[3], *Laura Tafe*[4]. [1]Lebanon, NH, [2]Dartmouth-Hitchcock Medical Center, Lebanon, NH, [3]Dartmouth-Hitchcock Medical Center, [4]Dartmouth-Hitchcock Med Ctr, Lebanon, NH

Background: The most common *EGFR* mutations in NSCLC are the activating exon 19 in frame deletions and the exon 21 p.L858R point mutation. Less common *EGFR* tyrosine kinase domain mutations have been described to have variable response to TKI targeted therapy. Treatment decision making can be even more challenging with compound *EGFR* mutations. Here, we describe our experience with compound *EGFR* mutations.

Design: In our institution, all lung adenocarcinomas are reflexively tested by targeted next generation sequencing (NGS) using the 50 gene AmpliSeq Cancer Hotspot Panel v2, the Archer® FusionPlex® Solid Tumor assay and FISH analysis for actionable genomic alterations.

Results: We identified 8 patients with compound *EGFR* mutations (May 2013-Aug.2017), most commonly p.S768I in exon 20 and p.G719 in exon 18. In 3 cases, where the mutations were within the same exon, the mutations were confirmed to be on the same allele by viewing the sequencing data in IGV (Figure 1). In the other 5 cases, the mutations were within different exons and different amplicons. In all 8 cases, the variant allelic fractions for both mutations were nearly identical, also supporting that both mutations are on the same allele. Five of the patients were female, age ranged from 64-88 years, and all were Caucasian, former smokers (15-45 pack years, when known). Three patients presented with stage IV disease, 4 with stage I disease, and one patient is still undergoing staging. The 3 patients with stage IV disease (3, 4 and 8) underwent therapy with EGFR TKIs. Patient 3 was initially treated with erlotinib and switched to afatinib after disease progression. Patient 4 was initially treated with carboplatin and pemetrexed and then treated with erlotinib at disease progression with stable response. Patient 8 was treated initially with afatinib with good response and then switched to carboplatin and pemetrexed at disease progression. Patient 6, did not receive an EGFR TKI and appeared to have a primary p.T790M mutation within the tumor at the same allelic fraction as the p.G719A mutation.

Patient	EGFR_1	exon_1	EGFR_2	exon_2
1	p.G719C	ex 18	p.E709V	ex 18
2	p.S768I	ex 20	p.L858R	ex 21
3	p.G719C	ex 18	p.S768I	ex 20
4	p.G719C	ex 18	p.S768I	ex 20
5	p.G719A	ex 18	p.S768I	ex 20
6	p.G719A	ex 18	p.T790M	ex 20
7	p.S768I	ex 20	p.V774M	ex 20
8	p.S768I	ex 20	p.V774M	ex 20

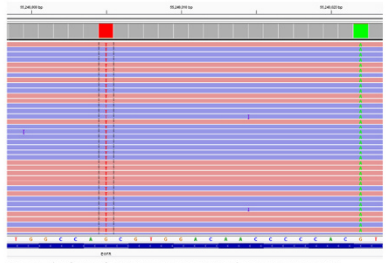

Figure 1. Identification of EGFR ex 20 c.2303G>T p.S768I and ex 20 c.2320G>A p.V774M mutations in cis (co-occurring in the same reads).

Conclusions: Compound *EGFR* mutations are a rare event which frequently occur in cis and includes a unique subset of *EGFR* mutant NSCLC patients of older age with a history of smoking and tumors that show variable responses to TKI therapy.

2081 Lymph node metastases in diffuse malignant mesothelioma of the pleura: Does the micropapillary pattern predict positive lymph nodes?

Nkechi Okonkwo[1], *Yang Zhang*[2], *Rachel E White*[3], *Allen Burke*[4]. [1]University of Maryland Medical Center, Baltimore, MD, [2]Ellicott City, MD, [3]University of Maryland, Baltimore, MD, [4]UMMS, Baltimore, MD

Background: The incidence of lymph node metastasis, concordance of histologic patterns between primary and metastastic deposits, and the rate of micropapillary growth pattern have not been studied in detail in diffuse malignant mesothelioma of the pleura.

Design: We retrospectively studied all diagnoses of mesothelioma of the pleura over a 3-year period. There were 57 patients, comprising 58 biopsies and 28 pleurectomies. Of these, 24 patients had pleurectomies and lymph node (LN) dissections.

Results: There were 18 men (aged 62 ± 13 years) and 6 women (64 ± 10 years). Mesotheliomas were epithelioid (17), and biphasic (7). In the primary epithelioid areas, the overall proportion of subtypes was solid (35%), tubular (27%), trabecular/cribriform (19%), micropapillary (15%), papillary (2%) and pleomorphic (2%). Thirteen primary tumors (54%) had micropapillary areas. Fifteen (63%)(6 of 7 biphasic and 9/17 epithelioid) tumors were positive for LN involvement. A mean of 6 (range 1-9) lymph node sites were sampled. All lymph node metastases of epithelioid type were epithelioid. Metastasis in biphasic were only biphasic (1 case); biphasic and epithelioid in different nodes (4 cases); and epithelioid, biphasic and sarcomatoid in different nodes (1 case). Rates of positivity were 5/7 intramammary (71%), 4/8 phrenic (50%), 9/20 posterior intercostal (45%), 2/5 lobar (40%), and 31/89 mediastinal (35%). A micropapillary growth pattern was present in 11/15 of tumors with lymph node metastasis versus 2/9 of those without a micropapillary pattern (p=0.01, chi square).

Conclusions: LN metastases are common in pleural mesotheliomas with the highest rates in intramammary, phrenic, and intercostal sites. Micropapillary areas are common, but unusually a small part of the tumor. Tumors with a micropapillary component have a relatively high rate of metastasis.

2082 Distinction of Chronic Hypersensitivity Pneumonitis from other Fibrosing Interstitial Lung Diseases in Lung Explants

Raghavendra Pillappa[1], *Eunhee Yi*[1], *Jay H Ryu*[1], *Anja Roden*[2]. [1]Mayo Clinic, Rochester, MN, [2]Mayo Clinic Rochester, Rochester, MN

Background: Distinguishing chronic hypersensitivity pneumonitis (CHP) from other fibrosing interstitial lung diseases (F-ILD) can be difficult. However, evidence suggests that patients with CHP might have a better outcome after lung transplantation than patients with UIP. We studied lung explants of patients with F-ILD to identify if we can distinguish CHP from UIP or other F-ILD.

Design: Lung explants with a diagnosis of CHP, UIP, non-specific interstitial pneumonia (NSIP) or chronic interstitial pneumonia (CIP) from institutional files (2002-2016) were reviewed by a pulmonary pathologist and a pathology trainee. Reports of HRCT were recorded; medical records were searched.

Results: Explants from 44 patients with a pre-transplant clinical diagnosis of UIP (n=26, 59.1%), CHP (6, 13.6%), NSIP (4, 9.1%), or connective tissue disease-associated F-ILD (CTD-ILD) (2, 4.5%), and cases with a differential consideration of CHP vs UIP (5, 11.4%) or CHP vs NSIP (1, 2.3%) were included. Pre-transplant HRCT suggested CHP (n=5, 11.4%), UIP (26, 59.1%), NSIP (5, 11.4%), CHP vs UIP (1, 2.3%) or other diagnoses / no specific diagnosis (7, 15.9%). Pre-transplant lung biopsies (reports available in 27) were reported as UIP (13), CHP (4), fibrotic NSIP (4), CIP (1), UIP vs CHP (1) and others (4).On histologic review of the lung explants, 21 (of 44, 47.7 %) cases were identified as possibly CHP (n=12) or suggestive of CHP (n=9). These cases included

6 (of 12, 50%) cases that were clinically (pre-transplantation) thought to be either CHP or CHP vs UIP/NSIP, 14 (of 26, 53.8%) cases of UIP, and 1 (of 4, 25%) case of NSIP. The other cases were histologically diagnosed as UIP (20 of 44, 45.4%) or fibrotic NSIP (3, 6.8%). Serology, available in 9 cases, was positive in 2 (of 9, 22.2%) which were histologically suggestive of CHP (pigeon breeders) or UIP (*Aspergillus fumigatus)*, respectively in the lung explants. More sections from the latter case will be evaluated for the possibility of CHP. Follow up was available in 43 patients. 17 (39.5 %) patients are alive at a median follow up of 60 months (range, 11-173) post-transplantation including 12 patients with histologic features of CHP in the explant (median follow up, 60 months, range, 11-173).

Conclusions: The histopathologic review of lung explants can help to establish a diagnosis of CHP in a subset of patients clinically and radiologically thought to have UIP. Our findings are important for prognosis, management and possibly treatment of lung allograft recipients.

2083 Beta-Catenin Expression in Familial Adenomatous Polyposis-Associated and Sporadic Sclerosing Pnemocytomas

Raghavendra Pillappa[1], *Brandon Larsen*[2], *Jennifer Boland*[3], *Anjali Saqi*[4], *Andras Khoor*[5], *Maxwell Smith*[2], *Henry Tazelaar*[6]. [1]Mayo Clinic, Rochester, MN, [2]Mayo Clinic Arizona, Scottsdale, AZ, [3]Mayo Clinic Rochester, Rochester, MN, [4]New York, NY, [5]Mayo Clinic, Jacksonville, FL, [6]Mayo Clinic, Scottsdale, AZ

Background: Sclerosing pneumocytoma (SP; formerly known as sclerosing hemangioma) is a rare benign neoplasm that usually arises sporadically, but SP has also been reported in 2 patients with familial adenomatous polyposis (FAP) syndrome. In both of the latter cases, SP was reported to display aberrant nuclear accumulation of beta-catenin, suggesting pathogenetic similarities with other FAP-associated neoplasms, but the role of beta-catenin in the pathogenesis of sporadic SP remains unknown.

Design: Institutional archives and consultation files of the authors were searched for cases of SP (1990-2017). Medical records were reviewed for any history of FAP, or FAP- or Gardner syndrome-associated tumors and outcome. Beta-catenin immunohistochemistry was performed on each tumor and stains were reviewed in a blinded fashion relative to the clinical history and FAP status.

Results: Eighteen patients (all women, mean age 56 years, range 17-75) were identified, including 2 with FAP and previous colectomy but no other FAP-associated tumors. Most SPs were solitary (17 cases, 94%); only 1 patient had multifocal disease but no history of FAP. Mean tumor size was 1.9 cm (range 0.1-3.6 cm), and most arose in the right lung (14, 78%). Two patients with sporadic SP had concurrent lung adenocarcinomas resected. Immunohistochemistry showed aberrant nuclear accumulation of beta-catenin in the cuboidal surface cells and stromal round cells in tumors from both patients with FAP, consistent with previous reports, as well as 2 sporadic tumors; the remaining cases showed only cytoplasmic and/or membranous immunoreactivity. In the 15 patients with available follow-up information, no tumors recurred and 14 were alive at the time of last follow-up (median follow-up 12.7 years, range 0.2 -25.1); the remaining patient died of unknown reasons 8.3 years after resection.

Conclusions: FAP-associated SP and some apparently sporadic SP show aberrant nuclear accumulation of beta-catenin. Most sporadic SP lack nuclear beta-catenin expression, suggesting possible differences in the molecular pathogenesis of syndromic and sporadic forms of SP. Beta-catenin immunohistochemistry may be useful to differentiate sporadic SP from FAP-associated tumors, and an abnormal nuclear pattern may warrant further workup for FAP. However, the mechanisms involved and importance of the WNT signaling pathway in tumorigenesis remain unknown.

2084 STK11 Mutations Are Associated With Lower PDL1 Expression in Lung Adenocarcinoma

Nicolas Piton[1], *Aude Lamy*[2], *Florian Guisier*[2], *Florent Marguet*[3], *Jean-Christophe Sabourin*[4]. [1]Rouen, Normandie, [2]Rouen University Hospital, [3]Barentin, [4]Hopital Charles Nicolle, Rouen

Background: Not all patients benefit from immunotherapy in lung carcinoma, and the expression of PDL1 by tumor cells seems to be an imperfect predictive biomarker. In terms of frequency, *STK11* is the third mutated gene in lung adenocarcinoma and is frequently associated with *KRAS* mutation. Experimental data suggest that *STK11*impacts PDL1 expression, and that an impaired *STK11* gene is associated with lower PDL1 expression. So as to improve the selection of eligible patients for immune checkpoint inhibitors, we decided to explore in further detail *STK11* as a predictive biomarker of PDL1 expression and to explore the association between the *KRAS* status of *STK11* mutated tumors and PDL1 expression.

Design: Lung adenocarcinomas harboring a *STK11* mutation were consecutively included in the study group, while a control group lacking a *STK11* mutation was randomly selected among lung adenocarcinomas genotyped between 12/21/2016 and 05/05/2017 using a 26-gene panel with high throughput sequencing. The effects of *STK11* mutations were predicted using online databases. Tumors were immunostained for PDL1 using the E1L3N clone. The percentage of PDL1 positive tumor cells was evaluated.

Results: We included 52 tumors harboring a *STK11* mutation, including 28 with a *KRAS* mutation, and 42 *STK11* wild-type tumors, including 17 with a *KRAS* mutation. Twelve tumors out of 52 (23%) in the *STK11* mutated group were positive for PDL1, compared to 19 out of 42 (45%) in the control group. Mean percentage of PDL1 positive tumor cells in the *STK11* mutated group was 9% (SD = 20), while mean percentage of PDL1 positive tumor cells in the *STK11* wild-type group was 25% (SD = 36) and the difference was statistically significant (p = 0.044) between the two groups. Among the 12 tumors harboring a *STK11* mutation and expressing PDL1, 5 also harbored a *KRAS* mutation. There was no statistically significant association between the presence of a *KRAS* mutation and the expression of PDL1 in the *STK11* mutated group. Five tumors expressing PDL1 harbored a *STK11* mutation described as pathogenic according to data in the literature.

Conclusions: We confirmed that PDL1 expression is dramatically lowered in *STK11* mutated lung adenocarcinomas compared to *STK11* wild-type tumors. In addition, we did not observe any association between PDL1 expression and *KRAS* mutation. The mechanism between *STK11* activity and PDL1 expression remains unclear and it seems that *STK11* could be an interesting surrogate marker of efficacy of immune checkpoint inhibitors.

2085 High Co-expression of PDL-1/PD-1, CD 8+ and CD45RO+ in Tumor-infiltrating lymphocytes (TILs) with EMT Activation Correlates with Aggressive Behavior and Poor Prognosis in High-Grade Pulmonary Neuroendocrine Tumors

Tabatha Prieto[1], *Vanessa Martins*[1], *Vera Luiza Capelozzi*[2], *Eduardo C da Silva*[3]. [1]Faculty of Medicine, University of São Paulo, [2]Faculty of Medicine University of Sao Paulo, Sao Paulo, [3]Barretos Cancer Hospital

Background: Pulmonary neuroendocrine tumors (PNETs) comprise various heterogeneous tumors, ranging from low-grade (AT/AC) and high-grade (LCNEC/SCLC). PD-1 and its ligand PD-L1, act as immune checkpoints and play a fundamental roles in the immune invasion of different tumors. Beyond that, studies have shown that EMT plays an important biological role in cancer progression, metastasis and drug resistance. Thus, our aim was to evaluate the clinical significance of PD-1/PDL-1, CD8 and CD45RO with the EMT activation in the malignancy of PNETs.

Design: We analyze 24 fresh frozen tumor-normal pairs for SCLC (n = 10), LCNEC (n = 4), AC (n = 5), TC (n = 5) and the gene expression was performed throught qRT-PCR analysis with a PCR Array System for the EMT pathway with 84 target genes.

For the immunohistochemistry, we analyze in both tumor and immune cells the PDL-1, PD-1, CD8 and CD45RO markers, and the results were correlated with clinicopathological characteristics and the expression of EMT genes.

Results: PD-L1 expression was higher in malignant cells for all pulmonary NETs (median H score, 136 vs 111 for SCLC, 155 vs 150 for LCNEC, 180 vs 25 for AC and 130 vs 41 for TC, respectively; P<0.01). Smoking status was significantly correlated with PD-1 in TILs expression (P<0.01). Lymphocytes naïve/memory T cells CD45RO was significantly higher in LCNEC than SCLC (median H score, 5.20 vs 78.75, P=0.03). No difference was found between the four PNETs and lymphocytes T cells CD8+. To understand the relationship between tumor cell PD-L1+ and other neuroendocrine lung tumor immune regulators and expression of EMT gene, we profiled *AKT1, COL1A2, COL3A1, COL5A2, DSP, EGFR, FR11, GSK3B, ILK, ITGA5, ITGAV, ITGB1, JAG1, MAP1B, MMP2, MMP3, SNAI2, SPARC, SPP1, STAT3, TCF3, TGF63, VPS13A, WNT5A* in 24 PNETs. By multivariate analysis, we found that the PD-L1 in tumoral cells was highly associated with EMT gene expression (SPP1 and MAP1B, p<0.05). Disease free survival and overall survival was significantly associated with higher expression of lymphocytes T cells CD8+ (Log rank 8.19; P<0.01), high expression of inhibitor PD-1 in immune cells (Log rank 7.67; P<0.01), and EMT gene expression for MAP1B (Log rank, 5.56; P=0.01).

Conclusions: High co-expression of PD-L1, PD-1, CD8+ and EMT gene signature are unfavorable prognostic factors for high-grade PNETs highlighting the importance of comprehensive assessment of both tumor and immune cells. Our results may support the use of quantitative immune profiling to study response and resistance to immunotherapy in pulmonary neuroendocrine tumors.

2086 Correlation of Pre-Operative Cancer Imaging Techniques with Post-Operative Macro and Microscopic Lung Pathology Images

Gabriel Reines March[1], *Xiangyang Ju*[2], *Stephen Marshall*[3], *Stephen J Harrow*[2], *Craig Dick*[4]. [1]NHS Greater Glasgow and Clyde, Glasgow, Lanarkshire, [2]NHS Greater Glasgow and Clyde, [3]University of Strathclyde, [4]NHS Greater Glasgow And Clyde, Glasgow, North Lanarksire

Background: This research project aims to investigate the performance of several PET radiotracers in lung cancer by aligning PET-CT and pathology imagery acquired from the same patients at different points in time. The discrimination of tumour substructures is of great importance in therapy planning, as a given treatment may be better adapted depending on the local characteristics of the carcinoma.

Design: Due to the high deformability of lung tissue, several intermediate steps must be used for merging pathology and pre-operative PET-CT in a coherent manner. Firstly, the tumour volume is reconstructed from the macroscopic images taken during dissection. For this purpose, an enhanced dissection protocol is used, where the lung specimen is placed in a bespoke slicing rig and embedded in agar to hold it in place. Using a threaded plunger, the specimen is pushed upwards in 5mm steps, sliced and photographed. This procedure allows us to obtain slices of uniform thickness. Secondly, microscopic digital slides of the cancerous tissue are merged with the macroscopic 3D model. Next, the whole volume is aligned to an ex-vivo CT scan of the specimen, taken immediately before pathological dissection. Finally, the pre-registered volume is fused with the pre-operative PET-CT scan, using a non-linear deformable model.

Results: Preliminary results obtained with a synthetic phantom allowed us to analyse the accuracy of the tumour 3D reconstruction algorithm from planar macroscopic slices. Using these findings, we could optimise the interpolation and segmentation routines for building an accurate 3D model of the carcinoma. During our first trial with lung tissue (on-going work), each cross-sectional slice was photographed, the tumour boundary was delineated in each image by a pathologist (CD), and from these contours a high-resolution 3D tumour model was built. Next, the corresponding microscopic digitised slices were merged. To date, five further patients have been identified and consented, therefore allowing us to test our algorithm on different cases and assess its performance.

Conclusions: We demonstrate a novel set of methods for co-registration of pre-operative PET-CT to macro and microscopically defined lung tumours. This proof of principle now allows interrogation of the raw data from scans using a range of tracers and the development of algorithms that identify substructure detail within a tumour mass, which could lead to tailored radiotherapy for individual cases based on tracer patterns and uptake.

2087 Computed Tomography Predicts the Pathologic TNM Stage of Thymic Epithelial Tumors in Most Cases

Anja Roden[1], *Megan J Hora*[2], *Sarah M Jenkins*[2], *Randolph S Marks*[2], *Darin White*[3]. [1]Mayo Clinic Rochester, Rochester, MN, [2]Mayo Clinic Rochester, [3]Mayo Clinic Rochester, Rochester, MN

Background: Treatment of thymic epithelial tumors (TET) depends on tumor stage. Accurate preoperative staging would facilitate treatment decisions for these neoplasms. We investigated the efficacy of CT studies (r) to predict the pathologic (p) tumor stage of TET using the 8th UICC/AJCC (TNM) staging.

Design: Resected TET (2006-2016) with preoperative CT scan and lymph node (LN) sampling were included. Slides were reviewed by a thoracic pathologist to confirm diagnosis and assess extent of invasion. CT scans were reviewed by two thoracic radiologists. 8th UICC/AJCC (TNM) and modified Masaoka staging were used for r and p staging. Medical records were reviewed. Statistical analysis was performed.

Results: 76 patients (33 men, 43.4%) (median age, 56.5 [28.1-87.3] years) underwent complete (69, 90.8%) or incomplete resection of thymoma (n=61, 80.3%) or thymic carcinoma (n=13, 17.1%). Sixteen patients received neoadjuvant therapy. Two cases of thymic carcinoma diagnosed on a pre-neoadjuvant therapy biopsy had no viable tumor in the resection specimen. A median of 4 LN (1-34; predominantly perithymic) were available for review. Percent agreement for TNM and modified Masaoka stage between r and p stage was 65.8% (κ, 0.42, Table) and 40.8% (κ, 0.23), respectively. CT studies overstaged 16 and understaged 10 TET, by TNM (Table). In 11 (of 26, 42.3%) cases disagreements occurred across adjacent categories (Table). Seven (of 50, 14%) pTNM stage I cases were interpreted as r stage III or IV; one of these had neoadjuvant radiation without preoperative repeat CT.

In a median follow-up of 3 years (0.1-10.5) 13 patients had metastases and/or recurrence; 13 died, 5 of disease. The 5-year disease-free survival was 75.6%; the 5-year overall survival was 73.4%. The p and r TNM and the r modified Masaoka stage were associated with overall survival (OS) (p=0.03, p<0.01, p<0.01, respectively); the p modified Masaoka stage trended towards worse OS (p=0.06). The p and r TNM and modified Masaoka staging were each associated with disease-free survival (p<0.01 for all).

Radiologic vs pathologic TNM stage of TET

Pathology	Radiology						
# Cases	I	II	IIIA	IIIB	IVA	IVB	Total
0	0	0	2	0	0	0	2
I	40	3	1	1	1	4	50
II	1	0	0	1	0	0	2
IIIA	3	3	2	0	0	1	9
IIIB	0	0	0	0	0	0	0
IVA	0	3	0	0	3	2	8
IVB	0	0	0	0	0	5	5
Total	44	9	5	2	4	12	76

Conclusions: CT studies using the new TNM staging predict p stage of most resected TET. TNM appears better than the modified Masaoka staging in CT studies predicting the p stage. However, a small percentage of patients will be overstaged and might undergo unnecessary neoadjuvant therapy.

2088 Comparison of EGFR Mutation Detection in Plasma Circulating Tumor DNA Using PNA Clamping and Droplet Digital PCR from Patients with Lung Adenocarcinoma

Mee Sook Roh[1], *Choonhee Son*[2]. [1]Dong-A University College of Medicine, Busan, [2]Dong-A University

Background: Circulating tumor DNA (ctDNA) has the potential to enable noninvasive detection for *EGFR* mutations in lung cancer patients, since it can provide similar molecular information as invasive tumor biopsies. However, the existing methods have limitations in sensitivity or in availability. We performed comparative and concordance analyses of peptide nucleic acid (PNA) clamping and droplet digital PCR (ddPCR) for detecting *EGFR* mutations in plasma ctDNA from patients with lung adenocarcinoma (AD).

Design: A total of 39 patients with newly diagnosed, treatment-naïve lung ADs (30 ADs with *EGFR* mutation and 9 ADs with wild type) were enrolled who provided both plasma samples and matched tumor tissue samples. The genomic DNAs were extracted from the plasma samples and extracted ctDNA was analyzed using two different methods PNA clamping-assisted fluorescence melting curve analysis (PNAc) and ddPCR to detect mutations in *EGFR* exon 18, 19, 20 and 21.

Results: Of 39 plasma samples, *EGFR* mutations were detected in 19 (48.7%) cases by PNAc and in 16 (41.0%) case by ddPCR. When the *EGFR* mutation status in tumor tissue was used as standard reference, the sensitivity and specificity for PNAc were 60.0% and 88.9%, respectively, whereas the sensitivity and specificity for ddPCR were 53.3% and 100%, respectively. The concordance rate between two methods was 82.1% (32/39). Seven cases showed discrepant results between two methods (5 cases; PNAc(mutant) /ddPCR(wild) and 2 cases: PNAc(wild)/ddPCR(mutant)). Of seven cases with discrepant results, 4 cases analyzed by PNAc were matched to tissue results, whereas 3 cases analyzed by ddPCR were matched to tissue results.

Plasma ctDNA analysis	Tumor-tissue analysis		Sensitivity (%)	Specificity (%)
	EGFR mutation (n=30)	Wild type (n=9)		
PNAc			60.0	88.9
EGFR mutation	18	1		
Wild	12	8		
ddPCR			53.3	100
EGFR mutation	16	0		
Wild	14	9		

Conclusions: The *EGFR* mutations detected by PNAc could be a relatively sensitive and specific method to noninvasively detect plasma *EGFR* mutations of patients with lung AD. Furthermore, the concordance rate between PNAc and ddPCR was high (82.1%). Our study showed that ctDNA could replace tumor-tissue analysis in routine molecular diagnostics using a commercially available and approved test. However, further investigations with a larger number of cases and various platforms would allow us to confirm the diagnostic performance and availability of plasma ctDNA for *EGFR* mutation detection in lung cancer patients.

2089 A Comparison of Antibodies HMB-45 and Cathepsin-K as Diagnostic Markers of Pulmonary Lymphangioleiomyomatosis

Ines Rolim[1], *Marquetta S Makupson*[2], *Aleksandra Lovrenski*[3], *Carol Farver*[1]. [1]Instituto Portugues de Oncologia de Lisboa, Francisco Gentil, Lisbon, [2]Cleveland Clinic, Cleveland, OH, [3]Institute for Pulmonary Diseases of Vojvodina, Medical Faculty University Novi Sad

Background: Pulmonary lymphangioleiomyomatosis (LAM) is a rare cystic lung disease affecting predominantly young women. According to the WHO, LAM was recently classified as a low-grade malignant soft tissue neoplasm from the family of perivascular epithelioid cell (PEC) tumors or PEComas. It is characterized by a proliferation of abnormal smooth muscle-like cells (LAM cells) along lymphatics, blood vessels and bronchioles, resulting in progressive respiratory failure. LAM cells coexpress myogenic and melanocytic markers, with HMB-45 as the gold-standard immunohistochemical diagnostic marker. Cathepsin K, a papain-like cysteine protease with high matrix (collagen, elastin)-degrading activity, is another potential marker for LAM. Despite its common use in other PEComa tumors, there are few data regarding its expression in pulmonary LAM.

Design: Twenty-two (22) specimens of pulmonary LAM were retrieved from the archives of the Department of Pathology. All cases were evaluated for protein expression of two antibodies, HMB-45 and Cathepsin-K, on consecutive sections of formalin-fixed, paraffin-embedded tissue. The intensity and the total area of the immunostaining were quantified using an Aperio Scan Scope and analyzed with an imaging software (Spectrum). Statistical analysis was performed using GraphPad software.

Results: The patients, all females, had a mean age of 45 years (28-69 yrs). In all cases, the percentage of LAM cells expressing Cathepsin-K was significantly higher than for HMB-45 and overall expression was statistically significantly higher (P=0.0137). Both antibodies had similar specificity with no false negative staining of internal negative controls (smooth muscle of airways and vessels in surrounding lung) (Figs 1a and 1b).

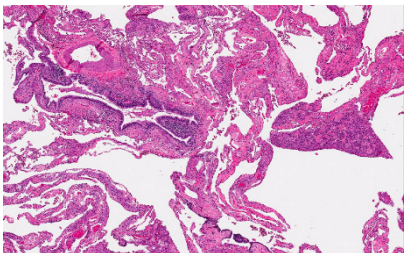

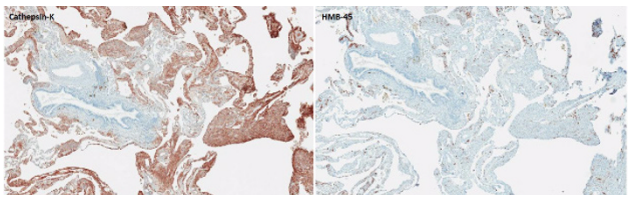

Conclusions: Our results indicate that Cathepsin-K is a more sensitive diagnostic marker for the diagnosis of pulmonary LAM, comparing to HMB-45. Further studies are ongoing to test for TFE3 expression and TFE3 rearrangement in LAM cells.

2090 Thymic Carcinoma-Associated Second Malignancies: A Single-Center Review

Rachel E Rominger[1], *Sunil Badve*[2], *Yesim Gokmen-Polar*[1]. [1]Indiana University School of Medicine, Indianapolis, IN, [2]Indiana Univ/Medicine, Indianapolis, IN

Background: Second malignancies are well-described in the setting of thymic tumors, although most of the prior research into this relationship has focused on thymoma. Little data is available regarding the incidence of second malignancies in thymic carcinoma, a rare malignancy accounting for less than 0.01% of new cancer diagnoses annually. The aim of this study was to identify whether thymic carcinoma is also associated with an increased incidence of second malignancies.

Design: Retrospective cases of histologically confirmed thymic carcinoma seen in the past 15 years were identified and available histological materials were reviewed applying the current WHO classification of thymic tumors (2015). Patient electronic medical records were searched for diagnoses of second malignancies.

Results: Clinical database review identified 184 cases of thymic carcinoma. In many cases, the original histological slides had been returned to referring institutions; this resulted in identification of histological materials for only 91 cases. Clinical data was available in 58 of these cases, although a complete medical history was not available for each case. A second malignancy was discovered for 13 patients (22.4%), with a total of 15 second malignancies identified. Eleven of these malignancies represented malignant neoplasms diagnosed before the patient's thymic carcinoma diagnosis (including one case each of small cell lung cancer, prostatic carcinoma, renal cell carcinoma, pituitary neoplasm, and Hodgkin's lymphoma, as well as two cases each of breast, bladder, and testicular cancer). Two malignancies were diagnosed concurrently with the thymic carcinoma (chondrosarcoma and renal cell carcinoma), and one malignancy developed after the thymic carcinoma diagnosis (acute lymphocytic leukemia).Two patients were identified with multiple second malignancies; one had two prior malignancies, and the second had both a prior and concurrent malignancy with their thymic carcinoma diagnosis. The true number of thymic carcinoma patients with second malignancies may be affected due to incomplete medical histories available for a large number of patients.

Conclusions: We for the first time describe the association of thymic carcinoma with second malignancies. In this limited series the association was strong association with approximately 22% of patients exhibiting second cancers prior to or following the diagnosis of thymic carcinoma. This relationship is consistent with the importance of thymic tissue in immune regulation.

2091 Utility of Programmed Cell Death Ligand 1 (PD-L1)/CD8 Dual Immunohistochemistry (IHC) in Predicting Response to Immunotherapy in Lung Cancer

Matthew Rosenbaum[1], *Tiffany Huynh*[1], *Marina Kem*[1], *Justin Gainor*[1], *Mari Mino-Kenudson*[1]. [1]Massachusetts General Hospital, Boston, MA

Disclosures:
Justin Gainor: *Consultant*, Bristol-Myers Squibb, Novartis, Genentech/Roche, Pfizer, Incyte, and Theravance, *Honorarium*, Bristol-Myers Squibb, Novartis, Genentech/Roche, Pfizer, Incyte, and Theravance

Background: Programmed Cell Death 1 (PD-1)/PD-L1 blockade is a part of the current treatment paradigm for advanced non-small cell lung cancer. IHC for PD-L1 has been used to guide patient selection for PD-L1/PD-1 blockade, but treatment response is highly variable. In this study we evaluated whether a combined assessment of tumor PD-L1 expression and immune microenvironment (CD8+ T cells) improves treatment response prediction in lung cancer.

Design: Our clinical database was queried for patients who had received PD-1 axis blockade at our hospital from 2014 to 2017. Available samples were stained for PD-L1 (clone E1L3N)/CD8 dual IHC. Tumor cell PD-L1 expression was evaluated in all samples, and CD8+ tumor infiltrating lymphocytes (TILs) and CD8+ stromal lymphocytes were evaluated in non-cytology samples (n=55). The results were compared to progression free survival (PFS).

Results: The study cohort consisted of 60 patients with 51 (85%) treated with PD-1 blockade as a second or later line of therapy. PD-L1 expression on ≥1% of tumor cells was seen in 50% of patients, while a high-level (≥50%) PD-L1 expression was seen in 16 (27%). Of 51 specimens with evaluable TILs, abundant CD8+ TILs were present in 14 (27%). 8 (17%) of 48 cases with evaluable stroma showed CD8+ T cells comprising ≥40% of stromal nucleated cells. PD-L1 expression on ≥1% of tumor cells was marginally associated with longer PFS (p= 0.095), while abundant CD8+ TILs and significant CD8+ stromal T cells were not individually associated with PFS. Within PD-L1+ cases where CD8+ T cells were evaluated (n=25), both abundant CD8+ TILs and significant CD8+ stromal T cells were seen in 3 (12%), and were significantly associated with reduced PFS (p=0.040).

Conclusions: In this cohort of lung cancer patients treated with PD-1 axis blockade mostly as a second or later line of therapy, PD-L1 expression was marginally associated with an improved PFS. PD-L1/CD8 dual assessment by IHC identified a decent minority who exhibited abundant tumor associated CD8+ T cells and failed to respond to the blockade despite the expression of PD-L1 on tumor cells. This phenomenon is counter-intuitive, but may be secondary to T-cell exhaustion following the prior chemo/radiation therapy, which may have led to the presentation of abundant tumor neoantigens to cytotoxic T cells already present in the tumor. A prospective study evaluating a role of PD-L1/CD8 dual assessment in predicting response to immunotherapy in the first line setting is underway.

2092 PREVIOUSLY PUBLISHED

2093 Small solid nests of lung adenocarcinoma are a prognostic and etiologic marker: a comparison study with a micropapillary pattern

Ryoko Saito[1], *Hironori Ninomiya*[2], *Sakae Okumura*[3], *Hironobu Sasano*[4], *Yuichi Ishikawa*[5]. [1]Tohoku University Graduate School of Medicine, Sendai-shi Aoba-ku, Miyagi-ken, [2]The Cancer Institute, Japanese Foundation for Cancer Research, [3]The Cancer Institute Hospital, Japanese Foundation for Cancer Research, [4]Tohoku University, Sendai-shi, [5]The Cancer Institute, Japanese Foundation for Cancer Research, Tokyo

Background: Tumor cell fragments, or pseudopapillary cell nests, in histology of lung adenocarcinoma are a histologic marker of poor prognosis, such as a micropapillary pattern. However, its etiologic implication is still controversial: in some studies the micropapillary pattern is related to non-smokers, but it is not the case in others, which may be due to vague definition of micropapillary patterns. In this study, we classified the pseudopapillary cell nest into two types: a narrowly-defined micropapillary pattern (NDMP) and a small solid nest (SSN). NDMP was defined as a corolla-like cell nest with glandular cell polarity and no fibrovascular core, and SSN as a solid tumor nest with less than 20 tumor cells and no glandular polarity.

Design: Using 436 invasive lung adenocarcinoma surgically resected at a cancer center hospital, we compared clinicopathological factors between SSN negative (<5%) and positive (=>5%), and NDMP negative and positive groups as well as among SSN dominant (SSN>NDMP>5%), NDMP dominant (NDMP>SSN>5%) and null (NDMP=<5%, SSN=<5%) groups.

Results: NDMP and SSN were independent factors for poor prognosis in all stages (p=0.026, p=0.001, respectively). In stage I, SSN positivity was a significant and independent poor prognostic factor (p=<0.0001) but NDMP positivity was not. The SSN dominant group showed poorer prognosis than the NDMP dominant group in all stages (p=0.050) and earlier stages (Stage I: p=0.043, Stage II: p=0.004). NDMP was negatively correlated with cumulative smoking (p=0.001) and SSN showed a marginally positive correlation (p=0.052).

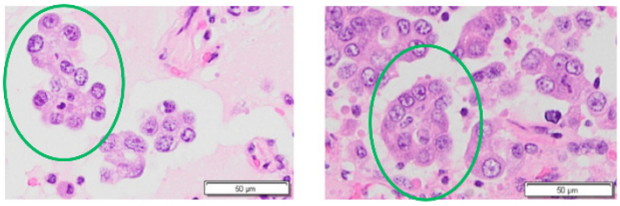

NDMP SSN

Conclusions: Both NDMP and SSN were prognostic factors, but distinction of NDMP and SSN revealed that SSN was a better prognostic indicator and that NDMP was associated with non-smoking and SSN with smoking.

2094 Negative Association Between PD1/PD-L1 Inhibitor Expression and ROS1, ALK and EGFR Mutations in Non-Small Cell Lung Cancer

Mónica Saiz[1], *Verónica Caamaño*[1], *Laura Zaldumbide*[2], *Ena Fernández-Lomana Idiondo*[3], *Aitziber Marcos Muñoz*, *Lorena Mosteiro*[1], *Veronica Velasco*[1], *Sefora Malaxetxebarria*[4], *Marta Gonzalez*[1], *Marta Atienza*[1], *Alexandre Nogueira*[1], *Dámaso Parrón*[1], *Ignacio Diaz de Lezcano*[5], *Jose I López*[1]. [1]Cruces University Hospital, [2]Cruces University Hospital, Barakaldo, Vizcaya, [3]Hospital Universitario de Cruces, Barakaldo, Blzkaia, [4]Cruces Universitary Hospital, [5]Cruces University Hospital, Barakaldo, País Vasco/Vizcaya

Background: Lung cancer is a highly prevalent neoplasm with high mortality rates in Western countries. EGFR, ALK and ROS1 mutations are considered the prototypical major receptor tyrosine kinase-targetable driver alterations in lung adenocarcinoma. On the other hand, PD1/PD-L1 is a promising therapeutic target because its inhibition restores the immune system of patients against tumor cells. Our aim in this study is to evaluate the relationships of these biomarkers in a consecutive series of 100 patients with non-small cell lung carcinoma

Design: Histological/immunohistochemical slides and molecular tests of 15 squamous cell carcinomas (SCC), 77 adenocarcinomas (ACA) and 8 large cell undifferentiated carcinomas (LCC) were retrieved from the pathology files for comparative study. Representative well preserved areas of tumors had been selected at the diagnostic time for biomarker testing following the standard step-wise protocol internationally accepted. PD-L1 was considered positive when ≥50% of cells were stained. ALK (Ventana, D5F3) ROS1 (Cell Signaling D4D6) and PD-L1 (Ventana SP263), ALK (ZytoLight SPEC) and ROS1 (ZytoLight SPEC) and EGFR (Roche, Cobas) were used for immunohistochemistry, FISH and RT-PCR, respectively.

Results: The series included 59 males and 41 females with an average age of 62 years (range (33-84). 19 cases were PD-L1+ (14 ACA, 3 SCC and 2 LCC), 12 were EGFR+ (all ACA), 3 were ALK+ (all ACA) and 1 was ROS1+ (ACA). A negative association between PD-L1 and EGFR expressions was detected (chi square test, p<0.001) in the series, with only 3 ACA being positive for both tests. Additionally, all ALK+ and ROS1+ cases were negative for PD-L1 (chi square test, p<0.001).

Conclusions: The percentage of EGFR, ALK, ROS1 and PD-L1 alterations in this series is comparable to previously published data. In addition, we have found a statistically significant negative association between the expression of immune checkpoint inhibitors and the presence of driver mutations.

2095 Analysis of MET Exon 14 Skipping Mutations and MET Gene Amplifications in Non Small-Cell Lung Cancer Patients

Marta Salido[1], *Sergi Clavé*[2], *Alba Dalmases*[3], *Lara Pijuan*[2], *Raquel Longaron*[4], *Marta Lorenzo*[5], *Álvaro Taus*[4], *Erica Torres*[4], *Pedro Rocha*[4], *Blanca Espinet*[6], *Beatriz Bellosillo*[3], *Edurne Arriola*[4]. [1]Hospital del Mar, Barcelona, [2]Hospital del Mar, Barcelona, [3]Barcelona, [4]Hospital del Mar, [5]Hospital del Mar-Parc de Salut Mar-IMIM, [6]IMIM-Hospital del Mar, Barcelona, Catalonia

Background: MET mutations leading to exon 14 skipping are likely to represent a novel and actionable driver oncogenic target in a small subgroup (4%) of NSCLC patients. However, the clinicopathological characteristics of NSCLC harboring *MET* mutations, and the correlation among mutations, and gene copy number alterations remain unclear. Our aim was to investigate the coexistence of M*ET* exon 14 skipping and *MET* copy number alterations (CNAs).

Design: A total of 222 paraffin-embedded NSCLC samples selected from 2013 to 2016 were included. Patient's characteristics were: median age 64 year-old, 72% were males, 84% were current or former smoker, 54% were diagnosed in advanced stage and 85% were adenocarcinomas. MET exon 14 and flanking intron mutations were studied by PCR-direct sequencing using DNA extracted from paraffin blocks. CNAs were analyzed by fluorescence in situ hybridization (FISH) with the MET / CEP7 probe (Abbott Molecular). Amplifications were defined as mean gene by mean centromere ratio ≥1.8, and highly amplified cases were defined by ratio ≥5.0. RT-PCR was performed to validate mutations leading to exon 14 skipping. Moreover, we collected clinical-pathological data together with *EGFR* and *KRAS* mutational status and *ALK*, *ROS1* and *RET* rearrangements.

Results: *MET* alterations were found in 24 patients (10.8%): 12 mutated and 13 amplified cases. Six of the 12 mutations (50%) were confirmed to lead exon 14 skipping. Regarding concurrent alterations, in one of these cases we identified also *MET* amplification, one case had *KRAS* p.G12C mutation and one had *EGFR* exon 19 deletion. Regarding clinical data among patients with *MET* alterations (n=24), 23 were men (96%), with a mean age of 62 years-old (range: 40-91), 16 were active smokers and 17 were diagnosed in the advanced stage (70.8%).

Conclusions: *MET* exon 14 skipping mutations define a small subgroup of patients with NSCLC. Rarely, *MET* gene amplification might coexist with *MET* mutation. Both, *MET* exon 14 skipping mutations and *MET* CNAs represent a new therapeutic target for patients with NSCLC and should be incorporated to the diagnostic protocols of these patients.

2096 Genomic Profiling of Micropapillary Adenocarcinoma of the Lung by Next Generation Sequencing

Christopher Sande[1], *Natalya Guseva*[2], *Aaron Stence*[2], *Jun Zhang*[2], *Deqin Ma*[3]. [1]University of Iowa, Iowa City, IA, [2]University of Iowa, [3]University of Iowa Hospitals and Clinics, Iowa City, IA

Background: Micropapillary carcinoma (MPC) is a newly added subtype of lung adenocarcinoma (ADC) in the 2011 WHO classification. MPC component >5% is associated with a high rate of recurrence, early metastasis, and worse prognosis. Although MPC subtype has been shown to be an independent prognostic factor for overall survival, the mechanism underlying its aggressiveness is poorly understood due to the lack of comprehensive genomic profiling. We evaluated 18 cases of microdissected MPC using an RNA- and DNA-based next generation sequencing (NGS) assay and correlated the findings with clinical information.

Design: Of 18 resection cases of ADC with >5% MPC, MPC areas were microdissected from optimal blocks of 11 primary and 7 lymph node (LN) tumors. Additionally, non-MPC areas in the same primary tumor or a different LN were tested in 4 cases, including 2 paired primary and metastatic tumors. Total nucleic acids were extracted from formalin-fixed, paraffin-embedded tissue, analyzed by an RNA-based (Archer FusionPlex CTL kit, ArcherDx) and/or DNA-based (Ion AmpliSeq Cancer Hotspot Panel, ThermoFisher) targeted NGS assay, and sequenced on MiSeq or Ion S5. Droplet digital PCR (Roche) was used to confirm the presence of low-level *EGFR* p.T790M mutation.

Results: Thirteen cases had positive LNs (72%), of which 5 had distant metastasis. Genomic aberrations were detected in 17/18 (94.4%) cases, including mutations in *KRAS* (7), *EGFR* (3), *NRAS* (1), *BRAF* (1), *TP53* in-frame deletion (1) and gain of function mutation (1) (p.R249S), gene fusions of *EML4-ALK* (2), *KIF5B-RET* (1), and the rare *MYH9-ROS1* (1). 16/18 cases (88.9%) had driver mutations. A low level of naïve tyrosine kinase inhibitor (TKI)-resistant *EGFR* mutation (p.T790M) was detected in 5/18 cases (27.8%) with or without TKI-sensitizing mutation. *EGFR*, *BRAF, NRAS, ALK*, and *ROS1* mutations were found in never/light smokers, while mutated *KRAS* was seen in heavy smokers. The genetic profiles of MPC and non-MPC areas of the same tumor as well as paired primary and metastasis were the same. Table 1.

Table 1. Molecular Findings with Clinical Information

Gene	Variant Detected (number of cases)	Age	Gender	Smoking Pack/year	TNM Staging	Specimen Site	Effect of Mutation	Targeted Therapy
KRAS	p.G12C (1)	65	M	50	T1aN2M0	L5 LN	Activating	None
	p.G12C (1)#	68	F	35	T3N1cM1	RML,2 blocks	Activating	None
	p.G12D (1)	82	F	2nd hand	T2bN1M0	RUL	Activating	None
	p.G12F (1)#	55	F	40-43	T2aN0M0	LUL	Activating	None
	p.G12V (1)	72	M	40	T1bN1M0	Hilar LN	Activating	None
	p.G12V (1)	73	F	Remote	T2bN1M0	RUL	Activating	None
	p.Q61H (1)	59	F	20	T1aN2M1b	Hilar LN	Activating	None
EGFR	p.L858R (1)#	70	F	Never	T2bN2M0	LLL,2 blocks	Activating	Yes
	p.A822T (1)a	73	F	10	T2aN1M0	LUL, RLL	VUS&	None
	p.E746_A750del (1)b	86	F	Never	T2aNxM1a	LUL, RLL	Activating	Yes
TP53	p.R249S (1) a	73	F	10	T2aN1M0	LUL, RLL	GOF	None
	p.N131del (1)	71	M	110	T1bN0M0	LUL	Inactivating	None
BRAF	p.V600E (1)	53	F	Never	T1bN1M0	LUL	Activating	Yes
NRAS	p.Q61L (1)	60	M	5	T1aN2M0	Level 5 LN	Activating	None
PTEN	p.P244Lfs*(1)b	86	F	Never	T2aNxM1a	LUL, RLL	Inactivating	None
ALK^	EML4-ALK (1)#	70	F	3, remote	T2aN2M1a	L5 LN, LUL	Activating	Yes
	EML4-ALK (1)	49	F	10	T3N0M0	LLL	Activating	Yes
ROS1^	MYH9-ROS1 (1)	41	F	Never	T1aN2M1b	L7 LN, RML	Activating	Yes
RET	KIF5B-RET (1)#	70	M	65-86	T3N2M0	Hilar LN	Activating	None

#With co-existing *EGFR* p.T790M mutation; aSame case; bSame case; ^Confirmed by FISH; L5/L7, level 5/7; RUL/RML/RLL/LUL/LLL, different lobes of the lung; LN, lymph node; VUS, variant of uncertain significance; GOF, gain of function.

Conclusions: MPCs in our cohort had an extremely high rate of driver mutations, which may account for the high metastatic rate and aggressiveness. The presence of *EGFR* p.T790M in TKI-naïve tumors suggests that a pre-existing minor TKI-resistant population exists in the tumor, which may progress rapidly after TKI therapy for sensitizing mutations. Identification of genetic variants by comprehensive molecular profiling may assist in management of these patients.

2097 EGFR Mutation Testing Using Liquid Biopsy Technology for Patients with Advanced EGFR-Mutant NSCLC

Jan Seitz[1], *Evgeny A Moskalev*[2], *Florian Fuchs*[3], *Florian Haller*[4], *Arndt Hartmann*[2]. [1]Bamberg, Bayern, [2]Institute of Pathology, Friedrich-Alexander University Erlangen-Nuremberg, [3]Department of Medicine, Pneumology, Friedrich-Alexander University of Erlangen-Nuremberg, [4]Erlangen, Germany

Background: Tyrosine kinase inhibitors (TKI), which target the epidermal growth factor receptor (EGFR), have become an alternative treatment option for patients with non-small cell lung cancer (NSCLC) by now. It has been demonstrated by many studies that activating *EGFR* gene mutations are effective markers for EGFR-TKI sensitivity. The aim of this study was to evaluate the presence of *EGFR* mutations in cfDNA in a cohort of patients with advanced EGFR-mutant NSCLC using next-generation sequencing (NGS) and digital droplet PCR (ddPCR).

Design: We evaluated the EGFR mutation status in 13 NSCLC patients with known primary EGFR mutations before or during TKI treatment. 10 ml blood samples were centrifuged to gain plasma for further processing and frozen at -20°C until cfDNA isolation. The Actionable Insights Tumor Panel and the Qiagen GeneReader workflow were used for NGS analysis. The remaining cfDNA was processed in a ddPCR investigating the T790M mutation status. Therefor the Bio-Rad PrimePCR Mutation Assay "ID: dHsaCP2000019" was used on a QX200 ddPCR System.

Results: In samples with positive detection of *EGFR* mutations in cfDNA by NGS, 100% concordance with the specific *EGFR* mutation was documented as determined previously in FFPE biopsies. In 6 of 13 samples, the primary activating EGFR mutation could be detected in cfDNA by NGS, with an allele frequency ranging 0.59% - 8.48%. Additionally, a secondary EGFR T790M mutation with an allele frequency of 1.81% could be detected in patient 6. In 3 of 13 cases a T790M mutation was detected in the analyzed cfDNA by ddPCR with a frequency of 0.38%, 0.72% and 1.86% for patient 6. The allele frequency by NGS for patient 6 was matched very well by ddPCR, altogether indicating a resistance to TKIs and the need for therapy adjustment. This patient received a 3rd generation EGFR TKI and showed good partial response.

In samples with positive detection of *EGFR* mutations in cfDNA by NGS, 100% concordance with the specific *EGFR* mutation was documented as determined previously in FFPE biopsies. In 6 of 13 samples, the primary activating EGFR mutation could be detected in cfDNA by NGS, with an allele frequency ranging 0.59% - 8.48%. Additionally, a secondary EGFR T790M mutation with an allele frequency of 1.81% could be detected in patient 6. In 3 of 13 cases a T790M mutation was detected in the analyzed cfDNA by ddPCR with a frequency of 0.38%, 0.72% and 1.86% for patient 6. The allele frequency by NGS for patient 6 was matched very well by ddPCR, altogether indicating a resistance to TKIs and the need for therapy adjustment. This patient received a 3rd generation EGFR TKI and showed good partial response.

Conclusions: Our results suggest that NGS and ddPCR are of adequate diagnostic accuracy in their respective fields of use. The wide-ranging examination of cfDNA by NGS panels and targeted analysis by the significantly higher sensitivity of ddPCR can be a valuable tool for analysis and detection of therapeutically relevant mutations. Also the short time needed for ddPCR analysis compared to a NGS run makes it a method of choice to support the important NGS results. The fluctuating amount of cfDNA in patients can be a challenge, however, if the amount needed isn't foreseeable. That could be solved by collecting more blood material in the future.

2098 Comparison of MTAP immunohistochemistry (IHC) with p16/CDKN2A deletions/loss and utility of MTAP and BAP1 IHC in the diagnosis of malignant pleural mesothelioma (MPM)

Maryam Shahi[1], *Takashi Eguchi*[1], *Marjorie Zauderer*[1], *William Travis*[1], *Achim Jungbluth*[1], *Denise Frosina*[1], *Miriam Fayad*[1], *Marina Asher*[1], *Prasad S Adusumilli*[1], *Marc Ladanyi*[1], *Jennifer L Sauter*[1]. [1]Memorial Sloan Kettering Cancer Center, New York, NY

Background: Homozygous deletion of *p16/CDKN2A* and loss of *BAP1* are the most common genetic alterations in MPM, with the former more frequent in sarcomatoid (S) and the later more frequent in epitheloid (E) subtypes. Homozygous co-deletion of methylthioadenosine phosphorylase (MTAP) occurs in the majority of mesotheliomas with *p16/CDKN2A* deletions. Herein, we investigate the sensitivity of MTAP and BAP1 IHC in MPM versus benign pleura (BP).

Design: MTAP (mAB EPR6893) IHC was performed on whole tissue sections (WTS) of 19 malignant mesothelioma (MM) with known *p16/CDKN2A* status by next generation sequencing (NGS). MTAP and BAP1 (mAb C4) IHC was performed on tissue microarray (TMA) with 243 pleural MM (194 E, 26 biphasic [B], 23 S) and on WTS of 20 BP. Loss of BAP1 (nuclear) and MTAP (cytoplasmic) immunoexpression was scored. Loss of MTAP expression by IHC was compared with *p16/CDKN2A* status by NGS. Sensitivity and specificity of both markers for MPM versus BP was determined.

Results: 9/10 MM with *p16/CDKN2A* loss by NGS showed loss of MTAP expression by IHC, and 9/9 MM with *p16/CDKN2A* wildtype by NGS demonstrated retained MTAP (overall correlation 94.5%). Proper internal controls for BAP1 and MTAP IHC were present in 234/243 (96%) and 228/243 (94%) TMA MPM cores, respectively. 19/20 and 20/20 WTS of BP showed proper internal controls for BAP1 and MTAP IHC, respectively. The specificity of BAP1 and MTAP IHC for MPM, versus BP, was 100% for each marker. BAP1 and MTAP sensitivity for MPM overall was 63% and 42% (63% and 42% in E, 58% and 46% in B, and 14% and 41% in S), respectively. When combined, the sensitivity BAP1 and MTAP IHC for MPM overall was 77%.

Conclusions: In-situ protein expression of MTAP by IHC correlates well with molecular *p16/CDKN2A* status detected by NGS and is a reliable, efficient and cost-effective method of detecting the presence of *p16/CDKN2A* deletion in MM. The interpretation of MTAP IHC is

straightforward for diagnostic pathology. Concurrent utilization of both BAP1 and MTAP IHC improves diagnostic sensitivity for MPM versus benign mesothelial proliferations than either marker alone.

2099 PD-L1 22C3 and 28-8 Expression in Malignant Mesotheliomas

Rachel Stewart[1], *David B. Chapel*[2], *Larissa Furtado*[1], *Aliya N Husain*[3], *Thomas Krausz*[4], *Georgios Deftereos*[1]. [1]University of Utah, Salt Lake City, UT, [2]Univ of Chicago Medicine, Chicago, IL, [3]University of Chicago, Chicago, IL, [4]The Univ. of Chicago Hosp, Chicago, IL

Background: Malignant mesothelioma (MM) is an aggressive neoplasm associated with poor prognosis and limited therapeutic options. Immunohistochemistry (IHC) assays for PD-L1 22C3 and 28-8 are approved by the US Food and Drug Administration (FDA) as companion and complementary diagnostics respectively, for predicting response to anti-PD-L1 targeted drugs pembrolizumab and nivolumab. Immune checkpoint inhibitors are now routinely used to treat advanced non-small cell lung carcinoma (NSCLC) and a variety of other solid tumors. Preliminary results from KEYNOTE-028, a nonrandomized, phase Ib trial, suggest that pembrolizumab has anti-tumor activity in advanced malignant pleural mesothelioma (MPM). However, the proportion of patients whose tumors express PD-L1 and their specific clinical characteristics remains unknown.

Design: In order to determine the proportion of MM cases expressing PD-L1, we stained 5 mm tissue microarrays (TMAs; n=134, including 1 pericardial, 117 pleural, and 16 peritoneal MMs) using two FDA approved clinical IHC makers for PD-L1 expression: Dako PD-L1 22C3 pharmDx and Dako PD-L1 28-8 pharmDx. TMA sections were scored independently by two pathologists who were blinded to clinical variables; discordances were resolved by a third pathologist. Scoring was dichotomized into positive (≥1% tumor cells staining) and negative (<1% tumor cells staining). Missing or uninterpretable tissue cores were excluded from analysis.

Results: Overall, 21% (27/127) of MMs were positive using the Dako 22C3 pharmDx assay, whereas 27% (32/119) of cases were positive using the Dako 28-8 pharmDx assay. No significant difference was observed in the rate of positivity between histologic subtypes (biphasic, epithelioid, sarcomatoid), patient sex, age, or T stage. However, the proportion of cases positive for PD-L1 expression was higher among peritoneal mesotheliomas when compared to pleural mesotheliomas (p=0.012 for 22C3; p=0.055 for 28-8).

Conclusions: Our results demonstrate that a significant proportion of MM cases expresses PD-L1. Moreover, our findings suggest that peritoneal MMs are more likely to express PD-L1. These findings support the potential use of PD-L1 expression as a biomarker in MM and may help to identify a subset of patients that may be candidates for immunotherapy.

2100 Clinicopathologic Features of BRCA-Mutant NSCLC Patients Characterized by Comprehensive Histologic Subtyping and Comprehensive Genomic Profiling

James Suh[1], *Adrienne Johnson*[2], *Laurie Gay*, *Garrett M Frampton*[3], *Linda Garland*[4], *Siraj Ali*[5], *Vincent A Miller*[3], *Philip M Stephens*[3], *Jeffrey S Ross*[2], *Julia A Elvin*[6]. [1]Foundation Medicine, Inc., Morrisville, NC, [2]Foundation Medicine, Cambridge, MA, [3]Foundation Medicine, [4]University of Arizona Cancer Center, Tucson, AZ, [5]Cambridge, MA, [6]Foundation Medicine, Inc., Cambridge, MA

Disclosures:
James Suh: *Employee*, Foundation Medicine, Inc.
Adrienne Johnson: *Employee*, Foundation Medicine, Inc.
Laurie Gay: *Employee*, Foundation Medicine, Inc.
Siraj Ali: *Employee*, Foundation Medicine, Inc.
Philip Stephens: *Employee*, Foundation Medicine, Inc.
Jeffrey Ross: *Employee*, Foundation Medicine, Inc.

Background: Two recent comprehensive genomic profiling studies identified *BRCA*-mutant NSCLC as a subset of patients who may benefit from potential PARP inhibition (Suh et al, Oncologist 2016 and Jordan et al, Cancer Discovery 2017). The morphology of *BRCA*-mutant breast and ovarian carcinomas has been described previously by multiple groups as poorly differentiated, including solid growth pattern and necrosis. Our aim was to investigate the clinicopathologic features and co-occurring genomic alterations (GA) of *BRCA*-mutant NSCLC patients, which have not been well characterized.

Design: DNA was extracted from 40 microns of FFPE sections from 6832 consecutive cases of lung adenocarcinoma, adenosquamous carcinoma, NSCLC-NOS and large cell carcinoma (2012-15). Comprehensive genomic profiling was performed using a hybrid-capture, adaptor ligation based next-generation sequencing assay to a mean coverage depth of 572X. GA (point mutations, small indels, copy number changes and rearrangements) involving up to 314 genes were recorded for each case. Comprehensive histologic subtyping and assessment of necrosis were performed on cases with GA involving *BRCA*.

Results: In this series, 201 (2.9%) NSCLC tumors harbored pathogenic *BRCA1* (n=80) or *BRCA2* (n=121) variants. The median age of *BRCA1*/*BRCA2*-mutant patients was 63 (range 29-88) versus 64 years for the entire cohort and 61% versus 53% were female (p-value = 0.0382). Of the 188 cases with at least one representative H&E slide available for review, 72 (38%) showed a predominant solid growth pattern whereas 19 (10%) were micropapillary, 25 (13%) were papillary, 26 (14%) were acinar, 4 (2%) were lepidic, 30 (16%) were NSCLC-NOS and 12 (6%) were invasive mucinous adenocarcinoma. Overall, 102 (54%) tumors were poorly differentiated and 48 (26%) contained necrosis. Interestingly, the proportion of *BRCA1*/*BRCA2*-mutant patients harboring a co-occurring GA involving *MET* (10% versus 5.6%) was nearly double that of the entire cohort (p-value = 0.0134).

Conclusions: *BRCA*-mutant NSCLC patients are more likely to be female, frequently show solid growth pattern and necrosis, closely resembling *BRCA*-mutant tumors of other anatomic sites, and more often harbor co-occurring GA involving *MET*. Recognition of these clinicopathologic features may help improve outcomes for this subset of NSCLC patients using the recently developed class of PARP inhibitors when other approaches fail.

2101 PD-L1/PD1 Expression in Poorly Differentiated Non Keratinizing Squamous Cell Carcinoma of the Thymus

David Suster[1], *Sara Higgins*[2], *German Pihan*[3], *Alexander Mackinnon*[4], *Saul Suster*[5]. [1]Boston, MA, [2]Brigham and Women's Hospital, Boston, MA, [3]Beth Israel Deaconess Medical Center, Boston, MA, [4]Medical College/WI, Milwaukee, WI, [5]The Medical College of Wisconsin, Milwaukee, WI

Background: Poorly differentiated non keratinizing squamous cell carcinoma of the thymus (PDNKSCC), also known as lymphoepithelioma-like thymic carcinoma, is a rare primary tumor of thymic origin. The mainstay treatment of these tumors is surgical and they tend to respond poorly to chemotherapy. The checkpoint protein programmed cell death ligand-1 (PD-L1) bound to its receptor (PD-1) has been demonstrated to be an important therapeutic target for many different tumors. To our knowledge no studies have exclusively examined PD-L1 expression in PDNKSCC. Expression of PD-L1/PD1 in PDNKSCC may indicate that these tumors are potential targets for inhibitor therapy.

Design: Twenty four cases of PDNKSCC were collected and reviewed. Tissue microarrays were created containing all cases using triplicate 2mm cores for each case. TMA's were stained with PD-L1 (Clone SP142, 1:30 dilution, Spring biosciences) and PD-1 (Clone NAT105, 1:50 dilution, Biocare). Cases were analyzed for intensity of staining and percentage of staining using a semi quantitative method (strength of staining: weak, moderate, or strong and percentage of staining: 0-33% [low], 34-66% [medium], and 67-100% [high]. The staining pattern (neoplastic cells versus tumor infiltrating lymphocytes) was documented for each case.

Results: 16/23 (69%) of cases showed some degree of membranous PD-L1 staining. Of the positive cases; 7 had weak staining, 2 had moderate staining and 7 had strong staining. 10 showed a high percentage of staining, 5 showed a moderate percentage of staining, and 1 case showed a low percentage of staining. Overall 9/24 (38%) cases had a combination of strong staining in a high percentage of tumor cells. PD-1 staining showed positivity in 16/24 (66%) cases amongst tumor infiltrating lymphocytes. The majority of these cases showed weak to moderate intensity of staining in a significant percentage of lymphocytes. All neoplastic cells in the tumors were negative for PD-1 staining.

Conclusions: Poorly differentiated non keratinizing squamous cell carcinoma of the thymus (PDNKSCC) is a rare tumor with limited treatment options outside of surgery. PD-L1/PD-1 inhibitor therapy has been used in other solid organ malignant tumors with high expression of PD-L1/PD-1 to some success. The high level of expression in PDNKSCC indicates that PD-L1/PD-1 blockade may be a viable therapeutic option for these patients.

2102 Adenocarcinoma with High-Grade Fetal Adenocarcinoma Component Has a Poor Prognosis Comparable to That of Micropapillary Adenocarcinoma: Clinicopathological, Immunohistochemical and Prognostic Analyses of 53 Cases

Masaki Suzuki[1], *Yukio Nakatani*[2], *Hiroyuki Ito*[3], *Hiroto Narimatsu*[3], *Kozo Yamada*[3], *Emi Yoshioka*[3], *Kota Washimi*[4], *Yoichiro Okubo*[3], *Kae Kawachi*[1], *Yohei Miyagi*[5], *Tomoyuki Yokose*[1]. [1]Kanagawa Cancer Center, Yokohama, Kanagawa, [2]Chiba University Hospital, Chiba, Japan, [3]Kanagawa Cancer Center, [4]Kanagawa Cancer Center, Yokohama-shi, Kanagawa, [5]Kanagawa Cancer Center Research Institute, Yokohama, Kanagawa

Background: Fetal adenocarcinoma is a rare variant of lung adenocarcinoma, which is subcategorized into low-grade (L-FLAC) and high-grade forms (H-FLAC). H-FLAC is prognostically worse than

L-FLAC, but the prognostic differences between H-FLAC and the major subtypes of lung adenocarcinoma are yet to be clarified.

Design: We reviewed 53 surgically resected lung cancers having an H-FLAC component in various proportions (years 1991-2016), and analyzed their clinicopathological, immunohistochemical and prognostic features. H-FLAC histology was defined as follows: 1) complex glandular, cribriform and papillary structures composed of columnar clear cells with pseudostratified nuclei and prominent nuclear atypia; 2) the apical border of the glands being flat; and 3) no morule formation. We performed prognostic analyses of H-FLAC-predominant (25 cases) and H-FLAC-nonpredominant (16 cases) subgroups (years 1991-2016). We further analyzed the prognostic differences between adenocarcinomas with an H-FLAC component (AC with H-FLAC, 36 cases) and major subtypes of adenocarcinoma without any H-FLAC component (1514 cases) (years 2000-2016).

Results: Lung cancers with an H-FLAC component predominantly occurred in elderly males with smoking history. Median tumor size was 33 mm. 29 patients were at stage I, 13 patients stage II, and 11 patients stage III. H-FLAC histology was combined with conventional-type adenocarcinoma (41 cases), squamous cell carcinoma (5 cases), large cell neuroendocrine carcinoma (5 cases), enteric adenocarcinoma (2 cases), and small cell carcinoma (1 case). The H-FLAC component showed immunopositivity for AFP (39%), Glypican-3 (37%), SALL4 (17%) and TTF-1 (64%). Five-year overall survival (OS) of H-FLAC-predominant and H-FLAC-nonpredominant subgroups were 44% and 56%, respectively (P=0.962). Five-year OS of lepidic-, acinar-, papillary-, solid-, and micropapillary-predominant adenocarcinomas, invasive mucinous adenocarcinomas, and AC with H-FLAC were 94%, 82%, 77%, 69%, 57%, 83%, and 40%, respectively (P<0.001). Both the univariate and multivariate analyses showed that AC with H-FLAC had significantly lower OS than the other histological subtypes except for the micropapillary-predominant subtype.

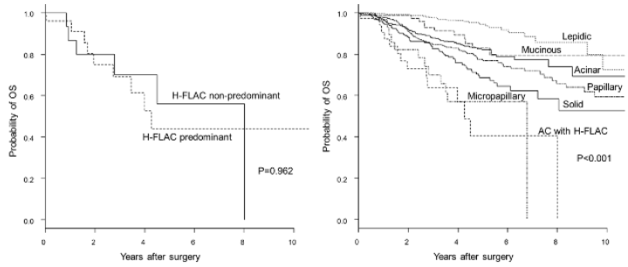

Conclusions: Our study demonstrated that lung adenocarcinomas with an H-FLAC component had a poor prognosis that was comparable to that of micropapillary adenocarcinoma. The presence of an H-FLAC component in lung adenocarcinomas should be recognized as an important prognostic marker.

2103 PREVIOUSLY PUBLISHED

2104 MET exon 14 skipping mutations are seen in early lung adenocarcinoma

Radhika Tandon[1], *Pierre Massion*[2], *Charles A Powell*[3], *Hideo Watanabe*[4], *Yong Zou*[5], *Alain Borczuk*[6]. [1]Weill Cornell Medicine, [2]Vanderbilt University, [3]Icahn School of Medicine at Mount Sinai, [4]Icahn School of Medicine at Mount Sinai, New York, NY, [5]Vanderbilt University Medical Center, Nashville, TN, [6]Cornell University Medical Center, New York, NY

Background: MET exon 14 skipping mutations have been described in 4% of lung adenocarcinomas and in up to 25% of pulmonary sarcomatoid carcinoma. As they are mutually exclusive with other trunk driver type oncogenic mutations such as KRAS and EGFR, it is assumed they are early events in adenocarcinogenesis. We describe 3 cases of early lung adenocarcinoma with MET exon 14 skipping mutations identified by sequencing and confirmed by RNA testing.

Design: A cohort consisting of 25 adenocarcinoma in situ and 32 minimally invasive adenocarcinoma were analyzed using a custom capture based next generation sequencing platform for 305 genes which included MET gene exon 14 skipping mutations (D1028* and Y1021F). RNA extracted from positive and negative cases were analyzed using Affymetrix Clariom-D arrays for alternative splicing. In addition, an RNA in-situ hybridization approach was used for MET exon 12/13, 14/15 and 13/15 junctions using the ACD BaseScope exon junction technology with tumor harboring known exon 14 skipping mutations used as positive control, and tumors without this class of mutation as negative control.

Results: Three cases (1 AIS and 2 MIA) were identified, 2 with D1028* and one with Y1021 mutations. Clariom-D alternative splicing with loss of exon 14 was confirmed when compared to adenocarcinomas without this mutation. BaseScope in situ hybridization showed the presence of MET 12/13 and MET 13/15 message in one of the MIA cases (Figure1 upper panel and lower panel respectively) as well as in positive controls. Two of the three cases were technically inadequate for BaseScope assay based on control probes, presumably related to specimen age.

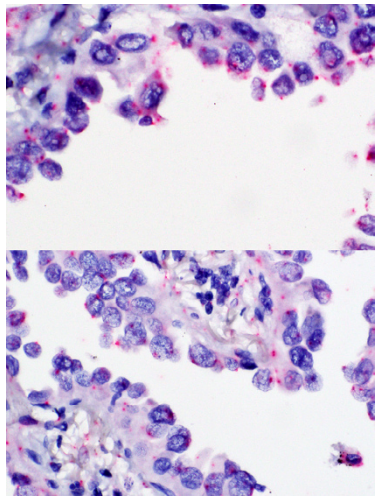

Conclusions: Three cases of AIS and MIA (5.3 %) were identified harboring mutually exclusive MET mutations resulting in exon 14 skipping at a rate similar to that described in more advanced disease. This supports the hypothesis that these mutations occur early in adenocarcinogenesis, including the sequence beginning with non-mucinous lepidic patterned tumors.

2105 The Value of reflex Gomori Methenamine Silver staining on post-transplant transbronchial biopsy specimens

Hamza Tariq[1], *Cynthia Forker*[1], *Daniel D Mais*[1]. [1]University of Texas Health Science Center at San Antonio, San Antonio, TX

Background: Fungal infections remain one of the major causes of morbidity and mortality in lung transplant recipients. The pulmonary allograft is especially prone to fungal infections due to the continuous and direct exposure to environmental microbes; the denervation of the allograft with subsequent impaired cough reflex and abnormal mucociliary clearance; and the aggressive immunosuppression following transplantation. Gomori Methenamine Silver (GMS) stain is routinely performed on all post-transplant transbronchial biopsies at most centers. We retrospectively analyzed the routine use of GMS staining at our institution in order to assess its utility and cost.

Design: A total of 1,027 transbronchial biopsies from lung transplant recipients over a seven year period from 2010 to 2017 were retrospectively reviewed. Hematoxylin and Eosin (H & E) stains were performed on all transbronchial biopsies using routine laboratory protocol. In addition reflex GMS staining was performed on all transbronchial biopsies using the automated Dako artisan link special stainer. A cost analysis was performed for reflex GMS staining on all transbronchial biopsies keeping in consideration the cost of the GMS kit and the reagents used for the automated stainer (95 % alcohol, 100 % alcohol, wash solution, 10 % bleach, artisan clearing solution and xylene).

Results: Out of the 1,027 specimens only one case was positive for fungal organisms on GMS stain. The technical cost of GMS staining on all post-transplant transbronchial biopsies was found to be $46 per specimen. The total cost of GMS stains on 1,026 transbronchial biopsies negative for fungi was $47,196. The average time taken by the automated stainer to perform GMS straining was 50 minutes for less than five slides and 85 minutes for more than five slides. Additional cost considerations include pathologist time spent analyzing GMS-stained slides and delays in issuing a report.

Conclusions: Reflex GMS staining on all post-transplant transbronchial biopsies has limited utility, leads to delays in issuing reports, and is associated with additional cost. Further study and consideration are required to determine clinicopathologic indications for GMS staining in particular cases.

2106 Loss of ATRX Expression Predicts Worse Prognosis in Pulmonary Carcinoid Tumors

Simone Terra[1], *Hao Xie*[1], *Jennifer Boland*[1], *Aaron S Mansfield*[1], *Anja Roden*[1]. [1]Mayo Clinic, Rochester, MN

Background: ATRX is a chromatin regulator which plays key roles in heterochromatin structure and genomic stability. Acquired mutations have been identified in various cancers. In pancreatic neuroendocrine

tumors, ATRX loss has been associated with worse prognosis. However, ATRX expression has not been studied in pulmonary carcinoid tumors (PCT). We investigated ATRX expression in PCT and its relationship with clinical outcome.

Design: Resected PCTs (1997-2017) were retrospectively identified from institutional pathology files. Clinical information was collected from medical records. ATRX immunohistochemistry (clone D-5) was performed on whole tumor sections. Percentage of tumor nuclei staining was recorded independently by a thoracic pathologist and a pathology trainee. Loss of ATRX expression was defined as <5% nuclear staining in tumor cells. All tumors were staged according to the 7th and 8th UICC/AJCC systems. Continuous variables were compared with Wilcoxon rank sum test. Categorical variables were compared with Fisher's exact test. Survival was estimated with Kaplan-Meier method and compared with log-rank test.

Results: The 76 studied patients included 35 men (46%), with a median age of 58.4 years (range, 14.8-86.3). Fifty-eight (76%) had typical PCT, and 18 (24%) had atypical PCT. The tumor was completely resected in 73 (96%) and incompletely resected in 3. Three (4%) cases had metastatic disease at diagnosis. Median tumor size was 2.5 cm (range, 0.8-8.3 cm). Necrosis, lymphovascular, and perineural invasion were present in 3 (4%), 4 (5%), and 4 (5%) cases, respectively. Atypical PCT had median ATRX nuclear expression of 15% [range, 0%-100%], significantly lower (p<0.001) than typical PCT with median ATRX expression of 100% [range, 0%-100%]. Of the 11 PCT that showed ATRX loss, 7 were atypical and 4 were typical PCT. ATRX loss was associated with higher mitotic activity (p=0.01), diagnosis of atypical PCT (p=0.002), and worse disease free survival (HR=4.2, 95% CI 1.04-17, p=0.04). PCTs with ATRX loss trended towards higher N-stage (p=0.05). The interclass correlation coefficient between two reviewers for nuclear ATRX expression was good (0.65, 95% CI 0.48-0.77).

Conclusions: Loss of ATRX expression predicts worse prognosis in pulmonary carcinoid tumors, and might be useful in patient management. Molecular studies are needed to elucidate the function of ATRX in the pathogenesis of these tumors.

2107 Temporal Heterogeneity of Programmed Cell Death-Ligand 1 Expression in Thymic Epithelial Tumors

Simone Terra[1], *Aaron S Mansfield*[1], *Anja Roden*[1]. [1]Mayo Clinic, Rochester, MN

Background: Programmed Cell Death-Ligand 1 (PD-L1) and Programmed Death Protein 1 (PD-1) blocking antibodies have been found to be promising immunotherapies for numerous malignancies. Studies have shown that PD-L1 is expressed in 54-70% of thymic carcinoma and 23-64% of thymoma. However, the temporal and spatial heterogeneity of its expression has not been studied in thymic epithelial tumors (TET). We compared the expression of PD-L1 between original and subsequent specimens of TET.

Design: Institutional pathology files (1979-2016) were searched for TET that had tissue from multiple time points. All cases were reviewed by a thoracic pathologist. PD-L1 expression by immunohistochemistry (clone SP263) was reviewed by two authors; membranous staining of tumor cells was scored as <1%, 1-10%, >10-50%, >50%. Statistical analysis was performed.

Results: Thirteen patients (8 men, median age at diagnosis, 48 years, range, 32-70) with thymomas (N=7, including 1 WHO type A, 2 B2, 4 B3), thymic carcinomas (N=5) or atypical thymic carcinoid tumor (N=1) were included. The first specimen was a primary TET from 12 patients, and a metastasis from 1 patient. The subsequent specimens were recurrences in 2 instances, and metastasis in 17 instances. In the initial specimen, PD-L1 expression was <1% (N=3), 1-10% (N=1), >10-50% (N=1) or >50% (N=8) as determined by one of the authors. Using the <1% tumor cell expression cutoff, the comparison of the original and subsequent specimens yielded 10 (77%) patients with concordant (8 all positive specimens; 2 all negative); and 3 (23%) with discordant specimens (2 positive first specimens, with negative subsequent metastasis; 1 negative primary tumor with positive metastasis) (kappa, 0.57) (Table). Using >50% tumor cell staining as cutoff all patients had concordant specimens including 8 (61.5%) positive; and, 5 (38.5%) negative cases (kappa, 1.0). Reviewers agreed on PD-L1 expression percentage in 28 (of 32, 87.5%) specimens (kappa 0.714).

Temporal heterogeneity of PD-L1 expression on tumor cells (cutoff <1%)

PD-L1 expression in initial specimen	PD-L1 expression in follow-up specimen/metastasis	N (%) (N=32)[a]
Neg*	Neg	2 (15.4)
Pos**	Pos	8 (61.5)
Pos	Neg	2 (15.4)
Neg	Pos	1 (7.7)

*Neg, negative; **Pos, positive; [a] Total number of specimens analyzed

Conclusions: Our findings show that disagreements in PD-L1 expression on tumor cells in TET occur between initial lesions and metastases/recurrences and should be considered when patients are treated with anti-PD-1 or anti-PD-L1 inhibitors.

2108 Clinical Implications of Submucosal Eosinophilia in Severe Asthma

Melissa Tjota[1], *Ayodeji Adegunsoye*[2], *Kyle Hogarth*[2], *Steven White*[2], *Jerry Krishnan*[3], *Aliya N Husain*[1]. [1]University of Chicago, Chicago, IL, [2]University of Chicago, [3]University of Illinois at Chicago

Background: Asthma is a chronic inflammatory disease of the lungs that affects over 200 million people worldwide with an annual mortality of 250,000 deaths. In poorly controlled asthma, endobronchial biopsy specimens may be obtained to optimize diagnostic accuracy and facilitate appropriate therapy. However, the impact of submucosal eosinophilia on clinical outcomes is not known.

Design: We conducted a retrospective study to investigate the clinical importance of submucosal eosinophilia in consecutive adult patients (n=220) at the Refractory Obstructive Lung Disease clinic over a ten-year period (2008-2017). All patients who had poorly controlled asthma despite respiratory inhaler education and guideline-recommended asthma therapy underwent endobronchial lung biopsy. Clinical data and demographics were obtained through review of the electronic medical records.

Results: One hundred and seventy-seven patients (80.5%) had submucosal eosinophilia present on endobronchial biopsy. When compared to patients without submucosal eosinophilia, patients with submucosal eosinophilia had increased intra-epithelial and submucosal cellularity, and a greater prevalence of thickened basement membrane with smooth muscle prominence. Patients with submucosal eosinophilia also had lower forced vital capacity (FVC) (75% vs. 82%, P=0.026), forced expiratory volume in the first second (FEV1) (67% vs. 78%, P=0.005), FEV1:FVC ratio (67% vs. 74%, P=0.018), and higher exhaled nitric oxide (41% vs. 15%, P=0.009) than those without. Compared to bronchoalveolar lavage eosinophilia, submucosal eosinophilia correlated more with diminished lung function. Importantly, submucosal eosinophilia more accurately predicted the reduction of asthma exacerbations with anti-IgE targeted therapy (omalizumab) (Figure 1).

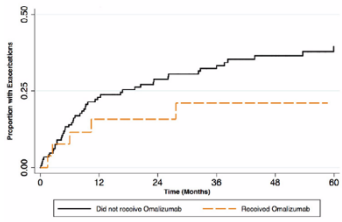

Figure 1. Omalizumab therapy reduces asthma exacerbations in patients with submucosal eosinophilia.

Conclusions: The results of our investigation suggest that incorporating the presence of submucosal eosinophilia into the clinical assessment for patients with severe asthma may help identify individuals who will respond to anti-IgE targeted therapy (omalizumab) to reduce exacerbations and improve long-term disease management.

2109 Effects of Neoadjuvant Therapy on Programmed Cell Death Ligand 1 (PD-L1) Expression and Immune Microenviroment in Non-Small Cell Lung Cancer (NSCLC)

Kristen Tomaszewski[1], *Tiffany Huynh*[1], *Marina Kem*[1], *Mari Mino-Kenudson*[1]. [1]Massachusetts General Hospital, Boston, MA

Background: Background: Programmed Cell Death 1 (PD-1)/PD-L1 blockade is a part of the current treatment paradigm for advanced NSCLC patients, and PD-L1 expression on tumor cells by immunohistochemistry (IHC) is used as a requisite or guidance in selecting patients for the blockade. Now, the efficacy of PD-1/PD-L1 blockade combined with chemotherapy or radiation is being evaluated. However, effects of chemotherapy and/or radiation on PD-L1 expression and tumor microenvironment have not been well studied in NSCLC.

Design: Design: Our clinical database was queried for patients who had undergone neoadjuvant chemo +/- radiation therapy followed by resection for stage IIIA NSCLC, and those with available pre-treatment (pre-Tx) and resection specimens were included in this study. Pre-Tx biopsy or cytology samples and representative sections of resections were stained for dual PD-L1 (clone E1L3N) and CD8 by IHC. Each sample was assessed for a fraction of tumor cells with membranous PD-L1 staining. CD8+ tumor infiltrating (TIL) and stromal T cells were also scored semiquantitatively (0-1) and with percentages (of all stromal nucleated cells), respectively, in non-cytology samples.

Results: Results: The study cohort consisted of 22 cases (16 [73%] female, mean age 64.8 years; 16 [73%] adenocarcinomas). PD-L1 expression was present in 3 (14%) pre-Tx samples (1%-5%/≥ 50% in 2/1), while 9 main tumor resections (41 %) showed PD-L1 expression (1%-5%/5%-10%/10%-25%/25%-50%/≥50% in 2/1/2/2/2). Abundant CD8+ TILs were seen in 2 (13%) of 15 non-cytology, pre-Tx samples and in 3 (14%) of resections. CD8+ T cells comprised a significant fraction (≥20%) of stromal cells in 2 (14%) of 14 pre-Tx samples and 8 (36%) of resections. Compared with pre-Tx samples, resection PD-L1 expression was significantly upregulated in 8 (36%), and was downregulated in 2 (9.1%). CD8+ TILs were increased and decreased in 1 (6.7%) each. In a subset of cases CD8+ stromal T cells were either increased (3, 21%) or distributed around the residual tumor nests as peritumoral cuffs (8, 36%), and 3/4 of cases with upregulated PD-L1 expression were associated with prominent CD8+ stromal cells (≥20% of stromal cells and/or peritumoral cuff).

Conclusions: Conclusion: Despite a small cohort size, the results suggest that chemo +/- radiation therapy frequently upregulates PD-L1 expression on tumor cells, often in association with prominent CD8+ T cells in NSCLC, supporting the rationale for PD-1/PD-L1 blockade combined with chemo/radiation therapy.

2110 Histological Findings in Lung Biopsies after Allogeneic Hematopoietic Stem Cell Transplantation

Guldeep Uppal[1], *Ashley Vogel*[2], *Dolores Grosso*[3], *Neal Flomenberg*[3], *John L Wagner*[3], *Jerald Gong*[4], *Stephen Peiper*[5]. [1]Glen Mills, PA, [2]Thomas Jefferson Univ, Philadelphia, PA, [3]Thomas Jefferson University, [4]Thomas Jefferson Medical College, Philadelphia, PA, [5]Sidney Kimmel Medical College, Philadelphia, PA

Background: Diffuse lung injury is a complication of stem cell transplantation (SCT) that occurs in 25–55% of SCT recipients and accounts for a major cause of transplant-related mortality. Graft-versus-host disease (GVHD) as a cause of lung injury has not been well studied.

Design: A retrospective study (2003-2017) evaluated lung biopsies from 36 allogeneic SCT recipients that raised at least a concern for GVHD upon interpretation. Histologic features specifically evaluated were: 1) lymphocytic bronchiolitis (LB), 2) bronchiolitis obliterans (BO), and 3) constrictive bronchiolitis (CB). Immunostaining for CD3, CD4, CD8, CD20, PD-1 was performed in 25 cases. Clinical data were retrieved from the electronic databases.

Results: Underlying diseases were AML (10), B-cell NHL (9), ALL (6), MM (5), Hodgkin lymphoma (3), MDS (2), and MPN (1). SCTs included haploidentical (26/36), matched unrelated (9/36), and HLA identical (1/36). The average time from transplant to lung biopsy was 10 months (2-60). BO was the most frequent (58%) pathology in (21/36), followed by LB in 35 % (13/36) and CB in 14% (5/36). Additional findings were interstitial pneumonitis of varying severity (14/36), organizing pneumonia (4/36), and diffuse alveolar damage (5/39). The evaluated cases showed CD8+ and PD1- T-cell infiltrate (80%, 20/25). Laboratory evidence of concomitant microbial infection was present in 8 cases with BO being the frequent pathologic feature (6/8). Concomitant, subsequent, and antecedent evidence of non-pulmonary GVHD was noted in one or more organs in 69% (25/36) patients. Pulmonary function test data were available in 22 patients. Of these 22 cases, 6 met NIH consensus criteria for lung GVHD. Histological features of these 6 cases were similar to the remaining 30 evaluated.

Conclusions: The overwhelming majority of cases (86%) had bronchial lesions, which are nonspecific and can be caused by other factors such as preparation therapies and infection. Thus, a definitive interpretation as GVHD was not possible on histological grounds. The differential diagnosis of these lesions is GVHD, drug-induced injury, or an infection. Importantly, despite its severity and need for aggressive therapy, pulmonary GVHD remains a difficult definitive diagnosis. There were no specific histological features to distinguish pulmonary GVHD from other pathologies.

2111 Case Series of Egfr Double Mutations in Patients with Lung Adenocarcinoma

Natalia Vilches[1], *Juan Pablo Flores Gutierrez*[2], *ORALIA BARBOZA*[3], *Karina E Lopez*[4], *Raquel Garza*[3]. [1]Hospital Universitario, Monterrey, NL, Mexico, [2]Guadalupe, NL, Mexcio, [3]Hospital Universitario, [4]Hospital Universitario, Monterrey, Nuevo León

Background: The introduction of targeted therapies has increased the survival time in a subset of patients with NSCLC. The National Comprehensive Cancer Network (NCCN) clinical practice guidelines in oncology recommend measuring the local EGFR gene mutations of NSCLC patients before treatment. Sensitivity to EGFR TKIs in patients with double or multiple mutations is not well described. In the literature there are few reported cases of double mutations. We present a series of six cases of Lung Adenocarcinoma with double mutations found between 2006 and 2017 in a hospital in Northern Mexico.

Design: 479 patients with Lung cancer were evaluated from 2006 to 2017. DNA extraction is performed using a commercial extraction kit, the process is performed by real time PCR in an automated platform in a closed circuit with a commercial kit. The DNA quantification quality control process is analyzed, validating with positive and negative controls, then analysis of the 29 known mutations of EGFR gene exons 18, 19, 20, 21.

Results: 479 cases, 141 (29.43%) patients had EGFR mutations, of which six (4.25%) had double exons EGFR mutations. Of the six cases with double mutations, male to female ratio was 1:1.The histological patterns reported in the double mutations were: 3 (50%) cases with acinar pattern, 2 (33.33%) with micropapillary pattern, and 1 (16.66%) solid pattern. The median age of the six patients is 54 years (range 38-78).

Table 1.- Mutations and histological pattern

	First mutation	Second mutation	Histological pattern	Age of patient
Case #1	L858R	L861Q	Acinar	52
Case #2	L858R	Deletion	Micropapillary	55
Case #3	Deletion	L861Q	Micropapillary	38
Case #4	Deletion	T790M	Solid	53
Case #5	Deletion	L861Q	Acinar	78
Case #6	Deletion	L858R	Acinar	55

Conclusions: EGFR co-mutation had a significantly lower mean progression-free survival than those with a single mutation (5.7 months vs. 12.3 months). The response rate to TKI was significantly worse in those with co-mutation compared to those without co-mutation (38% vs 89%). There are few studies evaluating all the characteristics of cases with double mutations, such as histological pattern and the mutations of EGFR gene exons. Further research on double mutations is suggested because of the impact on treatment and prognosis of the patient.

2112 Indoleamine-2,3-Dioxygenase (IDO-1) Expression in Non-Small Cell Lung Cancer (NSCLC): A Targetable Mechanism of Immune Resistance and Candidate for Dual Therapy with Anti-PD-1/PD-L1

Ashley Volaric[1], *Ryan Gentzler*[2], *Edward Stelow*[3], *Anne Mills*[1]. [1]Charlottesville, VA, [2]University of Virginia, [3]Univ. of Virginia Health System, Charlottesville, VA

Background: A subset of non-small cell lung cancers (NSCLC) express the checkpoint molecule programmed cell death ligand 1 (PD-L1) to escape immune detection. The interaction between programmed cell death-1(PD-1) and its ligand PD-L1 normally serves as a necessary brake on the immune response but allows for unchecked tumor growth when co-opted by cancer. Immunotherapy targeting the PD-1/PD-L1 axis has proven effective in some, but not all, PD-L1-expressing NSCLC. This could in part be due to the co-existence of other mechanisms of immune evasion. The immune regulatory molecule indoleamine-2,3-dioxygenase (IDO) is an enzyme that interferes with T cells through both starvation (via depletion of tryptophan) and toxicity (via generation of a toxic metabolite kynurenine). IDO can be expressed by malignant cells and is associated with worsened outcomes in a variety of tumor types. Targeted therapies are available against IDO, and early phase clinical trials combining IDO and PD-1 inhibitors have been promising. The co-expression of IDO and PD-L1 has not been thoroughly investigated and could provide a useful biomarker for identifying patients with the highest potential for dual immunotherapy.

Design: 102 cases of NSCLC [51 adenocarcinomas (AC), 42 squamous cell carcinomas (SCC) and 9 adenosquamous carcinomas (ASC)] were evaluated for IDO and PD-L1 expression by immunohistochemistry (Sigma Prestige, HPA 023072 and Ventana, SP263). Tumor staining extent was categorized for each stain as negative (<1%), 1-5%, 6-10%, 11-25%, 26-50%, and >50%.

Results: IDO expression is common in NSCLC (Table 1). In addition, subsets from all three tumor types show concomitant expression of PD-L1 and IDO of >1% while subsets of each tumor type demonstrate only IDO expression or PD-L1 expression. The variable patterns of PD-L1 and IDO expression are demonstrated histologically in Figures 1 and 2.

Table 1:

	AC (n=51)	SCC (n=42)	ASC (n=9)
IDO+ Tumor			
1-5%	18%	24%	0%
6-10%	8%	12%	22%
11-25%	6%	5%	22%
26-50%	6%	0%	0%
>50%	4%	2%	0%
PD-L1+ Tumor			
1-5%	18%	2%	0%
6-10%	6%	10%	0%
11-25%	8%	12%	11%
26-50%	4%	5%	22%
>50%	8%	31%	44%
IDO/PD-L1 coexpression	27%	26%	33%
IDO-only	14%	17%	11%
PD-L1-only	16%	33%	44%

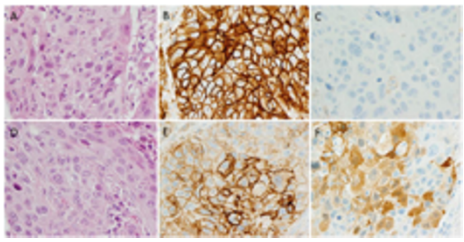

Figure 1: Examples of PD-L1 and IDO co-expression patterns in lung squamous cell carcinomas. The case on the top row (A) demonstrates strong membranous PD-L1 expression in all tumor cells (B). In contrast, IDO is completely negative (C). The case on the bottom row (D) shows diffuse but variably intense membranous PD-L1 positivity (E) with cytoplasmic co-expression of IDO in 50% of cells (F)

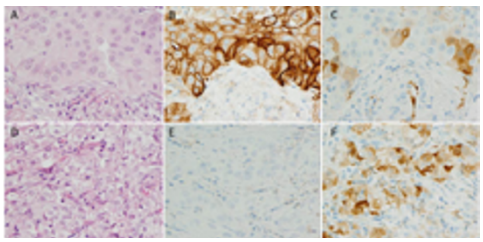

Figure 2: Examples of PD-L1 and IDO co-expression patterns in lung adenocarcinomas. The case on the top row (A) demonstrates membranous PD-L1 expression in 70% of tumor cells (B), while IDO shows patchy cytoplasmic positivity (C). The case on the bottom row (D) shows a complete absence of PD-L1 staining (E) with scattered IDO expression in 40% of tumor cells.

Conclusions: IDO and PD-L1 expression are common in NSCLC, with a subset of PD-L1+ NSCLC also expressing IDO. This suggests that IDO may be a mechanism of anti-PD-1/PD-L1 resistance in these tumors, and that dual therapy could be helpful in these cases. A smaller population of tumors shows PD-L1 or IDO expression in isolation, suggesting single-agent immunotherapy may be more appropriate for some tumors. Studies investigating the association between IDO expression and anti-PD-1/PD-L1 response in NSCLC are needed. Phase III trials evaluating the efficacy of IDO inhibitors in NSCLC are ongoing.

2113 Ki67 Index Should Be Incorporated Into the Classification of Pulmonary Carcinoid Tumors

Ann Walts[1], *Alberto Marchevsky*[2]. [1]Cedars-Sinai Medical Center, Los Angeles, CA, [2]Cedars-Sinai Med Ctr, West Hollywood, CA

Background: Pulmonary carcinoid tumors (PC) are classified by WHO as typical (TC) or atypical (AC) based on mitotic index (2 per 10 hpf) and/or presence of necrosis. Currently, WHO includes Ki67 index (Ki67%) as a feature in GI carcinoid tumors but not in PC. We have previously shown that histologic diagnosis and Ki67% are each independently associated with overall survival (OS) in patients with PC and that a 5% Ki67 cutoff provides the best fit for prognosis. In this study we assess whether this cutoff further stratifies pulmonary TCs for OS.

Design: 225 consecutive PC diagnosed as TC by WHO criteria with available Ki67% were retrieved from our pathology files and divided into Group A (TC with Ki67 ≥ 5%; n=38) and Group B (TC with Ki67 < 5%; n=187). Patient demographics and follow-up information including OS, presence/absence of tumor recurrence and time to recurrence were obtained. OS, and tumor recurrence, and time to recurrence were compared between the 2 groups using Kaplan-Meier methodology, chi-square statistics, and T-test, respectively.

Results: The 225 patients (142 females; 83 males) had a median age of 59 years (8-89 yrs) at diagnosis. TC ranged in size from 0.4 to 7.0 cm (median 2.0 cm) and included 123 pT1a, 44 pT1b, 38 pT2a, 6 pT2b and 14 pTx lesions. There is no significant difference in sex ratio, median age at diagnosis or median size of tumor between the 2 groups. As shown in the Kaplan-Meier plot below, despite longer follow-up in Group B (median 96.5 vs 63.0 mos.), OS is significantly worse in Group A patients (p=0.0089). Group A patients also experienced a higher percentage of tumor recurrences (12.5% vs 5.7%) and a shorter mean time to recurrence (38.0 vs 64.6 mos.) compared to Group B, but these differences did not reach statistical significance, possibly because only a small number of tumors recurred.

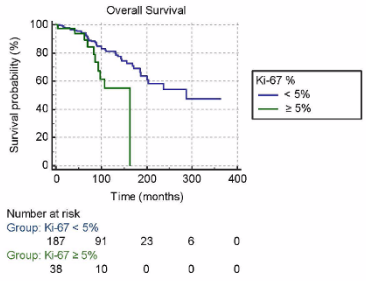

Conclusions: Our findings in this retrospective study indicate that a 5% cutoff value in Ki67% helps stratify TC patients and suggest that this cutoff should be incorporated as an additional diagnostic feature in the classification of PC. Confirmation in large prospective studies is needed to further support incorporation of Ki67% into the classification of PC.

2114 PD-L1 Expression is Related to Tumor Staging in NSCLC

Hangjun Wang[1], *Jason Agulnik*[2], *Goulnar Kasymjanova*[3], *Anna Y Wang*[2], *Victor Cohen*[2], *David Small*[2], *Carmela Pepe*[2], *Lama Sakr*[2], *Pierre O Fiset*[4], *Manon Auger*[5], *Sophie Camilleri-Broët*[6], *Mona Alameldin*[6], *George Chong*[6], *Leon van Kempen*[6], *Alan Spatz*[6]. [1]Verdun, QC, [2]Jewish General Hospital & McGill University, [3]JGH, Montreal, [4]McGill University Health Centre - Glen Site, Montreal, PQ, [5]Mt. Royal, QC, [6]McGill University Health Center & McGill University, Montreal, QC,

Background: PD-L1 is a predictive biomarker for guiding advanced lung cancer patients' treatment. Tumor proportion score (TPS) ≥50% by PD-L1 immunohistochemistry (IHC) testing is used to select patients with advanced non-small cell lung cancer for first line Pembrolizumab immunotherapy. Most of previous study on PD-L1 were tested on surgical resections or small biopsies. In this study, we evaluate PD-L1 expression on three different types of specimens including surgical resection, small biopsy and cytology cell block and correlate it with stage, tumor location and molecular alteration.

Design: A total of 1423 consecutive cases of non-small cell lung cancer (NSCLC), including 368 cytology cell blocks, 813 small biopsies and 242 surgical resections, were included in the study. PD-L1 expression was examined by staining with Dako PD-L1 IHC 22C3 pharmDx. TPS of ≥ 50% tumor cells was defined as positive. A total of 100 viable tumor cells were required for adequacy.

Results: Of the cytology cell blocks, 91% of the specimens had sufficient numbers of tumor cells, and the rate was equivalent to the rate of small biopsies (p>0.05). PD-L1 expression was positive in 42% of cytology cell blocks, close to small biopsies (36%, P=0.04), but higher than surgical resections (29%, p=0.001). This difference is only seen in non-squamous histology (mainly adenocarcinoma). The PD-L1 positive rate is not associated with EGFR, ALK or KRAS molecular alteration. It is only related to stage that the higher stage is more likely to be positive PD-L1 staining. There is no difference in PD-L1 positive rate between different metastatic sites.

Conclusions: Our results demonstrated that non-small cell lung cancer in higher stage is more likely to express PD-L1, especially in metastasis. It is possible that tumor cells have to express higher PD-L1 to enable them switch off the T cell surveillance to help them metastasis. PD-L1 IHC performed well with cytology cell blocks. As cytology cellblocks are commonly available from lung cancer patients, it can provide valuable resource for PD-L1 testing.

2115 PET-Positivity in Benign Lung Lesions: A Series of 120 Resected Nodules with Correlation between PET and Pathologic Features

Xiaoqiong Wang[1], *Sanjay Mukhopadhyay*[1]. [1]Cleveland Clinic, Cleveland, OH

Background: Benign lung nodules can be positive on positron emission tomography (PET), but it is unclear why standardized uptake values (SUVs) are elevated in some benign lesions but not in others. The aim of this study was to identify benign lung lesions that are more likely to be PET positive, to determine the range of SUVs in histologically confirmed benign nodules, and to correlate PET results with pathologic findings.

Design: Our pathology archives were queried to retrieve all benign lung nodules over a 13-year period. In order to exclude sampling error, cases were included in the study only if the nodule was completely resected. Other inclusion criteria were (1) PET findings available and (2) slides available for review. SUVs >2.5 were considered positive. All available H&E-stained slides and special stains for microorganisms were re-evaluated. In necrotizing granulomas, the granulomatous/inflammatory rim was classified as cellular (thick rim with numerous cells) or hypocellular (thin fibrous rim with few cells). In granulomas containing organisms, the number of organisms was classified as numerous (>=100) or few (<100). p values (two-tailed) were calculated using 2x2 contigency tables and Fisher's exact test. The significance threshold was set at .05.

Results: The results are summarized in Table 1. PET was positive in 54/120 (45%) resected benign lung nodules from 120 patients (64F/56M; 39-85y). SUVs ranged from 2.6 to 37.5; 95% were between 2.6 and 10. Necrotizing granulomas had the highest rate of PET positivity (54%) and hamartomas had the lowest (0%). In necrotizing granulomas, PET positivity varied by organism as follows: Histoplasma 18/40 (45%), Aspergillus 7/9 (78%), mycobacteria 6/7 (86%), Cryptococcus 2/4 (50%), Coccidioides 0/1 (0%), no organism found 13/23 (57%). PET-positive necrotizing granulomas were significantly more likely to have a cellular granulomatous rim (p<0.001) but PET positivity did not correlate with presence (p=0.33) or number of organisms (p=0.41).

	PET +/total with PET (%)	SUV 2.6-5	SUV 5.1-10	SUV>10	SUV N/A
Necrotizing granulomas	46/85 (54)	23	10	0	13
Hamartoma	0/19 (0)	0	0	0	0
Inflammatory myofibroblastic tumor	3/3 (100)	0	1	2	0
Others (abscess, pneumonia, sclerosing pneumocytoma)	5/13 (38)	2	1	0	2
TOTAL	54/120 (45)	25	12	2	15

Conclusions: SUVs in most PET-positive benign lung nodules fall between 2.6 and 10. SUV values beyond 10 are rare in benign lesions. The rate of PET positivity in benign lung nodules is highest in necrotizing granulomas and lowest in hamartomas. Among infectious necrotizing granulomas, those containing Aspergillus and mycobacteria have a higher proportion of PET positivity than those containing Histoplasma. In necrotizing granulomas, PET positivity correlates with cellularity rather than presence or number of organisms.

2116 Unique Correlation Between GTF2I Mutation and Spindle Cell Morphology in Thymomas (Type A and AB Thymomas)

Kirsty Wells[1], *Helene Schlecht*[2], *Angela Lamarca*[3], *George Papaxoinis*[4], *Emma Howard*[5], *Michael Bulman*[1], *Andrew Wallace*[1], *Fiona Blackhall*[3], *Yvonne Summers*[3], *Anne Marie Quinn*[6], *Daisuke Nonaka*[7]. [1]Central Manchester University Hospitals NHS Foundation Trust, [2]Central Manchester University Hospitals NHS Foundation Trust, Manchester, Greater Manchester, [3]The Christie NHS Foundation Trust, [4]Hippocration Hospital, [5]Liverpool Women's NHS Foundation Trust, [6]Manchester Greater M, Great Britain, [7]Guy's and St Thomas' NHS Foundation Trust, Gravesend, Kent

Background: Recent study with next generation sequencing has revealed frequent GTF2I mutation in thymomas, with the frequency being highest in type A and type AB, followed by B1, B2, B3 and thymic carcinoma. This has led to the conclusion that GTF2I mutation correlates with more indolent histology subtype and better prognosis. In this study, the presence and distribution of this mutation was tested in order to investigate the relation between GTF2I mutation status and histology subtype in thymic epithelial neoplasms.

Design: 108 thymic epithelial tumors were retrieved, reviewed and sub-classified according to WHO classification scheme. Genomic DNA was extracted from each tumor, and Sanger sequencing was performed to amplify the *GTF2I* 7:74146970 hotspot. Correlation between the GTF2I mutation status and a variety of clinical and pathological parameters was investigated.

Results: There were 16 cases of type A, including 7 atypical type A, 37 type AB, including one case with atypical features, 13 B1, 23 B2, 9 B3, 3 micronodular type, 2 metaplastic type, and 5 thymic carcinomas. 15 tumors failed the test. GTF2I mutation was observed in 80.9% of combined type A / AB group including those with atypical features; 78.6% of type A, 83.9% of type AB and 50% of micronodular type (1/2, with one test failure), while it was not expressed in type B, metaplastic type and thymic carcinoma (p<0.001). Among the GTF2I mutated tumors, seven cases of type AB were originally classified as type B1 (2 cases) and type B2 (5 cases), one type A as type B2, and one atypical type A as type B3. GTF2I mutation was observed in 37/71 (52.1%) patients with stages 1-2 and in 2/22 (9.1%) patients with stages 3-4 (p<0.001). Both thymoma histotype (p<0.001) and stage (p=0.001) were independently and significantly associated with GTF2I mutation. Advanced stage (hazard ratio [HR] 8.8, 95%CI 2.2-35.2, p=0.002), increased size (HR 0.96, 95%CI 0.93-0.99, p=0.002) and R1/2 margin (HR 11.5, 95%CI 1.3-102.7, p=0.029) were identified as prognostic factors.

Conclusions: GTF2I mutation appears unique in type A and AB thymomas, including those with atypical features, and micronodular type, all of which share a variable amount of spindle cell morphology, indicating they represent a group biologically distinct from type B thymomas. Indolent nature might be attributed to histology subtype rather than mere GTF2I mutation status. Subtle spindle cell component in type AB is easily overlooked, which may lead to inappropriate thymoma subtyping.

2117 The Role of Immunohistochemistry in the Evaluation of Rejection in Morphologically Normal-Appearing Lung Transplant Biopsies

Rachel E White[1], *Irina L Timofte*[2], *Nkechi Okonkwo*[3], *Allen Burke*[4]. [1]University of Maryland, Baltimore, MD, [2]University of Maryland, [3]University of Maryland Medical Center, Baltimore, MD, [4]UMMS, Baltimore, MD

Background: Diagnosis of graft rejection in lung transplant patients requires accurate and reliable interpretation of transbronchial lung biopsies. The significance of immunohistochemically positive (IHC)+ lung transplant biopsies with normal appearing routine sections has not been studied in detail.

Design: We studied retrospectively 211 biopsies from 51 patients, who had multiple consecutive biopsies in a one and one-half year period. Those patients with single biopsies were excluded. IHC stains for T-lymphocytes (CD3) were performed routinely. Acute cellular rejection was defined by ISHLT criteria. Borderline biopsies were defined as unremarkable on H&E staining but demonstrated increased CD3-positive cells by IHC. Emphasis was placed on "A" rejection only. Infection status at the time of biopsy was determined by culture for bacteria and fungi and PCR for viruses.

Results: There were 35 men (62 ± 12 years of age at biopsy) and 16 women (56 ± 15). Borderline biopsies (n=54) were present in 32 patients, and ≥ 1 biopsy with cellular rejection (n=36) present in 24. Borderline biopsies included 44 diffuse increase in the interstitium, 6 diffuse increase with scattered incomplete perivascular rings, and 4 with scattered rings with normal T-cell density. 56% of borderline biopsies occurred in patients with ≥ 1 biopsy with rejection, compared to 31% of normal biopsies (p. = .002). There was no correlation between biopsy diagnosis (negative, borderline, and rejection) and positive results for infection (p>0.2).

Conclusions: Inclusion of a "borderline" category by IHC may be useful at least in the discussion area of biopsies, as it seems to correlate somewhat with metachronous diagnoses of rejection.

2118 Pitfalls of PD-L1 Immunohistochemistry: A Comparison of 22C3 and SP263 antibodies Across Laboratories and Pathologists

Adam Wilberger[1], *Dara Aisner*[2], *Daniel T Merrick*[3]. [1]University of Colorado Hospital, Aurora, CO, [2]Denver, CO, [3]University of Colorado

Background: Multiple antibodies (Abs) for PD-L1 immunohistochemistry (IHC) testing are available commercially. Two of the available Abs are 22C3 Ab (Dako) for pembrolizumab and SP263 Ab (Ventana) for durvalumab. Pembrolizumab is an FDA-approved for treatment of non-small cell lung carcinoma (NSCLC) in PD-L1-positive patients with indications differing based on 22C3 PD-L1 expression of ≥1-49% (low positive expression) and ≥50% (high positive expression).

We are validating the SP263 Ab using 22C3 staining results at an outside laboratory as the comparator. Studies show comparable staining levels across Abs, suggesting cutoffs may cross-apply. However, studies have also shown moderate inter-observer variability in IHC interpretation. We aim to compare results of two PD-L1 Abs in relation to clinically actionable cutoffs while assessing inter-observer variability before and after a training session.

Design: 23 specimens of NSCLC previously sent to a reference

laboratory for 22C3 PD-L1 IHC were stained for SP263 Ab. 22C3 IHC was performed using the 22C3 pharmDx protocol on Dako Automated Link 48 platform (Dako, Carpinteria, CA, USA). SP263 IHC was performed at the University of Colorado on Ventana Benchmark staining systems (Ventana, Tucson, AZ, USA).

3 pathologists, blinded to the results of 22C3 IHC, independently scored the SP263 stain for proportion of tumor cells positive (membranous staining at any pattern and intensity). 17 cases were scored prior to and after interpretation training by a Ventana pathologist. 6 more cases were scored after training.

Results: Results of concordance and discordance are summarized in Table 1. For inter-observer agreement, kappa values for the 17 pre and post-training samples were 0.77 and 0.94, respectively. For all 23 cases post-training, kappa was 0.97.

Concordant Cases (SP263 Ab)					
			Negative	Low Positive	High Positive
Pre-training			9/17	3/17	3/17
Post-training			6/17	6/17	4/17
Post-training (All cases)			8/23	9/23	6/23
Discordant Cases (22C3 vs. SP263 Ab)					
Case No	22C3 (outside interpretation)	22C3 (our interpretation)	Obs 1 (SP263)	Obs 2 (SP263)	Obs3 (SP263)
#1	Low positive	Low positive	Negative	Negative	Negative
#12	Negative	Low positive	Low positive	Low positive	Low positive
#13	High positive	High positive	Low positive	Low positive	Low positive
#15	Negative	Low positive	Low positive	Low positive	Low positive

Conclusions: The data shows a concordance rate of 91.3% between the gold standard and SP263. The discordances in these cases could potentially lead to changes in patient care, as clinical thresholds were crossed, particularly the negative versus low positive (1% tumor cell staining), which impacts second line therapy selection. Additional cases are in process.

The most problematic cases both for agreement between antibodies and agreement between pathologists are those with a low-level of PD-L1 expression. The discordance of low-level staining may reflect differences in Ab clone, technical assay performance or interpretive challenges. Training of pathologists and thorough technicaal validation is paramount.

2119 Comparison of RNA in situ hybridisation (RISH) and immunohistochemistry for detection of PD-L1 expression in a panel of non-small cell lung carcinoma cell lines

Mark Wright[1], *Odharnaith O'Brien*[2], *Julie Mc Fadden*[3], *Henrik Thirstrup*[4], *Andreas Schønau*[4], *Lauren Brady*[5], *Lorraine Mc Carra*[3], *Marie Reidy*[3], *Umair Aleem*[3], *Anne-Marie Baird*[6], *Sinead Cuffe*[3], *Steven G Gray*[3], *Stephen Finn*[6]. [1]St. James's Hospital, Dublin 8, Leisnter, [2]Clonmel, [3]St. James's Hospital, [4]Visiopharm, [5]Trinity College Dublin, [6]University of Dublin, Trinity College, Dublin 8

Disclosures:
Henrik Thirstrup: *Employee*, Visiopharm
Andreas Schønau: *Employee*, Visiopharm A/S

Background: Immunohistochemical (IHC) assessment of PD-L1 protein expression using a variety of antibodies has rapidly become established as a companion or complementary methodology to identify candidate patients for PD-L1 immune-checkpoint targeted therapies in lung cancer. IHC is challenging in terms of laboratory methodology and pathologist interpretation. Furthermore, it is well known that patients respond to PD-L1 targeted therapies even in the absence of positive expression using IHC. Recently, RISH technology has improved significantly, and we propose that PD-L1 RISH could provide an alternative technology for the assessment of PD-L1, with improved dynamic range, thus providing the potential to identify additional patients for anti-PD-L1 therapy.

Design: A TMA was constructed comprising of eight highly annotated non-small cell lung carcinoma (NSCLC) formalin fixed cell lines in quadruplicate. PD-L1 status was assessed by IHC (DAKO 22C3) and read independently by a pulmonary pathologist. Sections of the same TMA were interrogated for PD-L1 mRNA expression by semi quantitative RISH using RNAScope technology. Image analysis was based on RNA abundance assessment (Visiopharm).

Results: As shown in table 1 these results demonstrate strong concordance between IHC and RISH for PD-L1 assessment, when resolved using an image analysis platform.

Table 1: Results comparing IHC and RISH on a panel of NSCLC cell lines scored by a pulmonary pathologist and image analysis

Cell Line	Immunohistochemistry (DAKO 22C3) Pathologist Scoring			RISH RNAScope Pathologist Scoring			RISH Image Analysis Scoring	
	Intensity	% positive	Expression	Score 1-5	0-100% Positive	Result	Composite Score 0-400	PD-L1 0-100%
MCF7	0	0%	No expression	0	0%	Negative	55.7654	0
H3122	1	50%	High expression	3	10%	Weak Positive	45.0389	8.3876
H1975	3	80%	High expression	5	90%	Positive	78.0689	97.5384
NCI H596	2	80%	High expression	5	80%	Positive	46.5875	58.8194
H460	2	50%	High expression	5	80%	Positive	121.8025	N/A
A549	1	50%	High expression	5	50%	Positive	77.6182	44.9184
HCC827	1	50%	High expression	5	50%	Positive	85.8926	42.9365
H2228	1	30%	Expressed	4	40%	Weak Positive	56.8198	23.5186

Conclusions: The data establish RISH with automated image analysis as a credible platform for PD-L1 RNA abundance assessment, which compares well with gold standard IHC. A prospective comparison of PD-L1 IHC with RISH in clinical samples will be used to further investigate the clinical utility of the technique.

2120 Identification of a novel CEP72-ROS1 fusion variant in non-small-cell lung cancer by next generation sequencing

Chunwei Xu[1], *Wenxian Wang*[2], *Yanping Chen*[3], *Youcai Zhu*[4], *Xinghui Liao*[4], *Wei Liu*[3], *Jianping Lu*[3], *Yanfang Guan*[5], *Rongrong Chen*[5], *Gang Chen*[6]. [1]Fujian Cancer Hospital, Fuzhou, Fujian, [2]Zhejiang Cancer Hospital, Hangzhou, Zhejiang, [3]Fujian Cancer Hospital, Fuzhou, China/Fujian, [4]Zhejiang Rongjun Hospital, Jiaxing, China/Zhejiang, [5]Geneplus-Beijing, Beijing, China/Beijing, [6]Fujian Cancer Hospital, Fu, China/Fujian

Background: ROS1 rearrangement is a validated therapeutic driver gene in non-small cell lung cancer and is a small subset (1%-2%) of NSCLC. A total of 15 different fusion partner genes of ROS1 in NSCLC have been reported. The multi-targeted MET/ALK/ROS1 tyrosine kinase inhibitor (TKI) crizotinib demonstrated remarkable efficacy in ROS1-rearranged NSCLC. Consequently, the detection assays of ROS1 have included fluorescence in situ hybridisation (FISH), immunohistochemistry and real-time PCR. The next-generation sequencing (NGS) assay covers a range of fusion genes and approaches to discover novel receptor-kinase rearrangements in lung cancer.

Design: Consequently, the detection assays of ROS1 have included fluorescence in situ hybridisation (FISH), immunohistochemistry and real-time PCR. The next-generation sequencing (NGS) assay covers a range of fusion genes and approaches to discover novel receptor-kinase rearrangements in lung cancer.

Results: A 63-year-old smoker male patient with stage IV NSCLC (TxNxM1) was detected a novel ROS1 fusion. Histological examination of the tumor showed lung adenocarcinoma. Then NGS analysis of the hydrothorax cell blocks revealed a novel CEP72-ROS1 rearrangement. This novel CEP72-ROS1 fusion variant is generated by the fusion of exons 1–11 of CEP72 on chromosome 5p15 to the exons 23–43 of ROS1 on chromosome 6q22. The predicted CEP72-ROS1 protein product contains 1202 amino acids comprising of the N-terminal amino acids 594–647 of CEP72 and C-terminal amino acids of 1-1148 of ROS1.

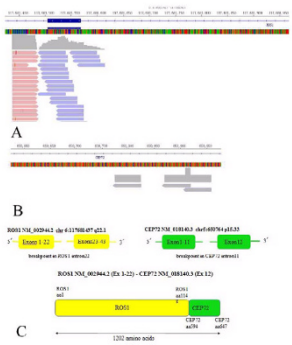

Conclusions: CEP72-ROS1 is a novel ROS1 fusion variant in NSCLC discovered by NGS and could be included in ROS1 detecting assay such as RT-PCR. And pleural effusion samples had good diagnostic performance in clinical practice.

2121 Histological factors predicting exacerbation of interstitial pneumonia in patients with resected lung cancer

Yukichika Yamamoto[1], *Mikiko Hashisako*[1], *Kazuto Ashizawa*[2], *Tomoshi Tsuchiya*[3], *Noriho Sakamoto*[4], *Naoya Yamasaki*[3], *Yuji Ishimatsu*[4], *Takeshi Nagayasu*[3], *Junya Fukuoka*[5]. [1]Nagasaki University Hospital, Nagasaki, [2]Nagasaki University Graduate School of Biomedical Sciences, [3]Nagasaki University, [4]Nagasaki University Graduate School of Biomedical Sciences, Nagasaki, [5]Nagasaki University Graduate School of Biomedical, Nagasaki

Background: In patients with lung cancer and interstitial pneumonia (IP), the progression of IP rivals lung cancer as a life-threating factor. Despite the clinical importance, evaluations of IP in lung cancer patients are limited. The aim of this study is to elucidate the histological characteristics related to the postoperative exacerbation of IP.

Design: During the period from October 2005 to December 2012, we investigated the patients who underwent pulmonary resection and were diagnosed with lung cancer combined with IP. We scored four histological characteristics of resected specimens (e.g. fibrotic focus, emphysema, granuloma, and microscopic honeycombing) into four grades: 0, 1, 2 and 3. We also classified patients based on guidelines of IPF: usual interstitial pneumonia (UIP), probable UIP, possible UIP and not UIP. We analyzed the association between above histological scores along with UIP diagnosis and postoperative exacerbation judged by CT images.

Results: 81 patients were diagnosed with lung cancer complicated by IP. 28 patients were died. The postoperative exacerbation of IP on CT images was observed in 19 patients. Histologically, the fibroblastic focus was observed in 30 patients (score 0, 51 [63%]; score 1, 24 [29.6%]; score 2, 6 [7.4%]; and score 3, 0 [0%]). The microscopic honeycombing was observed in 11 patients (13.6%). The proportion of diagnoses was as follows: UIP (n=8, 9.8%), probable UIP (n=14, 17.2%), possible UIP (n=30, 37%) and not UIP (n=29, 35.8%). When the patients with lung cancer have both the fibroblastic focus and the microscopic honeycombing in peripheral lung, it is likely to exacerbate interstitial opacity of CT images ($p<0.05$). Other histological characteristics were not associated with the exacerbation of IP.

Conclusions: Combination of fibroblastic focus and microscopic honeycombing is significantly associated with the exacerbation of IP in lung cancer patients.

2122 A Positive Feedback Loop of IL-17B-IL-17RB Activates ERK/β-catenin to Promote Lung Cancer Metastasis

Yi-Fang Yang[1], *Yi-Ning Chung*[2], *Shyng-Shiou F Yuan*[2]. [1]Kaohsiung Medical University Hospital, Kaohsiung, Taiwan, [2]Kaohsiung Medical University Hospital

Background: Inflammation contributes to the development and progression of cancer. However, the mechanisms by which inflammation contributes to cancer progression remain incompletely understood. Interleukin-17 (IL-17) is an inflammatory cytokine that functions in inflammation and cancer, as well as several other cellular processes. In this study, we investigated the roles and the prognostic value of IL-17 and the IL-17 receptor (IL-17R) in lung cancer.

Design: Gene expression microarray analysis followed by Kaplan-Meier survival curve was applied to study the association of different forms of IL-17 with the prognosis in lung cancer. Immunohistochemistry was used to analyze IL-17R expression in lung cancer tissues. *C*ell models and *mouse tail vein* model were applied to examine the functions of IL-17R. A kinase array was used to identify the signaling pathway that participates in IL-17-IL-17R signaling.

Results: Expression of IL-17RB was associated with lymph node metastasis and distant metastasis, as well as poor patient survival. IL-17RB overexpression significantly increased cancer cell invasion/migration and metastasis *in vitro* and *in vivo*. IL-17RB induced ERK phosphorylation, resulting in GSK3β inactivation and leading to β-catenin up-regulation. IL-17RB also participated in IL-17B synthesis via the ERK pathway.

Conclusions: IL-17RB activation is required for IL-17B-mediated ERK phosphorylation. IL-17B-IL-17RB signaling and ERK participate in a positive feedback loop that enhances invasion/migration ability in lung cancer cell lines. IL-17RB may therefore serve as an independent prognostic factor and a therapeutic target for lung cancer.

2123 Validation and Application of Predicted Tumor Mutational Burden (pTMB) Using a 130-Gene Sequencing Panel in Lung Adenocarcinoma

Soo-Ryum Yang[1], *David Steiner*[2], *Henning Stehr*[3], *Gerald Berry*[4], *James L Zehnder*[2], *Christian Kunder*[2]. [1]San Francisco, CA, [2]Stanford University School of Medicine, Stanford, CA [3]Stanford University, [4]Stanford University Med. Ctr., Stanford, CA

Background: Studies have shown that tumor mutational burden (TMB) derived from whole exome sequencing (WES) may predict response to immune checkpoint therapy in patients with advanced lung adenocarcinoma (LUAD). However, WES is not currently optimized for routine clinical use due to cost constraints and bioinformatics requirements. Recently, a novel algorithm was proposed that allows for estimation of total nonsynonymous exonic mutations from targeted clinical sequencing panels (Roszik et al. 2016). Herein, we customized the algorithm to our 130-gene next-generation sequencing (NGS) panel and calculated predicted TMB (pTMB) in a set of clinical LUAD samples in order to explore its validity and significance.

Design: TCGA data for LUAD samples (n = 230) were used to generate adjusted gene values for the 130 genes in our NGS panel. An independent WES LUAD cohort (n = 183) was used for *in silico* validation of the prediction algorithm (Imielinski et al. 2012). pTMB was calculated for 181 LUAD samples that were previously sequenced using our 130-gene NGS panel. The relationship between pTMB values and standard clinicopathologic variables including PD-L1 expression was analyzed.

Results: In our validation cohort, pTMB was significantly correlated with actual TMB (r = 0.83, P = 1.04E-47) and showed sensitivity, specificity, and accuracy of 81.6%, 82.3%, and 82.0% respectively when using a diagnostic threshold of 200 mutations. In our 181 LUAD samples, pTMB was significantly higher in smokers than in non-smokers (250 vs 121, P = 9.76E-06, Wilcoxon rank-sum test) and those with mutated vs wild type *KEAP1* (417 vs 152, P = 3.90E-03). No significant associations were seen for age, sex, clinical stage, and mutational status of driver oncogenes (*EGFR*, *KRAS*, *ALK*, *ROS1*, *RET*, *MET*, *BRAF*, *ARAF*, *NRAS*, *AKT1*, and *ERBB2*) and other recurrent tumor suppressors (*TP53* and *STK11*) (P > Bonferroni-corrected α = 5.56E-03). In addition, there was no association between pTMB and PD-L1 expression (P = 0.63).

Clinicopathologic correlates of predicted tumor mutational burden (pTMB) in 181 lung adenocarcinoma samples

Variable	Median pTMB	**P** value*
Age		0.869
< 68 years	167	
≥ 68 years	149	
Sex		0.892
Female	152	
Male	173	
Smoking**		9.76E-06
Yes	250	
No	121	
Stage		0.0402
I	87	
II	208	
III	214	
IV	167	
Driver oncogene status		0.0627
EGFR	120	
KRAS	221	
Kinase fusion	208	
Other oncogenic drivers	115	
Unknown	247	
TP53 status		0.0345
Mutant	186	
Wild type	151	
STK11 status		0.0741
Mutant	250	
Wild type	155	
KEAP1 status**		3.90E-03
Mutant	417	
Wild type	152	
PD-L1 expression		0.626
Positive	170	
Negative	152	

*Wilcoxon rank-sum test and Kruskal–Wallis rank-sum test as appropriate. ***P* < Bonferroni-corrected α = 5.56E-03. Kinase fusions included gene rearrangements involving kinase domains of *ALK*, *ROS1*, and *RET*. Other oncogenic drivers included activating genomic alterations involving *MET*, *BRAF*, *ARAF*, *NRAS*, *AKT1*, and *ERBB2*. PD-L1 expression (22C3 pharmDx antibody) was considered positive if tumor proportion score was ≥ 1%; negative if otherwise.

Conclusions: pTMB derived from a 130-gene NGS panel may be used to infer actual TMB with adequate performance. Furthermore, our analysis using pTMB confirmed the previously described association of mutation load with smoking history and revealed a potentially novel interaction with *KEAP1* mutations. Lack of association with PD-L1 expression suggests that TMB may represent an independent measurement of tumor immunogenicity in LUAD. Additional studies are needed to correlate pTMB with response to immune checkpoint therapy.

2124 Micropapillary Adenocarcinoma of Lung Is Associated With p53 Overepxression and EGFR Mutation

Yi-Chen Yeh[1], *Hsiang-Ling Ho*[2], *Teh-Ying Chou*[3]. [1]Taipei Veterans General Hospital, Taipei, [2]Taipei Veterans General Hospital, [3]Taipei Veterans General Hosp, Taipei, Taiwan

Background: The WHO 2015 classification of lung tumors classify lung adenocarcinoma into five predominant histological subtypes, including lepidic, acinar, papillary, micropapillary, and solid subtypes. Micropapillary subtype had been recognized as an indicator of poor prognosis. However, little is known about the molecular alternations associated with micropapillary histology. In this study, we investigated the association between micropapillary histology and p53 overexpression. We will also analyze the association between micropapillary histology and common driver mutations in lung adenocarcinomas, including epidermal growth factor receptor (EGFR) gene mutation and anaplastic lymphoma kinase (ALK) gene rearrangements.

Design: Totally 207 patients with lung adenocarcinoma who underwent surgical resection were enrolled. Immunohistochemical stain for p53 was performed on tissue microarrays constructed with one 3-mm cores of tumor tissue for each case. Correlations between p53 overexpression with patient characteristics, histologic subtype, EGFR mutation, ALK rearrangement and clinical outcome were analyzed.

Results: p53 overexpression was significantly associated with histologic subtype (P < 0.001). There were more lepidic predominant and papillary predominant tumors in p53-Low group (lepidic: 25.7%, papillary: 22.1%) than in p53-High group (lepidic: 5.3%, papillary: 7.4%). On the contrary, acinar, micropapillary and solid predominant tumors were more frequent in p53-High group (acinar: 47.9%, micropapillary: 17.0%, solid: 22.3%) than p53-Low group (acinar: 34.5%, micropapillary: 5.3%, solid: 12.4%). There was a trend toward worse overall survival in p53-High tumors, although the difference did not reach statistical significance (P = 0.076). Besides, p53-High tumors were associated with shorter recurrence-free interval than p53-Low tumors (P = 0.008). There were no significant association between p53 status and patient age, sex, smoking history, stage, EGFR mutation and ALK fusion. In addition, micropapillary predominant tumors were more prevalent in EGFR-mutated tumors than EGFR-WT tumors (14.0% vs. 3.8%), whereas solid predominant tumors were more prevalent in EGFR-WT tumors than EGFR-mutated tumors (25.6% vs. 12.0%).

	Total	p53-Low	p53-High	p53-Low vs. p53-High
	No. (%)	No. (%)	No. (%)	(P value)
Number	207 (100)	113 (100)	94 (100)	
Age(years)	65.4±10.9	66.0±11.1	64.7±10.6	P = 0.38
Median	67	68	65.5	
Range	36-88	36-83	41-88	
Sex				
Female	88 (42.5)	47 (41.6)	41 (43.6)	P = 0.77
Male	119 (57.5)	66 (58.4)	53 (56.4)	
Smoking				
Never	94 (65.3)	52 (61.2)	42 (71.2)	P = 0.22
Smoker	50 (34.7)	33 (38.8)	17 (28.8)	
Stage				
I	120 (58.8)	71 (63.4)	49 (53.3)	P = 0.14
II-IV	84 (41.2)	41 (36.6)	43 (46.7)	
Histologic subtype				
Lepidic	34 (16.4)	29 (25.7)	5 (5.3)	P < 0.001
Acinar	84 (40.6)	39 (34.5)	45 (47.9)	
Papillary	32 (15.5)	25 (22.1)	7 (7.4)	
Micropapillary	22 (10.6)	6 (5.3)	16 (17.0)	
Solid	35 (16.9)	14 (12.4)	21 (22.3)	
EGFR				
Wild type	78 (43.8)	43 (43.4)	35 (44.3)	P = 0.91
Mutated	100 (56.2)	56 (56.66)	44 (55.7)	
ALK fusion				
Negative	169 (94.9)	93 (93.9)	76 (96.2)	P = 0.49
Positive	9 (5.1)	6 (6.1)	3 (3.8)	

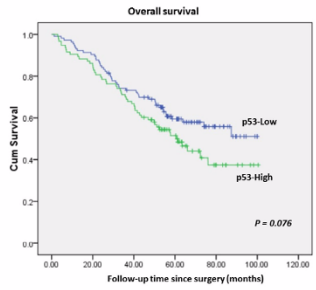

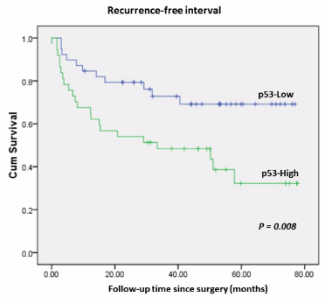

Conclusions: We showed that micropapillary predominant adenocarcinomas tend to show p53 protein overexpression, and more commonly harbor EGFR mutation than other histologic subtypes.

2125 Epidemiology of Interstitial Lung Disease in Autopsy Cases of Elderly Patients

Xiaotun Zhang[1], *Eunhee Yi*[1], *Jay H Ryu*[1], *Anja Roden*[2]. [1]Mayo Clinic, Rochester, MN, [2]Mayo Clinic Rochester, Rochester, MN

Background: Evidence suggests that idiopathic pulmonary fibrosis (IPF) is the most common interstitial lung disease (ILD) in elderly. However, the epidemiology of ILD in that patient population is still not fully elucidated given the relative lack of surgical lung biopsies in elderly patients. We have studied lungs obtained during autopsies from elderly patients to identify the distribution of ILDs in this population.

Design: Pathology files (1995-2014) were searched for a spectrum of ILDs. A subset of cases that did not have a distinct diagnosis in the pathology report was re-reviewed by a thoracic pathologist. All cases will be re-reviewed by the time of the conference to confirm the diagnosis. Medical records were studied. An age cutoff of 70 years to define elderly was used.

Results: Most (47 of 66, 71.2%) cases were identified with usual interstitial pneumonia (UIP). However, cases of hypersensitivity pneumonitis (HP) (5, 7.6%), sarcoidosis (4, 6.1%), granulomatosis with polyangiitis (GPA) (2, 3.0%), non-specific interstitial pneumonia (NSIP) (2, 3.0%), Pulmonary Langerhans cell histiocytosis (PLCH) (1, 1.5%), pneumoconiosis (1, 1.5%) and fibrosing interstitial pneumonia, NOS (4, 6.1%) were also found. Table 1 summarizes clinicopathologic features and causes of death of all cases.

Table 1 Clinicopathologic features and cause of death of elderly patients with ILD

ILD	Number of cases N	Age at Death (yrs) Median (Range)	Male N (%)	Smoking Hx N			CTD* N (%)	Cause of Death - ILD N (%)
				Yes	No	Un-known		
UIP	47	76 (70->89)	32 (68)	22	15	10	9 (19.1)	30 (63.8)
HP	5	82 (71-89)	2 (40)	0	1	4	0	1 (20)
Sarcoid-osis	4	80.5 (77-86)	1 (25)	1	1	2	0	3 (75)
NSIP	2	81 (73-89)	0	0	1	1	2 (100)	1 (50)
GPA	2	82 (79-85)	1(50)	1	0	1	0	1 (50)
PLCH	1	>89	1	1	0	0	0	0
Pneumo-coniosis	1	>89	1	1	0	0	0	1 (100)
FIP**, NOS	4	82.5 (77->89)	3 (75)	2	1	1	0	2 (50)

*CTD, connective tissue disease; ** FIP, fibrosing interstitial pneumonia

Conclusions: While we confirm that UIP is the most common ILD in elderly, other ILDs are not infrequent in this age population. Furthermore, some elderly patients with UIP have an associated connective tissue disease (CTD). The majority of patients die of the underlying ILD. Our study shows that elderly patients with ILD should not be assumed to have UIP or idiopathic pulmonary fibrosis without appropriate evaluation.

2126 Use ALK immunohistochemistry (IHC) assay to screen for ALK+ lung adenocarcinoma: equivocal staining pattern is a practical challenge

Christopher Q Zhang[1], *Hong Yin*[2], *Shaobo Zhu*[2], *Zongming Eric Chen*[2]. [1]Lafayette College, [2]Geisinger Medical Center, Danville, PA

Background: For identifying ALK+ lung adenocarcinoma, the recently FDA approved IHC assay has several advantages over the traditional FISH test. It is faster, cheaper, and probably easier to interpret. With a compatible sensitivity and specificity to FISH assay, it is the ideal method for the task. However, in reality, ALK IHC assay still faces many technical challenges. Here, we present data to show "equivocal staining pattern" in IHC test is a real problem and recommend a 3-tier scoring system to replace the dichotic scoring.

Design: To verify ALK IHC test performance, concurrent FISH and IHC testing was performed using 126 consecutive clinical samples, including cytology specimens and tissues obtained from biopsy procedure and surgical resection. For IHC, Ventana ALK (D5F3) CDx assay was performed using Benchmark Ultra platform according to vendor's instruction. For FISH analysis, Vysis ALK break apart FISH probe kit was used and results interpreted according to vendor's instruction.

Results: Using recommended dichotic scoring system, ALK IHC unequivocally identified 4 positive and 103 negative samples, in complete accordance with FISH results. However, 19 (15%) samples were hard to score because tumors cells and background non-tumor cells both showed variable granular cytoplasmic staining. They were labelled as "indeterminate" at the time of testing. These were all cytology specimens, containing limited tumor cells with abundant non-tumor cells including macrophages and other inflammatory cells in background. Many specimens also contained necrotic tumor debris. In most samples, the intensity of granular staining in tumor cells appeared weaker compared to that seen in macrophages in the same specimen. However, in other samples, the tumor cells showed moderate to strong granular cytoplasmic staining indistinguishable from true positive pattern. FISH analysis revealed 1 positive and 18 negative for ALK gene rearrangement. Had the dichotic scoring system forcefully applied, many of the sample would incorrectly identified as either positive or negative.

Conclusions: For identifying ALK+ lung adenocarcinoma, the IHC test can function as an effective screen tool. However, in practice, due to specimen complexity, "equivocal staining pattern" does exist. To ensure accurate interpretation, adding an "indeterminate" category into the current dichotic scoring system is necessary. Our data also suggest that FISH confirmation is only needed for these IHC "indeterminate" samples.

2127 Assessment of Programmed Death Ligand-1 (PD-L1) Expression in Lung Adenocarcinoma at Primary and Metastatic Sites: Value of Testing all Available Specimen Sites and Types

Haijun (Steve) Zhou[1], *Ritu Nayar*[1]. [1]Northwestern University, Chicago, IL

Background: Immunotherapy targeting PD-1/PD-L1 has emerged as a promising therapeutic strategy for lung adenocarcinoma. PD-L1 immunostaining result is primarily the gatekeeper for enrolling patients into the FDA approved treatment or related clinical trials especially for patients with unresectable tumor or late stage disease with metastasis. The nature of heterogeneous PD-L1 expression in the tumoral tissue may potentially cause false negative interpretation on small biopsy specimens.

Design: We retrospectively reviewed clinically performed PD-L1 immunostaining (SP142 clone) cases of adenocarcinoma specimens in needle core biopsies and cell block preparations from primary sites and metastases including fluids in our hospital from January 2016 to September 2017. Semi-quantitative score (0/1/2/3) was given according to percent of PD-L1 positive tumor cells (TCs) (TC 0 for <1%, TC 1 for 1-4%, TC 2 for 5-49%, and TC 3 for ≥50%) and percent tumor area with PD-L1 positive tumor-infiltrating immune cells (ICs) (IC 0 for <1%, IC 1 for 1-4%, IC 2 for 5-9% and IC 3 for ≥10%).

Results: Adenocarcinoma cases that were scored either TC 1/2/3 or IC 1/2/3 accounted for 57% in primary needle core biopsies (48 of 84 cases), 51% in metastatic site biopsies (39 of 77 cases) and 57% in metastatic fluids (13 of 23 cases). 10 of total 174 patients have repeated PD-L1 immunostaining studies at different anatomical sites. Interestingly, 6 of 10 (60%) patients had significantly different expression levels of PD-L1 in different anatomic sites: 3 patients had TC 3 or IC 3 PD-L1 expression on metastatic sites (1 mediastinal lymph node, 1 pelvic soft tissue and 1 pleural fluid) with TC 0 or IC 0 on primary tumor site. 2 patients each had two lung masses biopsied with PD-L1 studies showing TC3 on one mass and TC0 or TC2 on the other mass respectively. One patient's initial lymph node staging biopsy showed TC 0 and IC 0 PD-L1 expression while the primary tumor core biopsy showed IC 2 PD-L1 expression.

Conclusions: Needle core biopsy and cytology cell block preparations are valuable resources for PD-L1 testing. For patients with multiple available specimens (primary or metastatic sites including fluids), every specimen should be tested with PD-L1 so as not miss potential candidates for frontline immune checkpoint inhibitor therapy.

2128 Tissue Handling Effects on PD-L1 Immunohistochemistry Staining

Sina Zomorrodian[1], *Sarwat Gilani*[1], *Rocco Lafaro*[2], *Ximing Yang*[3], *John T Fallon*[1], *Minghao Zhong*[1]. [1]Westchester Medical Center at New York Medical College, Valhalla, New York, [3]Westchester Medical Center, [4]Northwestern University, Chicago, IL

Background: Anti-PD-L1/PD-1 immunotherapies offer an attractive treatment option for various cancers. Published data support strong PD-L1 expression as an effective tumor biomarker in predicting therapeutic response. Thus, accurately evaluating PD-L1 expression is essential. However, data regarding the effect of different tissue handling procedures on PD-L1 immunohistochemistry (IHC) staining has not been published to date. We evaluated the effect of tissue handling variables, such as formalin fixation time, decalcification, alcohol fixation and ischemic time on PD-L1 IHC staining.

Design: Placenta (a PD-L1 positive tissue) was used for all procedures. Both 22C3 and SP263 antibody clones were used for staining. To test ischemic time, fresh placentas were divided into pieces of similar size and placed in closed containers at room temperature for 0, 2, 4, 8, 12 and 24 hours before fixation. In terms of fixative type, separate placentas were placed in either 10% neutral buffered formalin or 95%

alcohol for 12, 24, 36 and 72 hours. Decalcification regimens of 0.5, 1, 6 and 24 hours were followed by standard formalin fixation of placenta. Also, FFPE tissue from a known PD-L1 positive lung adenocarcinoma was reversely processed and underwent decalcification as mentioned. All specimens were submitted for routine processing and paraffin embedding after the various regimens. Tissue microarrays were constructed to minimize IHC staining variation. IHC results were evaluated by pathologists.

Results: Tissue with ischemic times of up to 24 hours didn't show significant change in PD-L1 staining. Ischemic times from 24-96 hours resulted in slight dimming of PD-L1 detection from 3+ to 2+. The use of 95% alcohol compared to 10% neutral buffered formalin did not produce an appreciable difference in PD-L1 detection. Prolonged fixation regimens yielded no effect on PDL-1 staining. Decalcification yielded a slight effect, as staining decreased from 3+ to 2+ after 3 hours. Specimen that was placed in decal for 8 hours without any prior calcification showed noticeably attenuated staining. The two clones (22C3 and SP263) yielded similar results.

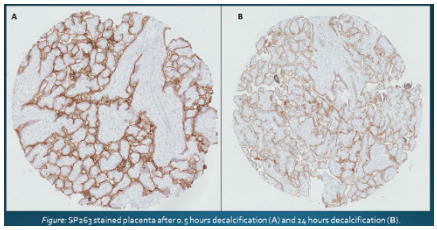

Figure: SP263 stained placenta after 0.5 hours decalcification (A) and 24 hours decalcification (B).

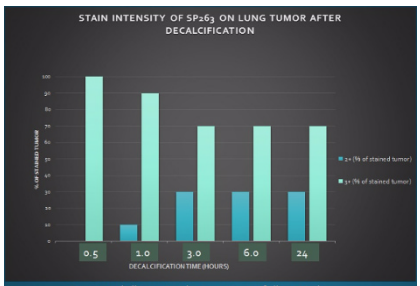

Figure: Graph illustrating the percentage of all *positively* stained tumor cells that stain 2+ and 3+ (1+ staining was not observed in the lung tumor specimens).

Conclusions: This is the first study on the effect of different tissue handling protocols on PD-L1 IHC staining. The data demonstrates that ischemic time, decalcification and lack of fixation will effect PD-L1 IHC staining. Specific guidelines for the handling of PD-L1 stained specimens should be provided to the pathology community, based on results from further studies.

Table 1. Distribution of PD-L1 in malignant cells and lymphocytes T Cell CD3+CD45RO+ from primary and metastatic tumors stratified according to histologic types.

PD-L1 in Malignant Cells					
Histologic Types	Tumor	Mean	Std. Deviation		
	ADC		Prim	0,55	1,93
			Met	0,30	1,44
	SCC		Prim	2,36	7,50
			Met	0,46	1,32
	LCC		Prim	0,35	0,89
			Met	0,40	0,38
	LCNEC		Prim	9,47	23,17
			Met	12,31	32,68

Lymphocytes T Cell CD3+CD45RO+					
Histologic Types	Tumor	Mean	Std. Deviation		
	ADC		Prim	770,81	623,07
			Met	584,71	413,51
	SCC		Prim	664,09	670,21
			Met	335,79	324,05
	LCC		Prim	655,60	309,50
			Met	641,67	499,84
	LCNEC		Prim	663,16	411,55
			Met	673,43	549,84

FIG. 2034

Table. Clinical, imaging and pathologic features of study group

Tumors Studied	Case No.	Age (yrs), Gender, smoking status	Presentation and Imaging	Histology	IHC Profile CD34 STAT6 TTF-1	**NAB2-STAT6** fusion by NGS	Treatment and Follow-up
Intrapulmonary (AFs)	1	63/F, unknown	Incidental, 0.8 cm nodule, RUL, not PET	No mitoses (low risk)	Diff + Diff+ Epi +	Positive	Resection, NED at11 yrs.
	2	75/F, non-smoker	Incidental, 1.6 cm nodule, RML, no FDG uptake	No mitoses (low risk)	Diff + Diff+ Epi +	Positive	Resection, NED 10 yrs
	3	44/F, non-smoker	Incidental, 2.7 cm nodule, RUL, mildly increased FDG PET avidity	No mitoses (low risk)	Diff+ Diff+ Epi+	Positive	Resection, NED at 8 months
	4	83/M, ex-smoker	Incidental, 3.0 cm nodule, RLL, mildly increased FDG PET avidity	No mitoses (low risk)	Diff + Diff+ Epi +	Positive	Resection, NED at 15 yrs.
	5	57/M, non-smoker	Incidental, 1.8 cm nodule, RUL, No FDG uptake	No mitoses (low risk)	Diff + Diff + Epi. +	Positive	Resection, NED at 12 yrs.
Hybrid Tumors	1	40/F unknown	Incidental, 2.5 cm, RUL, No FDG uptake	No mitoses (low risk)	Diff + Diff + Epi +	Negative	Resection, NED at 4 yrs
	2	63/F, non-smoker	History of breast cancer, 2.3 cm nodule, RLL, mildly increased FDG PET avidity	1 mitosis per 10 HPFs (low risk)	Diff. + Diff + Epi. +	Positive	Resection, NED at 4 yrs.
Typical SFTs	1	72/M, non-smoker	Hypoglycemia and weight loss, 24.5 cm mass, LLL, no PET	Focal atypia, 7 mitoses per 10 HPFs (high risk)	Diff + Diff + N/A	Not done	Resection, NED at 2 yrs.
	2	72/M, ex-smoker	Incidental, 3.0 cm nodule, RUL, No FDG uptake	7 mitoses/ 10 HPFs (moderate risk)	Foc + Diff + N/A	Not done	Resection, NED at 1 yr.
	3	48/F, non-smoker	Chest symptoms, 13.7 cm mass, RLL, no PET	No mitoses (low risk)	Diff + Diff + N/A	Not done	Resection, NED at 8 yrs.
	4	32/M, non-smoker	Presentation unknown, 5.0 cm exophytic, LLL, No PET	<2 mitoses/ 10HPFs (low risk)	Diff + Diff + Epi. +	Not done	Resection, NED at 3 yrs.

FIG. 2077

Results:	Total No.	Age Range (Ave)	M:F	Lepidic	Acinar	Papillary	Micropapillary	Solid	Poorly Differentiated (PD)	Moderately Differentiated	Well Differentiated	Not classified (NC)	Comments
BRAF +	4	46 to 81 (63.5)	1:0	0	0	0	0	1 (25%)	2 (50%)	0	0	1 (25%)	NC: psammoma
BRAF -	310	35 to >89 (62.5)	1:1.3	4 (1.3%)	27 (8.7%)	16 (5.2%)	7 (2.3%)	50 (16.1%)	89 (28.7%)	20 (6.5%)	1 (0.3%)	96 (30.1%)	PD: sarcomatoid, cribriform, mucinous, or neuroendocrine.
				BRAF + (4 cases)									
Smoking status/history				100% smokers									
Stage at diagnosis				75% Stage IV; 25% Stage 1a									